Electrical and Optical Investigations on Discotic Liquid Crystal Composite Systems

By

Supreet

Thesis submitted to Thapar University, Patiala for the award

of the degree of

Doctor of Philosophy

School of Physics & Materials Science

Thapar University

Patiala - 147 004

INDIA

2014

DEDICATED TO

MY BELOVED

PARENTS

THAPAR UNIVERSITY, PATIALA

CERTIFICATE

This is to certify that the thesis entitled **"*Electrical and Optical Investigations on Discotic Liquid Crystal Composite Systems*"** submitted by ***Supreet***, for the award of the degree of **DOCTOR OF PHILOSOPHY** of Thapar University, Patiala, Punjab, India, is her original experimental investigation and conclusions. The subject matter of this thesis has not been previously published or submitted to any other university for the award of any other degree, diploma, associateship, fellowship or any other similar title.

Prof. K. K. Raina

(Supervisor)

Distinguished Professor

And Deputy Director

Thapar University, Patiala

Prof. Sandeep Kumar

(Supervisor)

Professor

Raman Research Institute

Bangalore

ACKNOWLEDGEMENTS

I am very grateful to my thesis supervisors Prof. K. K. Raina and Prof. Sandeep Kumar for giving me the opportunity to work under their guidance. There are no adequate words to explain their keen interest, immense patience, kind advice, sustained encouragement, and constant help during this time. It was a great experience to work with them and learn so many things from them both as a researcher and as a human being.

I would like to express my deep gratitude to Dr. Pratibha R. (Raman Research Institute, Bangalore), for giving me a chance to collaborate with her and to utilize her laboratory for my experimental work related to the thesis. I thank her for her keen interest in my research work and many valuable discussions that I had with her.

I would also like to thank my committee members Dr. Kulvir Singh, Dr. Puneet Sharma and Dr. Rajeev Mehta for their constant encouragement and sharing their valuable comments and suggestions. I also thank Dr. Manoj K. Sharma (HOD, SPMS) and Dr. O. P. Pandey (Dean Research and Sponsored Projects) for their constant support.

I am thankful to all other Soft Condensed Matter faculty members, research students, and my friends in Raman Research Institute for their support and valuable suggestions.

I also thank various other departments of RRI and the administration, RRI library staff, computer section, workshop, transport, security, canteen, hostel and clinic for their constant support throughout my stay in RRI.

My sincere thanks to everyone at RRI especially "*Jaladarshini family (we peers at RRI)"* for their unconditional love, support, and cooperation which made my stay a wonderful experience. I love you all. I was lucky to have Dr. Manveen Kaur, Dr. Gudveen Sawhney, Dr. Lavanya Khanna, Rishi Kumar, Geatanjali Dhir, Dr. Jaspal Singh Patra as my friends,

Dr. Neeraj Sharma, Dr. Ravi Kumar Shukla, Dr. Dinesh Pathak, Dr. Praveen Kumar as my seniors, Mrs. Manju Arora, Dr. Rekha Rani, Dr. Renu Rani, Ramneek Kaur, Gurpreet Kaur, as my labmates, Hitesh Mehtani as my junior in Thapar University, Patiala.

I have earned good experiences of life from them. God bless you all.

I am also grateful to staff of SPMS, Thapar University, Patiala who always helped me whenever I approached them for any help.

My deep gratitude to my beloved parents, my sister, my brother, my adorable niece *Mehreen*, my beloved husband *Nitin Gogna*, my in-laws, for being a constant source of affectionate encouragement and help throughout my research work.

And above all, I thank the Almighty for being there with me all the times. I praise you Lord.

(Supreet)

Contents

Chapter 1: INTRODUCTION

Chapter 2: Materials and Experimental Techniques

Chapter 3: Characterization of Pure and ZnO Nanoparticles Dispersed Rufigallol Based Discotic Liquid Crystal

Chapter 4: Dispersion of Gold Nanoparticles in Discotic Liquid Crystals Comprise of Triphenylene Core

Chapter 5:Induction, Variation, and Stabilization of Mesomorphic Properties of Disc-Like Molecules Composites Based on Charge Transfer Complex of Disc-like Molecule and TNF

Chapter 6: Summary

List of Figures

List of Tables

List of abbreviations used in this Thesis

LC	Liquid Crystal	LCD	Liquid Crystal Display
Sm	Smectic	N_D	Discotic Nematic
Col	Columnar	N*	Chiral Nematic
1D	One Dimensional	N_D*	Chiral Discotic Nematic
2D	Two Dimensional	N_L	Nematic Lateral
N_{Col}	Columnar Nematic	Col_h	Columnar Hexagonal
Col_p	Columnar Plastic	Col_r	Columnar Rectangular
Col_{ob}	Columnar Oblique	Col_{tet}	Columnar Tetragonal
Col_L	Columnar Lamellar	UV	Ultraviolet
H	Helical	POM	Polarizing Optical Microscopy
DLC	Discotic Liquid Crystal	DSC	Differential Scanning Calorimetry
XRD	X-ray Diffraction	CT	Charge Transfer
FT-IR	Fourier Transform Infrared	FET	Field Effect Transistor
LED	Light Emitting Diode	LB	Langmuir Blodget
TOF	Time of Flight	NMR	Nuclear Magnetic Resonance
HBC	Hexabenzocoronene	PAH	Polyaromatic Hydrocarbon
TP	Triphenylene	TNF	Trinitrofluorenone
Pc	Phthalocyanine	I	Isotropic
ITO	Indium Tin Oxide	Cr	Crystalline
CNT	Carbon Nanotube	τ	Relaxation Time

ε’	Dielectric permittivity	ε”	Dielectric losses
λ	Wavelength	OPV	Organic Photovoltaic

CPI Complementary Polytopic Interaction

PR-TRMC Pulse Radiolysis Time Resolved Microwave Conductivity

List of Publications

In journals:

1. Supreet, S. Kumar, K. K. Raina and R. Pratibha. Enhanced stability of the columnar matrix in a discotic liquid crystal by insertion of ZnO nanoparticles, Liquid Crystals, 2013; 40:228–236.
2. Supreet, S. Kumar, R. Pratibha and K.K. Raina. Effect of dispersion of gold nanoparticles on the optical and electrical properties of discotic liquid crystal, Liquid Crystals, 2014;41:933-39.
3. Supreet, S. Kumar, Rishi Kumar, R. Pratibha and K.K. Raina. Gold Nanoparticles in Columnar Matrix of Discotic Liquid Crystal, AIP Conference Proceeding, 2013;1536:67-68.
4. Rishi Kumar, Supreet, and K. K. Raina. Morphological responses of polymer dispersed liquid crystal composites for photonic display applications, AIP Conference Proceeding, 2013;1536:743-744.
5. Supreet, S. Kumar, R. Pratibha K. K. Raina. Orientational Order Parameter Measurements of Discotic Liquid Crystal, AIP Conference Proceeding, 2013;1591:180-182.
6. Dielectric and thermodynamic studies of columnar hexagonal phase in discotic Liquid crystal

   Supreet, S. Kumar, K.K. Raina, and R. Pratibha
7. Induced smectic A phase in binary mixtures of a non mesomorphic compound composed of disc-like molecules and 2, 4, 7-trinitrofluorenone

   Supreet, S. Kumar, K.K. Raina, and R. Pratibha

In Conference Proceedings:

1. Supreet, S. Kumar, R. Pratibha and K. K. Raina. Dielectric and Thermo-physical Studies of Discotic Liquid Crystal Dispersed with Gold Nanoparticles, International Workshop on Soft Matter Chemistry, Nov. 9-11, 2011, organized by Raman Research Institute, Bangalore, pp 42.

2. Supreet, K. K. Raina, Sandeep Kumar. Dielectric spectroscopy of nematic liquid crystals disperesed with discotic liquid crystals, 18th National conference on liquid crystal, Nov. 15-17 2011, organized by NERIST, Itanagar, Arunachal Pradesh, Nov. 15-17 2011, pp 66.

3. Supreet, R. Pratibha , S. Kumar and K. K. Raina. ZnO-Columnar Hexagonal Discotic Nanocomposites: Dielectric and Thermophysical Properties, 23rd Annual General Meeting-Materials Research Society of India (MRSI), February 13-15, 2012, organized by Thapar University, Patiala, pp 148.

4. Supreet-, R. Pratibha , S. Kumar and K. K. Raina. Induced smectic A phase in binary mixtures of a non mesomorphic compound composed of disc-like molecules and 2, 4, 7-trinitrofluorenone, 19th National conference on liquid crystals, Nov 21-22, 2012, organized by Thapar University, Patiala, pp 52.

5. Supreet, R. Pratibha, S. Kumar and K. K. Raina. Thermophysical studies on rufigallol based discotic liquid crystal, NCFM, Sept 24-25, 2012, organized by GVMGC Sonipat, Haryana, pp 23.

6. Supreet, Pratibha R., Sandeep Kumar, and K.K. Raina. Charge transfer complex of discotic liquid crystal, DAVIET-2013, May 30-31, 2013, organized by DAVIET, Jalandhar, Punjab, pp 34.

7. Supreet, Pratibha R., Sandeep Kumar, and K.K. Raina. Thermal analysis and X-ray study of disc like molecules forming columnar mesophase, National Conference on Recent Developments in Physics (NCRDP-2014), March 29-30, 2014, organized by S. D. (PG) College, Sonipat, Haryana.

8. Supreet, Pratibha R., Sandeep Kumar, and K.K. Raina. Gold Nanoparticles-Discotic Liquid Crystal Composite Systems for Opto-Electronic Devices, International conference on electron microscopy (EMSI-2014), July 9-11, 2014, organized by Delhi University, Delhi.

CHAPTER 1

INTRODUCTION

Abstract: This is an introductory chapter to liquid crystals in general like their classification and their important significance in material science, life science, nanoscience and their dominance in electro-optical display devices. The chapter begins with an over view of thermotropic liquid crystals and their brief history and focuses in greater detail on the physical properties of discotic liquid crystals, making them ideal candidates for various optical and electronic devices such as optical compensation films, photocopiers, laser printers, photovoltaic cells, light emitting diodes, field effect transistors, gas sensors and holographic data storage.

1.1 Soft Matter

Soft matter is an inevitable part of everyday life. It covers large variety of system from living cells to paints, soaps detergent solutions, milk, toothpaste, liquid crystals, gels etc. soft matter (or soft condensed matter) research is a driving force for a broad range of innovative field. Materials of interest in soft condensed matter physics are complex fluids, micro emulsions, surfactant mesophases, liquid crystals etc.

Liquid crystals (LC) are well known today to a broad community. Induced by the applications of liquid crystals in optoelectronics displays such as watches, calculators, laptops computers, flat panel televisions etc. and for thermography in the mid 1960's, LC has been extensively used in numerous other applications such as temperature sensing, solvents in chemical reactions, in chromatography, in spectroscopy, in holography etc. LC's can be potentially used as new functional materials for electron, ion, molecular transporting, sensory, catalytic, optical and bio-active materials. LCs can also be used as templates for synthesis of nanomaterials and serve as model system for biomembranes etc.

1.2 What are LIQUID CRYSTALS?

It is generally accepted that there are three common states of matter: solid, liquid and gas [1]. Most substances exhibit only these three states as the temperature is varied. There are, however many organic compound composed of molecules with pronounced geometric shape anisotropy like a rod or a disc do not immediately transform to liquid phase when heated beyond the melting temperature but exhibit more than a single transition from solid to liquid showing the existence of one or more intermediate phases, exhibiting the properties of both solids and liquids. This phase possesses some degree of orientational ordering and sometimes some positional ordering of the anisotropic molecules. This is the mysterious and fascinating

liquid crystalline state. LC phase is also referred to as mesophase and the constituents of the mesophase are called mesogens. Mesogens can be acyclic, heterocyclic, isocyclic, aromatic, organo-mettalic, steroids, organic acid salts etc. Liquid crystals have also been called as the fourth state of matter and have been recognized as a true thermodynamically stable state of matter.

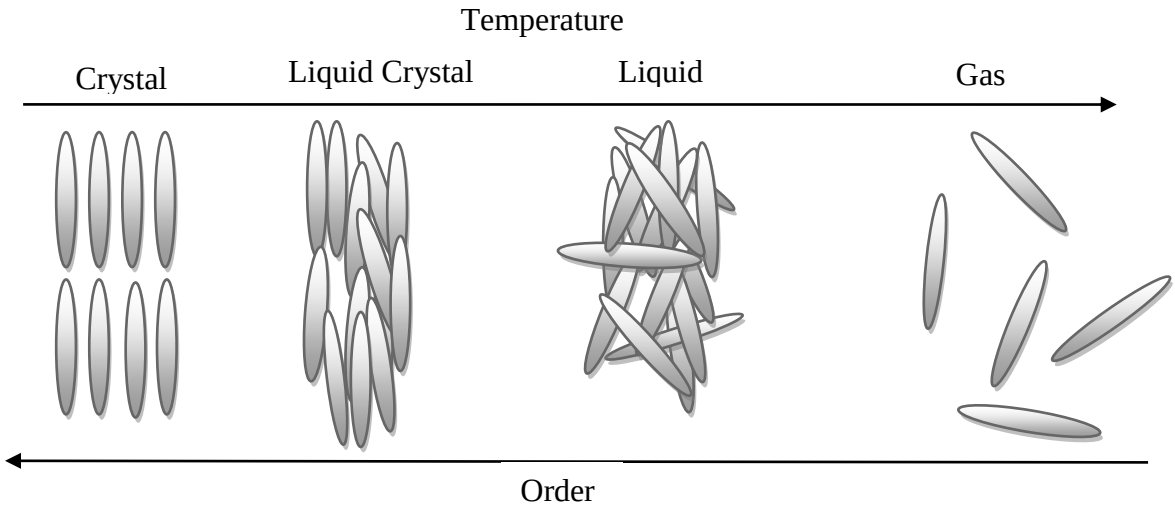

Figure 1.1 Schematic representations of different states of matter and molecular ordering present in them.

In the simplest LC phase, one molecular axis tends to point along a preferred direction as the molecules undergo diffusion. The preferred direction is called the *director* and is denoted by ***n***. To quantify just how much order is present in a material, an order parameter (*S*) is defined. Traditionally, the order parameter is given as follows:

$$S = \frac{< 3cos^2\theta - 1 >}{2}$$

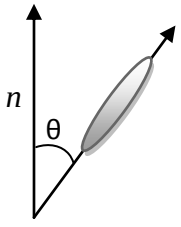

where theta (θ) is the angle between the director and the long axis of each molecule. The brackets denote an average over all of the molecules in the sample.

Typical values for the order parameter of a liquid crystal range between 0.3 and 0.9, with the exact value a function of temperature, as a result of kinetic molecular motion. This is illustrated below for a nematic liquid crystal material.

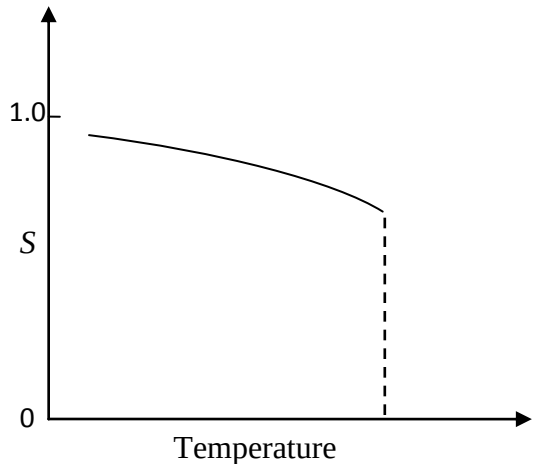

Figure 1.2 Typical temperature dependence of the nematic order parameter *S* with temperature.

1.3 Discovery of Liquid Crystals

The story of liquid crystals started around 1850 with a few European investigators who observed some new and interesting phenomena but who never fully realized exactly what was exactly happening in their experiments [2].

In 1888, an Austrian botanist and chemist, Friedrich Reinitzer synthesized several esters of cholesterol, a natural product occurring in plants and animals. He observed that these compounds at certain temperature changes from the crystalline solid phase to an opaque liquid which transform at a higher temperature to an optically clear liquid. These phases were

reproducible with increasing and decreasing temperature in several compounds. He himself was not able to explain this curious phenomenon of double melting [3]. He sent these samples to Otto Lehmann, who was professor of physics (successor of Heinrich Hertz) at the technical High School of Karlsruhe. Lehmann intuitively argued that the optical anisotropy of these liquids would be due to elongated molecules which are oriented parallel with long axes [4]. Eventually he realized that the cloudy liquid was a new state of matter and coined the name "liquid crystal," illustrating that it was something between a liquid and a solid, sharing important properties of both. Reinitzer is usually called the discoverer of LCs [5]. Up till 1890 all the liquid crystalline substances that had been investigated naturally occurring and it was then that the first synthetic liquid crystal, pazoxyanisole, was produced by Gatterman and Ritschke. Subsequently more liquid crystals were synthesized and it is now possible to produce liquid crystals with specific predetermined material properties. One of the important contributors in the field of liquid crystals was the German chemist Daniel Vorlander, who worked in Halle. He and his coworkers synthesized many new liquid crystalline substances and were the first to observe a single substance that possessed more than one LC phase. Dr. Vorlander in 1908 established his rule that liquid crystalline compounds must have a molecular shape as linear as possible [6, 7]. In 1922 the French scientist G. Friedel produced the first classification scheme of LCs [8], dividing them into three different types of mesogens (materials able to sustain mesophases), based upon the level of order the molecules possessed in the bulk material:

(a) nematic (from the Greek word nematos meaning "thread"),

(b) Smectic (from the Greek word smectos meaning "soap"), and

(c) Cholesteric (better defined as Chiral nematic) [9].

In the 1960s, a French theoretical physicist, Pierre-Gilles de Gennes, who had been working with magnetism and superconductivity, turned his interest to liquid crystals and soon found fascinating analogies between liquid crystals and superconductors as well as magnetic materials. His work was rewarded with the Nobel Prize in Physics 1991. The modern development of liquid crystal science has since been deeply influenced by the work of Pierre-Gilles de Gennes [10].

In 1977, Chandrasekhar and his coworkers in India reported that not only rod-like molecules but also compounds with disc-like molecular shape are able to form LC phases [11]. In 1986, liquid crystals formed by board-like (lath-like) were reported [12]. From the Greek word for board, these phases are called "sanidic". Recently however there has been much interest in the so-called 'banana' phases formed by bent-core molecules [13].

1.4 Classification of Liquid Crystals

There are various ways of classifying liquid crystals [14,15]. The most widely used classification of liquid crystals is into two major categories; (a) *Thermotropic* liquid crystals (Mesophase formation is temperature dependent), and (b) *Lyotropic* liquid crystals (Mesophase formation is solvent and concentration dependent). A*mphotropic* liquid crystal compound displays both thermotropic and lyotropic liquid crystalline phases [16]. Classification of liquid crystals is shown in Figure 1.3.

1.5. Thermotropic Liquid Crystal

For thermotropic LCs, the transition to the liquid crystal state is induced by a purely thermal process. Thermotropic LCs form thermally activated mesogenic phases that extend from the crystal melting temperature, T_m, up to the clearing or isotropic temperature, T_i. If temperature is too high, the rise in energy and therefore in motion of the components will induce a phase

change: the LC will become an isotropic liquid. If, on the contrary, temperature is too low to support a thermotropic LC phase, the LC will become a crystal. The liquid crystallinity of thermotropic LC appears only in a particular temperature range.

Based on the shape of the mesogenic molecules, thermotropic LCs are classified into three main groups: (a) calamitic (rod-like); (b) bent-core (bad rods, boomerang, banana-like), and (c) discotic (disc-like) LCs.

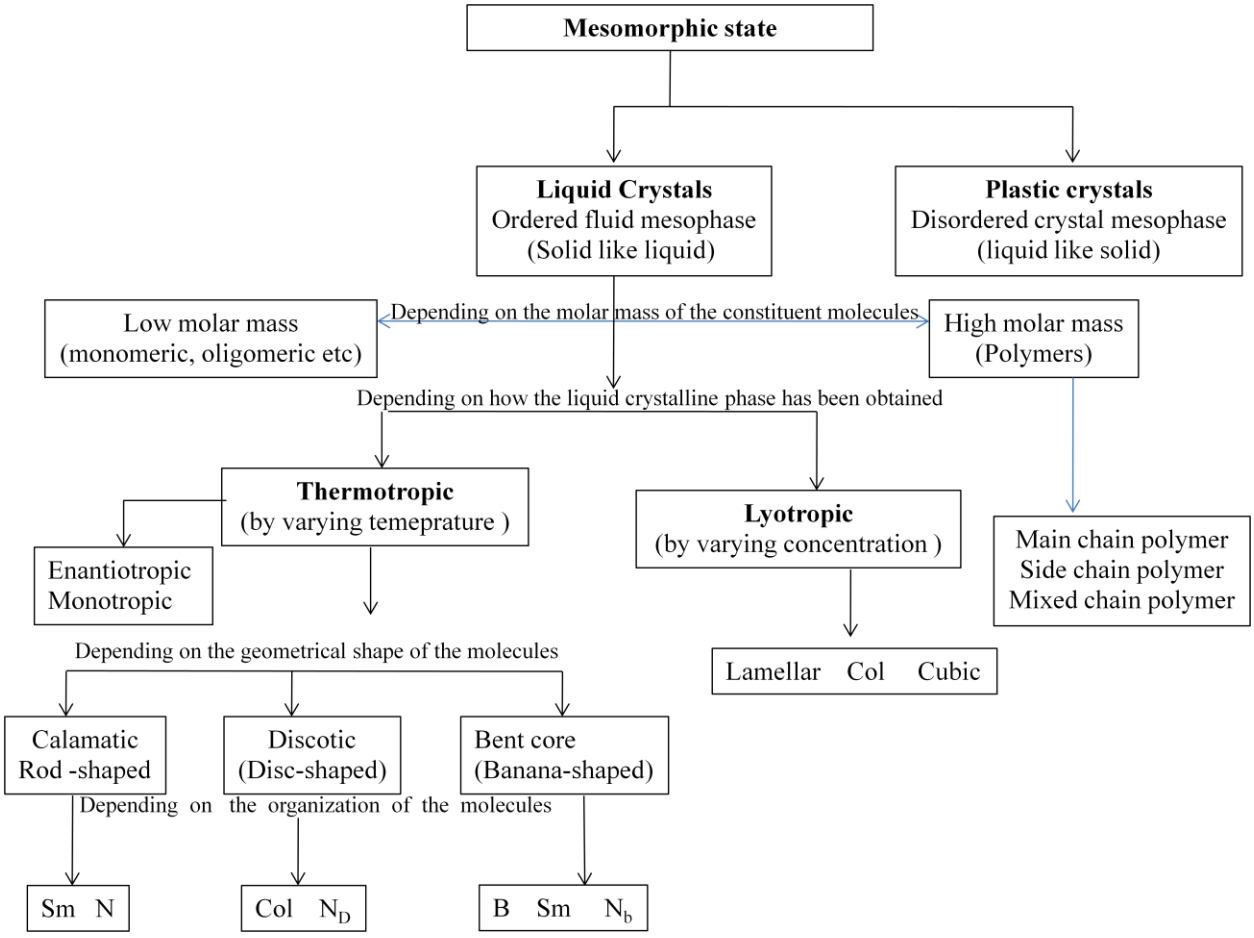

Figure 1. 3 Classification of liquid crystals.

1.6 Calamatic Liquid Crystals

Specifically, for a substance to be a calamitic liquid crystal, its molecules must have an elongated shape, they must have some rigidity in the central region, and their ends should be flexible. The flexibility of the ends of the molecule seems to help the molecule to position itself between the other molecules and ensure the fluidity of the phase.

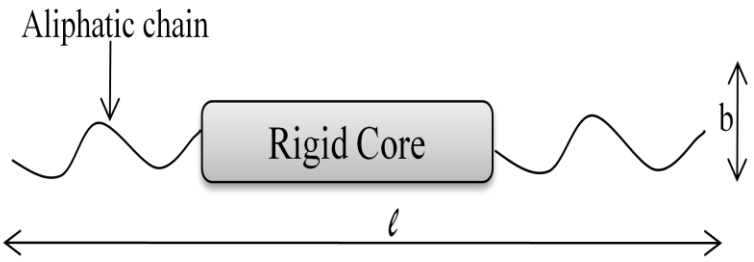

Figure 1.4 Cartoon representation of calamitic LCs, where length(*l*) >> breadth(b).

Calamitic LCs generally exhibit two types of mesophases:

(a) nematic

(b) smectic

1.6.1 Nematic Liquid Crystal Phase

The simplest liquid crystal phase is called the nematic phase (N). It is characterized by a high degree of long range orientational order but no translational order. A schematic diagram of a nematic phase is shown in Fig. 1.5. A uniformly aligned nematic has a preferred direction, often described in terms of a unit vector called the director, n. Viewed under a polarizing microscope, the nematic phase is seen as thread schlieren texture and the defect regions linking these domains appear as dark threads [17].

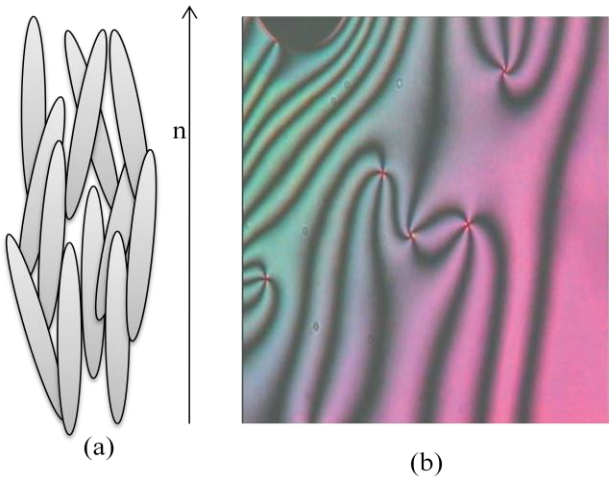

Figure 1.5 (a) Cartoon representation of N phase. (b) Schlieren texture of a nematic phase under planar anchoring conditions [17].

1.6.2 Chiral Nematic Liquid Crystal Phase

When a nematic phase is incorporated with a chiral molecule, it leads to the formation of a structure as a stack of very thin 2-D nematic like layers with the director in each layer twisted with those above and below (as shown in Figure 1.6). In this structure, the directors actually form in a continuous helical pattern about the layer normal. The distance over which the director rotates by 360◦ is called the chiral pitch and is generally of the order of hundreds of nanometres, the wavelength of visible light. Cholesteric phase is also defined as the chiral nematic phase, represented by N*.

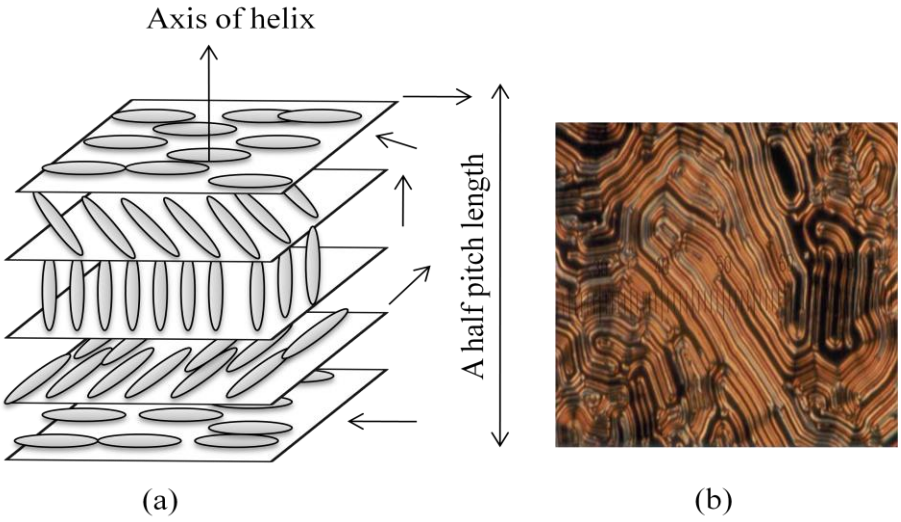

Figure 1.6 (a) Schematic representation of the cholesteric phase. (b) Fingerprint texture of a cholesteric phase [17].

1.6.3 Smectic Liquid Crystal Phase

Smectic liquid crystals have a layered structure as presented in Fig 1.7 (a, b). The position of smectic molecules is correlated in some ordered patterns. The centers of gravity of the elongated molecules are arranged in equidistant layers with well-defined layer spacing or periodicity [18,19]. The smectic phase is denoted by the symbol “Sm”. The long axes of smectic molecules are parallel to a preferred direction that may be normal to the planes (smectic A) or tilted by a certain angle (smectic C). Typical textures of smectic liquid crystals, such as fan-shaped and Schlieren textures, are presented in Fig.1.7 (c and d). A number of different types of smectic liquid crystals are known which differ from each other in the way of layer formation. The increased order means that the smectic state is more "solid-like" than the nematic. Smectic ‑ A, B, C, D, E, F, G, H, I. A number of different classes of smectics have been recognized. However, SmA and SmC mesophases are more commonly encountered.

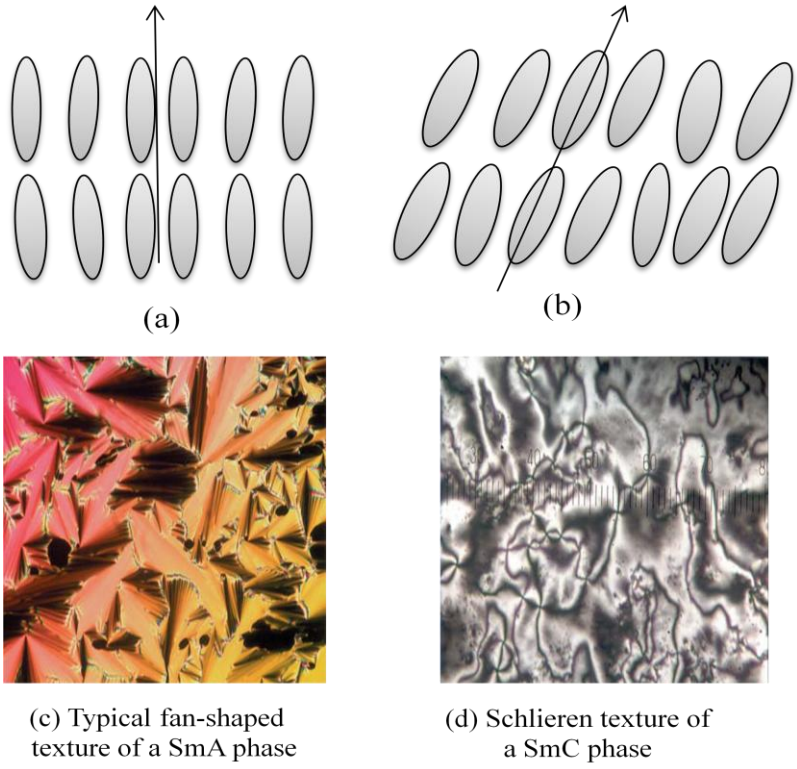

Figure 1.7 (a) Smectic A and (b) Smectic C liquid crystal phases and there respective textures [17].

1.6.4 Smectic C* Liquid Crystal Phase

As in the nematic, the smectic-C mesophase has a chiral state designated C*. Consistent with the smectic-C, the director makes a tilt angle with respect to the smectic layer. The difference is that this angle rotates from layer to layer forming a helix. However, a single layer of the chiral smectic C phase is ferroelectric and so by unwinding the helix (by external forces such as surface interactions), a true ferroelectric phase is generated [20,21]. In the chiral smectic C phase, the molecular chirality in conjunction with molecular tilt makes the smectic layers polar and the polarity can be switched by application of appropriate electric field.

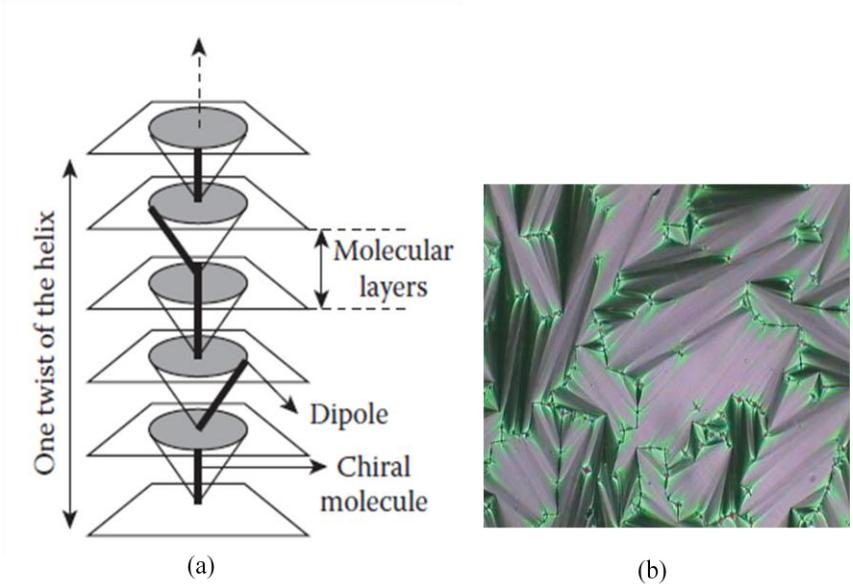

Figure 1.8 (a) Schematic diagram of a SmC* liquid crystal. (b) Fan-shaped textures of the SmC*[17].

1.6.5 Ferroelectric Liquid Crystal Phase

Although the overall polarization of the SmC* phase is zero, each layer in the phase structure has a polarization associated with it. If, therefore the helical structure of the SmC* is unwound, it is possible to generate a polarized phase since the polarization is no longer being cancelled out by the constantly changing direction of polarization vector.

Unwinding the helix of SmC* phase can give rise to three possible sub phases; (i) ferroelectric, (ii) ferrielectric, and (iii) antiferroelectric phase.

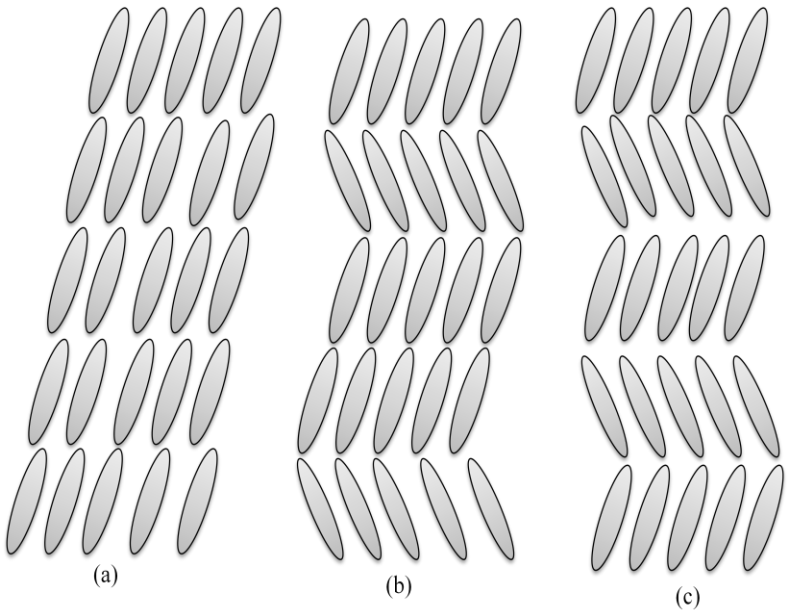

Figure 1.9 Structures of (a) ferro-, (b) ferri-, and anti-ferroelectric SmC* phase.

1.6.6 Bent Core Liquid Crystals

Recently in 1996, it has been recognized that molecules that possess a bent molecular shape can exhibit mesomorphism. To date eight banana phases named B1 through B8 have been discovered and like smectic phases the B nomenclature was derived from the order in which they were discovered. Out of the eight banana phases, the B1 and B2 phases are the most often observed. Bent-shaped molecules provide access to mesophase with polar order and supramolecular chirality despite the mesogens being achiral [22].

1.7 Lyotropic Liquid Crystal Phases

The molecules that make up lyotropic liquid crystals are surfactants consisting of two distinct parts: a polar, often ionic, head and a nonpolar, often hydrocarbon tail. (Not all surfactants, however, form lyotropic liquid crystals.) Following the rule of "like dissolves like," the head is attracted to water, or *hydrophilic*, and the tail is repelled by water, or *hydrophobic*.

Figure 1.10 Schematic diagram of ampliphilic molecule.

A schematic is shown in Figure 1.10. When these are dissolved in an appropriate solvent (having enough high concentration) they self-assemble so that the polar (hydrophilic) heads protect the non-polar (hydrophobic) tails. These structures are known as micelles. At low surfactant concentrations these are roughly spherical. As the surfactant concentration increases then other phases are formed. The micellar phases can also be inversed. Lyotropic liquid crystals are found in countless everyday situations. Soaps and detergents form lyotropic liquid crystals when they combine with water. In the kitchen, cake batters may harbor the liquid crystals as well. Most importantly, biological membranes display lyotropic liquid crystalline behavior.

1.8 Discotic Liquid Crystal

1.8.1 Brief History and Introduction

The origin of LC phases is rooted in molecular geometry. Before 1970's, it was believed that only rod-like structures could give rise to mesomorphism. In September, 1977 S. Chandrasekhar and his colleagues at Raman Research Institute, Bangalore designed and synthesized a number of disc like structure consisted of benzene hexa-*n*-alkanoates and investigated their possible mesomorphism in this novel molecular architecture by thermodynamic, optical, and x-ray studies [22,23].

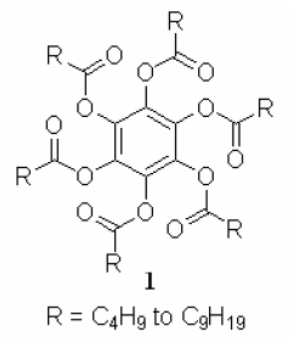

Figure 1.11 Molecular structure of the first series of discotic LCs discovered: the benzenehexa- n-alkanoate derivatives.

A general illustration of disc like molecule is given in Figure 1.12. As can be seen, the molecular diameter (*d*) is much greater than disc thickness (*t*), imparting the form anisotropy to the molecular structure. Disc-shaped molecules orient along their short axis and have tendency to lie on top of each other forming one dimensional stack which further self assemble into two dimensional various lattices (discotic columnar phase), which represents orientational and positional ordering.

DLCs are typically made of a central discotic core substituted by 3–12 saturated chains of three or more carbon atoms. These materials often have two-, three-, four-, or six-fold rotational symmetry. The liquid crystallinity results from the microsegregation of the two constituents: the crystalline character is promoted by the interaction between the conjugated cores while the liquid character originates from the melting of the saturated alkyl chains in the mesophase.

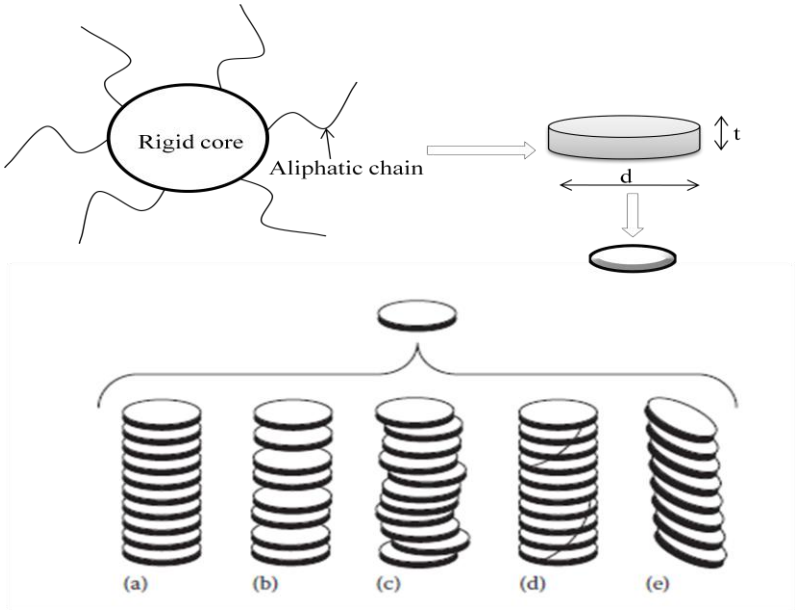

Figure 1.12 Cartoon representation of the general shape of discotic LCs, where d>>t and different kinds of columnar self assembly of discotic mesogens: (a) ordered column, (b) and (c) disordered columns, (d) helical column, and (e) tilted column. These self-assembled columns selforganize into different types of 2D columnar lattices.

By tailoring the shape, size and nature of the central core as well as the type of the attached side chains, compounds with different ability to self-organize into different mesophase morphologies can be synthesized.

1.8.2 Classification of Discotic Liquid Crystal

Just as calamitic molecules can exhibit various types of mesomorphism, discotic molecules can also exhibit various different types of mesomorphism. Mesophases formed by disc-shaped molecules are primarily four types: (1) nematic, (2) smectic, (3) columnar, and (4) cubic. The columnar phase is most commonly observed in discotics followed by nematic phase whereas the other phases are rarely observed. Most of the discotics exhibit only one type of mesophase but a few examples are known to exhibit polymorphism [24].

1.8.3 Nematic Phase of Discotic Mesogens

The nematic phases of disc-shaped mesogens can be sub-divided into three types:

(a) nematic discotic (N_D)

(b) chiral nematic (N_D*) and

(c) nematic columnar (N_{col}).

Nematic discotic (N_D) is the least ordered mesophase, where the molecules have only orientational order being aligned on average with the director. There is no positional order. The nematic phase of disc-shaped molecules is usually not miscible with the nematic phase of rod-like molecules, though they exhibit similar fluid schlieren texture. Unlike the usual rod-shaped nematic, discotic nematic phase is optical negative, the director being the preferred axis of orientation of the disc-normals. Chiral version of this phase have been discovered which just like its calamitic analogue possesses twist to the director, thus generating a helix. The columnar nematic phase (N_{Col}) is characterized by a columnar stacking of the molecules. However these columns do not form 2D lattice structures. They possess positional short-range order and an orientational long-range order.

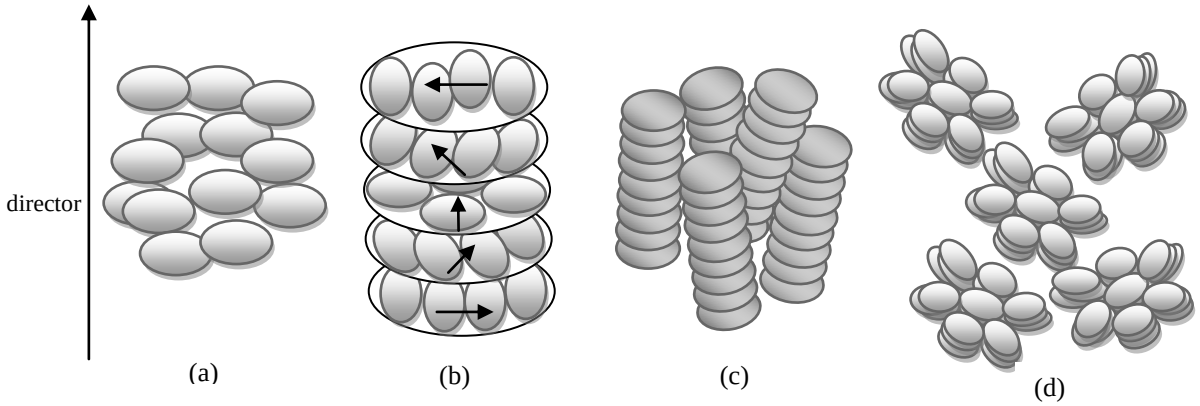

Figure 1.13 Structure of various nematic phases exhibited by discotic mesogens: (a) discotic nematic, (b) chiral nematic, (c) columnar nematic, and (d) nematic lateral.

Recently, another nematic phase has been reported, where the disc-shaped molecules aggregate into large superstructure, and these supramolecular aggregates show a nematic arrangement. The phase is referred to as the nematic lateral phase (N_L) due to the strong lateral interactions [24].

1.8.4 Smectic Phases of Discotic Mesogens

When there is an uneven distribution of the peripheral chains or there is reduced number of peripheral chains, the discotic mesogens exhibit smectic mesophase which is very rare in DLC. Like calamitic smectic mesophases, in discotic smectic mesophases the discs are arranged in a layered manner separated by sub layers of peripheral chains [25]. Since the molecular rotations about their long molecular axes will be restricted in the layers, they are expected to exhibit biaxial smectic phases.

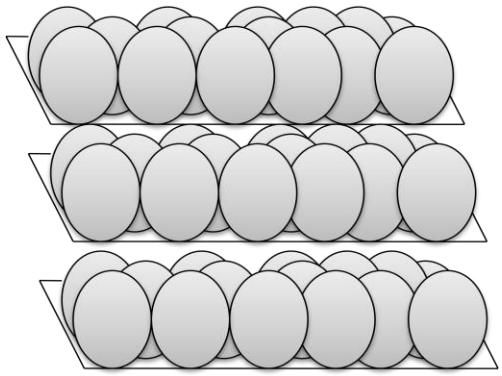

Figure 1.14 Smectic phase of discotic mesogen.

1.8.5 Columnar Phase of Discotic Mesogens

A majority of discotic liquid crystals (DLCs) form columnar mesophases probably due to intense π-π interactions of polyaromatic cores. The core-core separation in a columnar mesophases is usually of the order of 3.5 Å so that there is considerable overlap of π−orbitals and molecules self-assemble one on the top of the other in columns and these so-formed columns self-organize in various 2D lattices (Figure 1.15). The molecules may be arranged in a regular ordered manner or disordered. Depending on the order in the molecular stacking in the columns and two-dimensional lattice symmetry of the column packing the dynamics of the molecules within the columns, the columnar mesophases may be classified in seven classes:

(a) Columnar hexagonal mesophase (Col_h),

(b) Columnar rectangular mesophase (Col_r),

(c) Columnar oblique phase (Col_{ob}),

(d) Columnar plastic phase (Col_p),

(e) Columnar helical phase (H),

(f) Columnar square (tetragonal) phase (Col_{tet}), and

(g) Columnar lamellar phase (Col_L).

1.8.5.1 The Columnar Hexagonal Mesophase (Col_h)

Columnar hexagonal mesophase (Col_h) is probably the most widely observed columnar mesophase. It comprises of several columns of molecules packed in a hexagonal pattern (Figure 1.15 (a)). The most likely reason for the observation of hexagonal columnar mesophase is due to symmetrical shape of the synthesized molecule of discotic mesogen which lead to the most efficient packing for a disc shape molecule which is hexagonal

packing. The basic hexagonal columnar phase structure has singular C_6 axis, six C_2 axes and σ_h mirror plane as symmetry operations (Figure 1.16). Col_h mesophase can be characterized via POM which shows focal conic, fan-shaped, mosaic, and dendritic textures under crossed polarizer. However XRD is must to confirm the phase.

1.8.5.2 The Rectangular Columnar Phase (Col_r)

When the molecules in the columns are tilted with respect to columns axis, columns do not opt for the hexagonal pattern rather they pack in rectangular columnar pattern (Figure 1.15(b)). Since the molecules in the tilted columns that exist in the in rectangular columnar pattern have ability to recognize their required orientation with respect to their neighboring columns [26], they have stronger core-core interaction than that in hexagonal pattern. Crossover from columnar rectangular to hexagonal mesophases has been observed with increasing side-chain lengths. Depending on the mutual orientation of the molecules (ellipses) and the number of columns per unit cell in the lattice, Col_r phases have been divided into three different types. In all three types of molecular organization in Col_r phase liquid like ordering along the columns and the average orientation of the constituent molecules of the column is not necessarily normal to columnar axes. Most commonly broken fan-shaped textures are more common for columnar rectangular mesophase.

1.8.5.3 The Columnar Oblique Mesophase (Col_{ob})

The phase structure of columnar oblique phase (Figure 1.15 (d)) shows the arrangement of tiled (usually) columns in oblique manner with respective to one another. In Col_{ob} phase the average of the plane of the molecules is not necessarily normal to the columnar axes. The Col_{ob} mesophase posses liquid like ordering along the column axes. Very strong core-core interaction between the molecules is required to exhibit the phase. Therefore the Col_{ob} is least

observed in all columnar mesophase. Fan-shaped textures and spiral textures are characteristics for Col_{ob} phase [27].

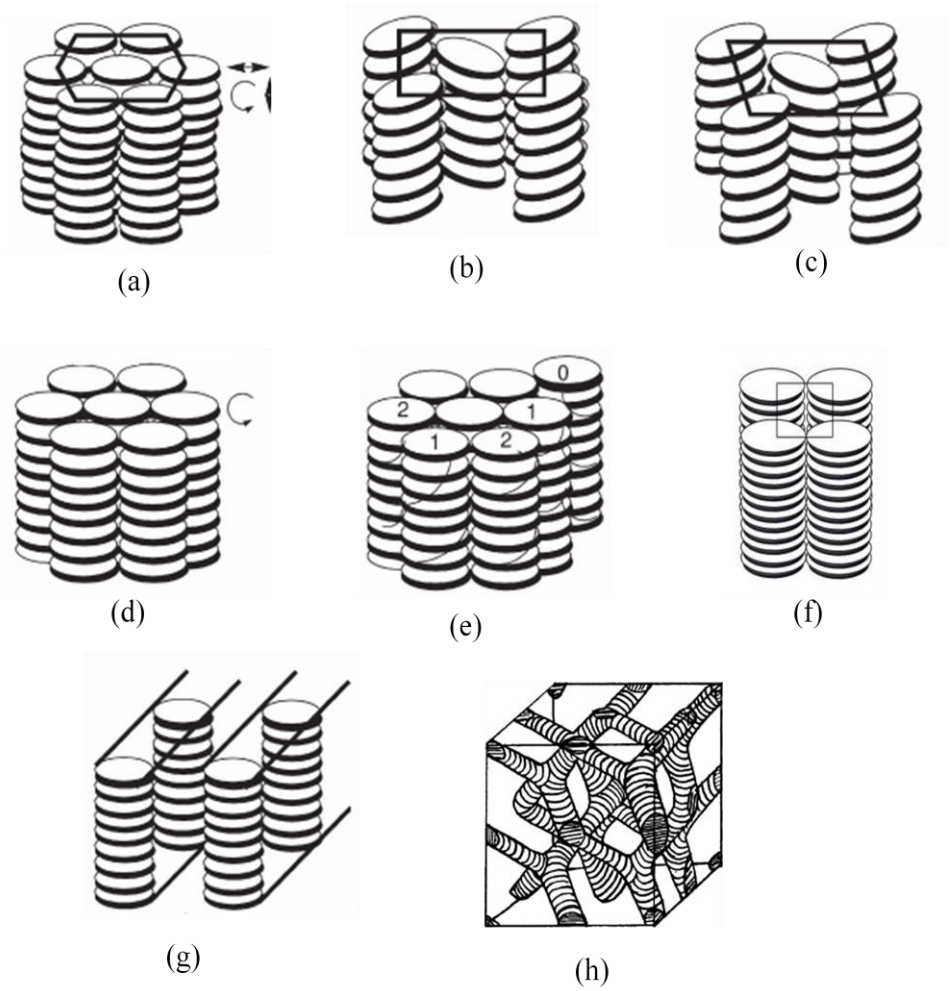

Figure 1.15 Schematic representation of (a) hexagonal columnar phase (b) rectangular columnar phase (c) columnar oblique phase (d) columnar plastic phase (e) helical phase (f) columnar square (tetragonal) phase (Col_{tet}) (g) columnar lamellar phase (Col_L) and (h) cubic phase.

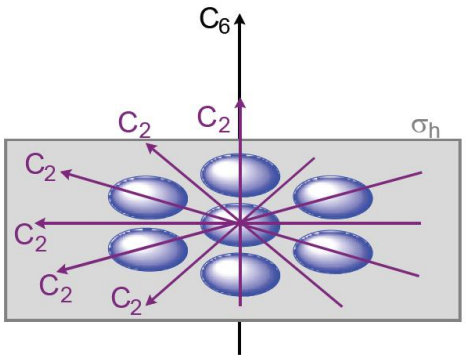

Figure 1. 16 Schematic representation of symmetry operation in Col_h phase.

1.8.5.4 The Columnar Plastic Mesophase (Col_p)

The columnar plastic mesophase (Col_p) [28] phase is characterized by 3D crystal-like order of the center of mass of the molecules but the columns are arranged in a 2D hexagonal lattice, while the discs within the columns are able to rotate about the column axis (Figure 1.15 (d)). It is the presence of the diffuse peak due to the alkyl chains in x-ray diffraction profile that differentiates this phase from a truly crystalline phase. These features point to the fact that the plastic phase has a 3-dimensional positional order with the absence of any sliding motion of one column with respect to its neighbor, a feature characteristic of the Col phase. But the presence of the diffuse peak due to the alkyl chains points to the presence of a rotational degree of freedom for the discs to rotate about the column axis.

1.8.5.5 The Columnar Helical (H) Phase

In The columnar helical (H) phase [29], there is a helicodal stacking of the discotic (usually triphenylene) cores within each column, the helical period being disproportionate with the intermolecular (intracolumnar) spacing. In addition, a three-column superlattice develops as a result of the frustration caused by molecular interdigitation in the group of three columns. In the superlattice, the third column is displaced by half an intracolumnar distance vertically

with respect to the other two columns. Schematic representation of H phase is shown in Figure 1.15 (e).

1.8.5.6 The Columnar Lamellar Mesophase

In this phase discotic molecules stack to form columns and these columns are arranged in layers, where the columns in layers can slide. But the columns in different layers do not possess any positional (translational) correlation. X-ray studies have suggested layered structure. Molecules posses liquid like nature within the layers [30].

1.8.5.7 The Columnar Square (tetragonal) Phase

The columnar square phase otherwise known as the tetragonal phase (Col_{tet}) is shown in Figure 1.15 (g). Here the columns are upright and they are arranged in a square lattice. Like columnar hexagonal phase, this phase also exhibit spontaneous homeotropic alignment of the columns [31].

1. 9 Cubic Phase

Cubic phases are common in lyotropic liquid crystals, however some discotic phthalocyanine derivatives [31c-d] exhibit bicontinuous cubic phase which consist of interwoven but not connected branched columns.

1.10 Identification and Characterization of Discotic Liquid Crystal

There are three basic techniques for identification and characterization of mesophase [24c]:

(a) Polarizing optical microscopy (POM)

(b) Differential scanning calorimetry (DSC)

(c) X-ray diffraction (XRD)

POM is most powerful and first in line technique for identification of mesophase from its characteristic texture and approximate idea of phase transition temperature. DSC is used to determine the temperatures of phase transitions and enthalpy changes related to each transition. DSC thermogram gives an excellent indication of the number of the mesophase and precise measurement of their respective transition temperatures. XRD is the ultimate technique in mesophase morphology identification as it provides accurate and direct information regarding molecular positioning and orientation and makes it possible to determine the precise mesophase at a given temperature. It also provides much deeper insight into the various microstructures adopted in the self assembly of the mesogens in the mesophase.

Solid state NMR is another one of the most powerful tools for the study of the molecular dynamics. This technique allows one to derive independent conclusions about the rotation of the core or about peripheral mobility of side chains.

POM, DSC, and XRD techniques will be discussed in details in chapter 2.

1.11 Alignment of Discotic Liquid Crystal

Alignment of discotic liquid crystal plays very important role and aligned samples are required for various purposes such as to understand the detailed supramolecular order in the columnar phase (ordered, disordered, orthogonal, and tilted arrangement of discs, etc.), to evaluate the electronic properties and charge migration efficiency of the columns and conductivity anisotropy of the columnar phase which are very important for their potential use in electronic devices as organic semiconductors. Discotic molecules can adopt two characteristic orientations, which are required for electronic devices with different geometries.

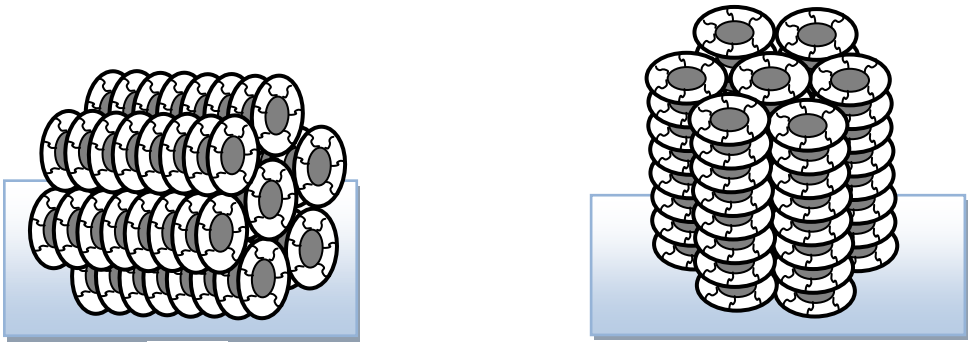

(a) (b)

Figure 1.17 Schematic representation of (a) planar and (b) homeotropic alignment configurations of discotic columnar phases.

1.11.1 Planar Alignment

A uniaxial planar alignment (Figure 1.17 (a)) with the columns parallel to the substrate but with long columnar axes pointing in the same direction is obviously preferable for electronic devices such as field effect transistors (FET). There are number of ways to achieve a uniaxial alignment of columns: Langmuir–Blodgett (LB) films, (SAM: self-assembled monolayer, epitaxial growth method, the zone processing methods, surface treatment, IR radiations, influence of magnetic or electric filed, use of sacrificial layer, etc. Details of these methods are out of the scope of the thesis.

1.11.2 Homeotropic Alignment

The face-on orientation (homeotropic alignment) (Figure 1.17 (b)) of discotic molecules is usually a preferred mode of deposition. The face-on orientation of discotic molecules obtained by slow cooling of the material from the isotropic phase can initiate the formation of homeotropic alignment on a macroscopic scale. The molecules arranged on the surface act

as nucleation sites at which new discs self-assemble in columns. Typically, this process occurs during annealing at the isotropic liquid to mesophase transition where the mesophase viscosity is low.

1.12 Physical Properties of Discotic Liquid Crystal

1.12.1 Electrical Conductivity

Majority of DLCs form columnar mesophase phase due to efficient polyaromatic π-π interactions. The core-core distance along the column direction is usually in the order of 3.5 Å whereas the distances between the centers of cores in adjacent columns is dictated by the size of the mesogens and is typically of the order of 20-40 Å. Flexible alkyl chains around the cores substantially insulate the column from the neighboring column. As a result of the assembly of discotic aromatic mesogens into columnar stacks with typical intercore distances of about 3.5 Å, an overlap of the π*–π* LUMOs (lowest-unoccupied molecular orbitals) should be possible, which would lead to a conduction band for charge transport along the column axis. Conductivity is, therefore, anticipated to be significantly higher along the column axis; therefore, the DLC columns are sometimes referred to as quasi-one-dimensional.

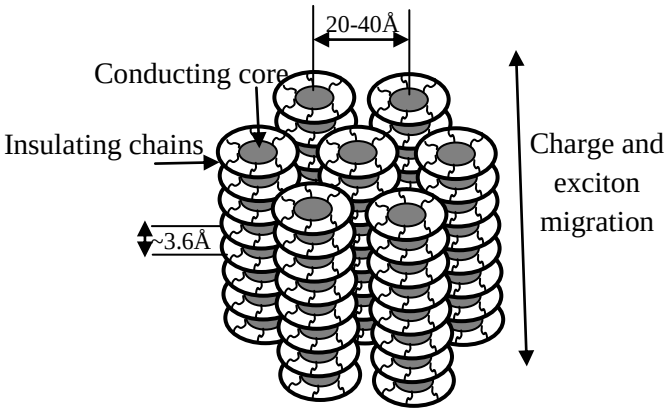

Figure 1.18 Energy and charge migration in discotic liquid crystals.

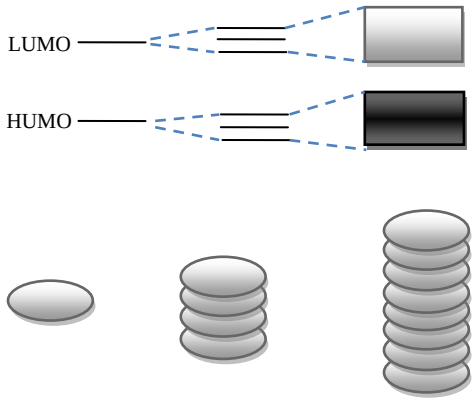

Figure 1. 19 Electronic band formation from a single molecule (left) to the column (right).

For studying charge transport in discotic liquid crystals, the time-of-flight (TOF) technique, which relies on charge photogeneration, is most widely used.

1.12.2 Optical Properties

Liquid crystals (LCs) are optically anisotropic media whose properties, as the name suggests, depend on the direction in the medium. The optical properties of a material can be visualized using a geometrical representation of the dielectric tensor, known as the index ellipsoid. The intercepts of the ellipsoid surface with its three principal axes give the principal refractive indices of the medium. If the system is isotropic, that is, the properties are independent of direction, the index ellipsoid becomes a sphere. The most common liquid-crystalline phases have one optic axis (they are optically uniaxial), with two principal refractive indices n_o and n_e (the ordinary and the extraordinary refractive index, respectively). The index ellipsoid in this case is an ellipsoid of revolution. Moreover, liquid crystals are most often uniaxial positive, which indicates that the value of n_o (the refractive index of the light propagating along the optic axis) is lower than that of n_e (the refractive index of the light propagating perpendicular, but with polarization parallel, to the optic axis). Many discotic LC phases, like the nematic and the columnar phases, are optically uniaxial, but with negative anisotropy,

that is, $n_o > n_e$, which makes the index ellipsoid oblate (Figure 1.20). This property has been fundamental for the application of discotic films as optical compensators for LC displays. The magnitude of the optical anisotropy $\Delta n = n_{\parallel} - n_{\perp}$ is generally lower for discotics than calamitics. Experimental values are scarce, but some reports

give values in the range of -0.08 to -0.04 [32].

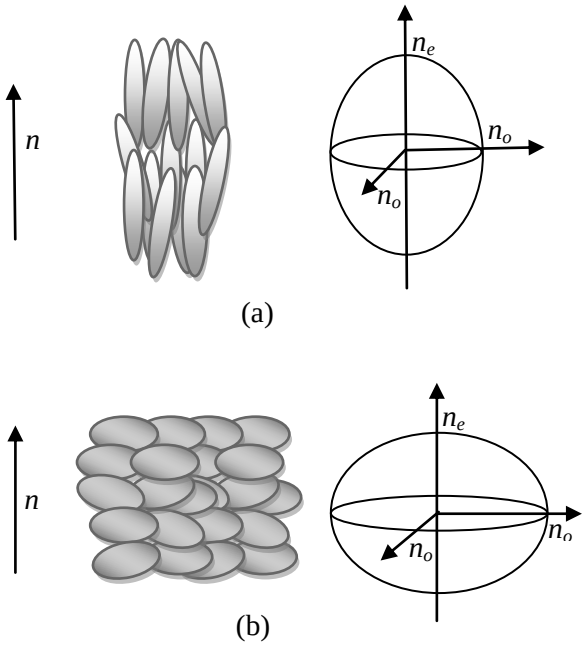

Figure 1.20 Index ellipsoids for (a) uniaxial positive ($n_e > n_o$) and (b) negative ($n_e < n_o$) liquid crystals.

1.12.3 Dielectric Properties

Another physical property that is crucially affected by the anisotropic nature of liquid crystals is the dielectric permittivity (ε). The dielectric permittivity of a compound is a measure of interaction of a permanent or induced electrical dipole of the compound with an electrical field, thus compounds which contain groups which induce strong dipoles, such as

cyano or fluoro substituent, will interact strongly with an applied electric field. The anisotropic nature of liquid crystalline materials means that the permittivity of a compound will be different when measured perpendicular or parallel to the director. Thus the dielectric anisotropy is calculated as $\Delta\varepsilon=\varepsilon_{\parallel}-\varepsilon_{\perp}$. Dielectric anisotropy $\Delta\varepsilon$ of columnar mesophase is generally positive. $\Delta\varepsilon$ shows a surprising high value, comparable to those found for nematic and smectic liquid crystals with strong permanent dipolar moments [33].

The dielectric anisotropy of a material is highly important for display devices, where the ability to switch the orientation of a molecule and to do so at high speed when an electrical field is applied, is essential. Thus, large magnitudes (either positive or negative depending on the application) of $\Delta\varepsilon$ are extremely important.

Measurements of the real part ε' and imaginary part ε'' of the dielectric susceptibility has given us valuable insight into the mechanisms of dipolar relaxation and thermal dipolar production of discotic liquid crystal materials. Details of dielectric spectroscopy will be discussed in chapter 2.

1.12.4 Electro-optical Properties

In contrast to calamitic LCs, columnar LCs cannot be used as switching units [34,35]. This is mainly due to the fact that these disc-shaped molecules do not have a central dipole moment, typically have a much higher viscosity than rod-shaped molecules of similar molecular weight, and are therefore difficult to orient by an electric field. Even if switching is possible, that is, reorientation of the bulk sample, switching times are too slow as compared to the corresponding nematic or smectic compounds. However, this does not mean that columnar mesogens are completely useless for display applications. They are used as optical compensating films in LCDs as discussed in section 1.14.1.

1.13 Features That Work Towards Practical Device Applications

DLCs may form efficient π-π columnar stacks that produce high charge-carrier mobilities, the magnitude of which is fundamentally determined by the degree of order and π-π molecular orbital overlap within the columnar stacks. Charge transport within the stack, i.e., in a one-dimensional manner, is therefore built into the design scheme. The structure of the conjugated core of the discoid materials govern their molecular-level electronic properties, whereas the change in the peripheral flexible chains and aromatic cores control their self-assembly in both solution and bulk phase; the overall electronic properties of the materials, therefore, depend on both core and substituent structure.

The ease of film formation is another key feature of smart materials for organic-based electronic and optoelectronic devices. Because some DLCs have a predisposition to self-assemble into columnar stacks, ease of processability is inherent, although orientation of the columnar stacks in the direction required for the device function can be challenging. Furthermore, because of their liquid-character, DLCs possess the capacity to self-heal structural defects such as grain boundaries and consequently have the ability of attaining several square millimeters large single domains of several micrometers film thickness. The advantageous properties of DLCs, therefore, include long-range self-assembling (order), self-healing (dynamics), ease of processing, high solubility in organic solvents, and high charge-carrier mobility. For high performance devices these properties play very crucial role e.g. the charge carrier mobility ultimately controls the switching speed of the field-effect transistor, the intensity of the light emitting diode, and the separation of charges in photovoltaic cells.

1.14 Applications of Discotic Liquid Crystal

1.14.1 Optical Compensating Film

In previous years of liquid crystal displays a persistent problem of 'angle of view' was always faced [36]. The brightness, contrast, and sharpness of focus are only optimal when the display is viewed at a certain angle. Furthermore an image inversion is observed because of the positive birefringence of the liquid-crystal layer. The loss of image quality when viewed off-centre is intrinsic to uncompensated liquid crystal displays because oriented liquid crystal films are optically birefringent. However, because the sign of the optical birefringence for calamitic liquid crystals is positive and that for discotic liquid crystals is negative the birefringence of a calamitic display can effectively be cancelled by adding a layer of discotic, as shown in Figure 1.21. In a compensated display based on this principle, only the calamitic layer needs to be 'switchable'; it is only the birefringence of the 'on' state of the calamitic that needs to be compensated so a passive (non-switchable) compensating layer is all that is required. However, the problem of compensating the optics of real displays is a little more complex.

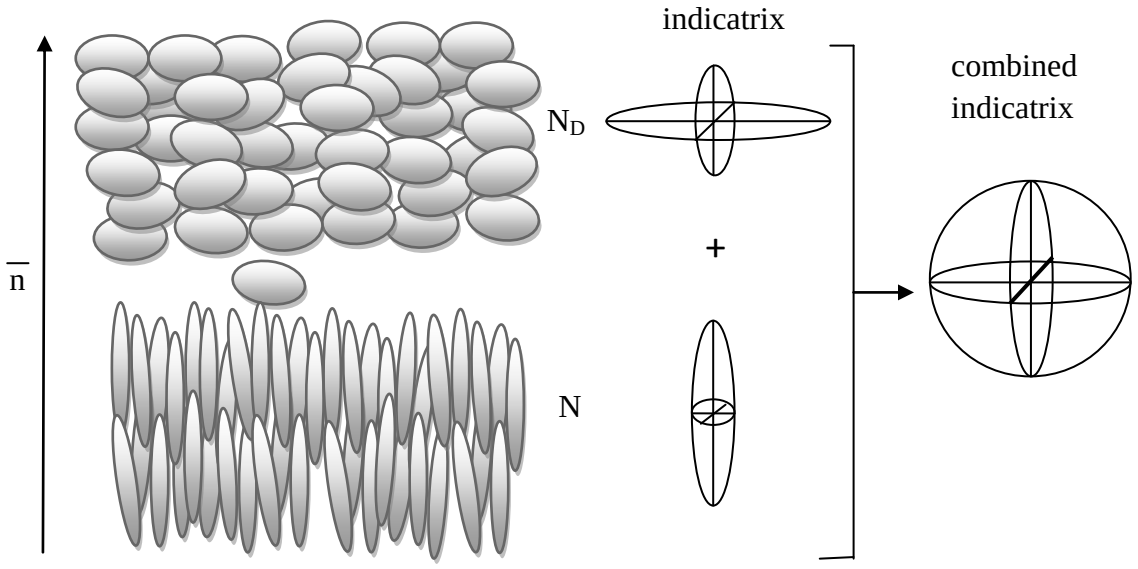

Figure 1.21. How, when the directors n are aligned, the optical birefringence (represented by the indicatrix), of the N phase of a calamitic liquid crystal can be cancelled by a film of the ND phase of a discotic liquid crystal.

Fuji has recently commercialized an optical phase compensation film using a triphenylene-based crosslinked polymer to overcome these problems.

1.14.2 Discotics in Xerographic Processes

To achieve a high contrast potential for image development, the photoreceptor must be an insulator or have low conductivity in the dark and become conductive on exposure to light. A highly sensitive photoconductor not only requires less energy to generate the electrostatic image, but also increases the speed of the Xerox process. Thus, photosensitivity and dark conductivity of a certain material must be assessed. In addition, the lifetime and processibility of the material must be considered. While copier applications require that the photoconductor is sensitive in the visible region, the corresponding photoconducting materials of laser printers are sensitive in the IR Region. Classes of compounds which are particularly well studied for photoconducting devices that operate in the visible region are the perylene bisimides such as compound. On the other hand phthalocyanines have a strong absorption both in the visible and near infrared region. Eichhorn *et al.* discovered that mixtures, which contained amphotropic phthalocyanines with a different substitution pattern, display much higher inter- and intracolumnar order than the single compounds [37]. In addition, macroscopic homeotropic alignment was simply achieved by mechanical shearing, thus providing an easy way to orient the material for laser printers.

1.14.3 Discotics in Organic Light-Emitting Diodes

An OLED is a device, in which light is generated by electrical excitation. In a single layer OLED, a thin film of an organic emitter is sandwiched between a transparent anode (ITO) and a metallic cathode. A multilayer device consists of separate hole-transporting layer, emitter layer and electron transporting layer. For OLED applications, columnar perylene derivatives have been successfully used. The research groups of Kitzerow and Bock [38] described an all-columnar bilayer OLED that consisted of fluorescent columnar 3,4,9,10-tetra(alkoxycarbonyl)perylenes as the luminescent electron transport layer combined with columnar hexaalkoxytriphenylenes as the hole transport layer. A particular advantage of columnar LCs in such devices is their ability to expel defects in an annealing process which leads to increased lifetimes

1.14.4 Discotics in Organic Field–effect Transistors

The self-assembly properties of columnar LCs, in combination with their ability to provide anisotropic charge-carrier transport along the channel, makes them viable candidates for OFETs. A typical OFET device is shown in Figure 1.22. For a p-type semiconductor, conduction of charge between the source and the drain electrodes is governed by the gate voltage. When the gate is biased negatively, carriers accumulate in the channel between source and drain. The drain current is then proportional to the material mobility. The extraordinary hole mobility for aligned hexa *peri*-hexabenzocoronene (μ = 0.5-1.0 X 10 -3 $cm^2V^{-1}S^{-1}$) films on oriented PTFE has been used by the research group of Mullen [39]. The solution processibility, uniaxial parallel orientation and promising material and device stability under ambient conditions pave the way to the industrial production of these OFETs.

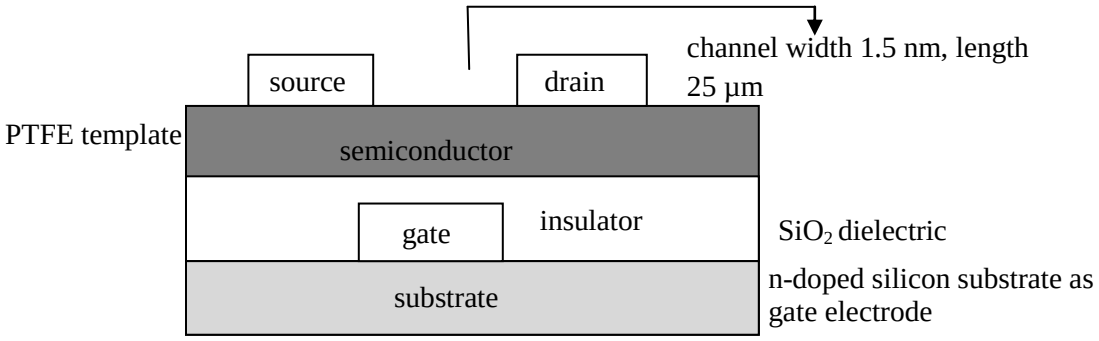

Figure 1.22 Schematic representation of an organic field effect transistor.

1.14.5 Discotic Liquid Crystals as Photosynthetic Light Harvesting Materials

The photovoltaic effect requires (a) the absorption of solar radiation and the photogeneration of electrons and holes, and (b) the charge separation, and the transport of electrons and holes for collection at the cathode and anode, respectively. The photosensitivity of semiconducting organic materials can be enhanced by blending donor and acceptor molecules to optimize photoinduced charge separation. Gregg *et al*. studied photovoltaic effects in symmetrical cells filled with discotic liquid crystalline porphyrin complexes [40]. Photovoltaic effect comparable with that of some of the better organic solar cells was found. However, the authors did not study the charge mobility in the mesophases itself but utilized the liquid crystalline properties to fill the cells and to promote macroscopic order, which on cooling, forms polycrystalline films. Schmit-Mende *et al*. utilized discotic liquid crystalline hexabenzocoronene as the hole transporting layer and a perylene dye to construct a p/n type photovoltaic solar cell [41]. Mullen and coworkers have shown in a seminal contribution [41, 42] that thin film prepared by self-organization of a mixture of columnar LC and crystalline-conjugated materials directly from a xylene solution showed a photovoltaic response with external quantum efficiencies greater than 34% at 490 nm and power efficiencies up to 2%.

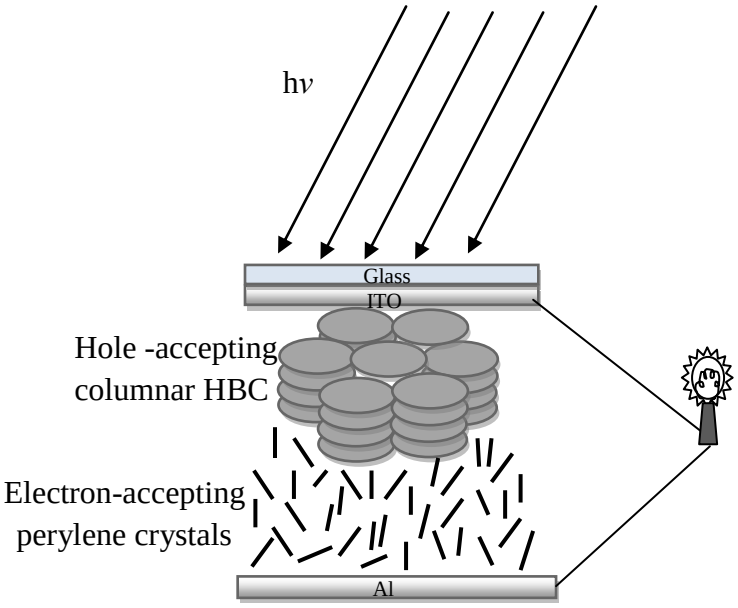

Figure 1.23 Schematic diagram of a discotic-based photovoltaic solar cell.

1.14.6 Discotics as Gas Sensors

In discotics, there are more degrees of freedom at the surface which encourage disorder in the stacks. When a lateral field is applied to a homeotropic film, conduction is likely to be dominated by that of the disordered surface since in the bulk it would be perpendicular to the columns. If the fluctuation and thermodynamics of liquid crystal surfaces are influenced by exposer to gases the response could be simply and cheaply measured by looking at the conductance change giving a simple gas sensor. Structural changes do not require strong electronic coupling or charge transfer reactions to surface states, so sensor built on these principles could also work for detecting weakly interacting non-polar gases. The adsorbate produces a change in the order of the surface and this in turn changes the conductivity. This is relatively easy to measure. Furthermore, self-organized molecular dynamics prefer to keep charge and uncharged impurities near the free surface of the liquid crystals. Discotic liquid

crystals can therefore be used as very sensitive gas sensors for both polar and non-polar molecules [43].

Also, the facile formation of ordered columnar superstructures from the discotic molecules in the bulk state and their high stability in the mesophase qualify them as precursors toward novel carbon nanostructures. Pyrolysis of well-defined discotic molecules in the bulk state produces novel carbon nano and microstructures [44].

1.15 Aim of This Research Work

The field of the discotic liquid crystals is in exploratory stages, although, more than 3000 discotic liquid crystals have been synthesized. The possibility to tune the properties by simple mixing with each other liquid crystalline or non-liquid crystalline materials and metal/non-metal nanoparticles seems very interesting and has opened new horizons in area of liquid crystal research. The incorporation of nanomaterials in the supramolecular order of the columnar phase forming discotic liquid crystals would provide materials that possess the properties of the nanomaterial as well as the processing, handling and self-assembling properties of DLCs. Because of the unique properties of DLC and nanomaterials, the electrical and optical properties of DLC composites are unique and contribute for the understanding their fundamental aspects. Our attempt was on understanding the science behind the dispersed discotic liquid crystal composite systems as studied by their electrical and optical behavior. Electrical properties such as electrical conductivity and dependence of dielectric permittivity on applied electric field, frequency and temperature were investigated. Polarized Optical Microscopy (POM), UV-visible spectroscopy, and IR- dichroic technique allowed us to detect and analyze liquid crystalline optical properties throughout a material.

The purpose of exploring these parameters is that these parameters are very crucial for understanding and optimizing the performance of liquid crystal devices.

References

[1] P. J. Collings, *Nature's delicate Phase of Matter*, Princeton University Press, (1990).

[2] W. J. Heintz, *Prakt. Chem*. 66, 1–51, (1855).

[3] F. Reinitzer, *Wiener Monatsh. Chem.*, 9, 421, (1888).

[4] F. Reinitzer, *Liq. Cryst.*, 5, 7, (1989).

[5] T. J. Sluckin, D. A. Dunmur, and H. Stegemeyer. Crystals That Flow: Classic Papers from the History of Liquid Crystals, *Taylor & Francis*, London, U.K., (2004).

[6] W. J. Heintz, *Prakt. Chem*. 66, 1–51, (1855).

[7] D. Vorlander, *Kristallinisch-Flussige Substanzen,* Enke, Stuttgart, Germany, (1905).

[8] G. Friedel, *Ann. Physique*, 18, 273, (1922).

[9] H. Sackmann, *Liq. Cryst.*, 5, 43-55 (1989).

[10] P. G. de Gennes and J. Prost, *The Physics of Liquid Crystals*, 2nd ed. Oxford University Prss, New York (1993).

[11] S. Chandrasekhar, B. K. Sadashiva and K. A. Suresh, *Pramana*, 9, 471, (1977).

[12] O. H. Schönherr, J. H. Wendorff, H. Ringsdorf, Peter Tschirner, Makromol. *Chem. Rap. Commu*., 7, 791, (1986).

[13] T. Niori, T. Sekine, J. Watanabe, T. Furukawa, H. Takazoe, *J. Mater. Chem*., 6, 1231, (1996).

[14] P. G. de Gennes, *Physics of Liquid Crystals*,Oxford, (1976).

[15] Shri Singh, *Liquid Crystals: Fundamentals*, World Scientific, Science, (2002)

[16] C. Tschierske, *Curr. Opin. Colloid Interface Sci*. 7, 355–370, (2002).

[17] I. Dierking, *Textures of Liquid Crystals*, Wiley-VCH,Technology & Engineering, (2003).

[18] G. W. Gray, J. W. Goodby, Smectic *Liquid Crystals: Textures and Structures*, Leonard Hill, Glasgow, U.K., (1984).

[19] J. P. F. Lagerwall, and F. Giesselmann, F. *ChemPhysChem* 7, 20–45, (2006).

[20] S. T. Lagerwall, *Ferroelectric and Antiferroelectric Liquid Crystals*, Wiley-VCH, Weinheim, Germany, (1999).

[21] I. Musevic, R. Blinc, B. Zeks, *The Physics of Ferroelectric and Antiferroelectric Liquid Crystals*, World Scientific, Singapore, (2000).

[22] S. Kumar, *Chemistry of Discotic Liquid Crystals: From Monomers to Polymers*, CRC Press, Boca Raton, FL, (2011).

[23] S. Chandrasekhar, B. K. Sadashiva, K. A. Suresh, N. V. Madhusudana, S. Kumar, R. Shashidhar, G. Venkatesh, *Journal de Physique*, 1979, 40, C3-120. Proceedings of the 7th international liquid crystal conference held in 1978 at Bordeaux, (1979).

[24] (a) S. Kumar, *Chem. Soc. Rev*., 35, 83, (2006); (b) T. Kato, T. Yasuda, Y. Kamikawa and M. Yoshio, *Chem. Commun*., 729, (2009); (c) S. Laschat, A. Baro, N. Steinke, F. Giesselmann, C. Hagele, G. Scalia, R. Judele, E. Kapatsina, S. Sauer, A. Schreivogel, M. Tosoni, *Angew. Chem. Int. Ed.*, 46, 4832, (2007); (d) S. Sergeyev, W. Pisula, Y. H. Geerts, *Chem. Soc. Rev*., 36, 1902, (2007); (e) J. Wu, W. Pisula, K. Mullen, *Chem. Rev*., 107, 718, (2007); (f) Y. Shimizu, K. Oikawa, K. Nakayama, D. Guillon, J. Mater. Chem., 17, 4223, (2007); (g) N. Boden, R. J. Bushby, J. Clements, B. Movaghar, *J. Mater. Chem*., 9, 2081, (1999); (h) R. J. Bushby, O. R. Lozman, *Curr. Opin. Solid State Mater. Sci.*, 6, 569, (2002);

(i) R. J. Bushby, O. R. Lozman, *Curr. Opin. Colloid Interface Sci*., 7, 343, (2002); (j) H. Takezoe, K. Kishikawa, E. Gorecka, *J. Mater. Chem*., 16, 2412, (2006); (k) K. Ohta, K. Hatsusaka, M. Sugibayashi, M. Ariyoshi, K. Ban, F. Maeda, R. Naito, K. Nishizawa, A. M. van de Craats, J. M. Warman, *Mol. Cryst. Liq. Cryst*., 397, 25, (2003); (l) P. H. J. Kouwer, W. F. Jager, W. J. Misj and S. J. Picken, *Macromolecules*, 34, 7582, (2001); (m) S. Chandrasekhar, *Liq. Cryst*., 14, 3, (1993); (n) S. Chandrasekhar and G. S. Ranganath, Rep. *Prog. Phys*., 53, 57, (1990).

[25] (a) D. W. Bruce, D. A. Dunmur, L. S. Santa, and M. A. Wali, *J. Mater. Chem*., 2, 363, (1992); (b) B. Alameddine, O. F. Aebischer, W. Amrein, B. Donnio, R. Deschenaux, D. Guillon, C. Savary, D. Scanu, O. Schidegger, T. A. Jenny, *Chem. Mater*., 17, 4798, (2005).

[26] (a) A. M. Levelut, *J. Chem. Phys*., 80, 149, (1983); (b) F. C. Frank, S. Chandrasekhar, *J. Phys*., 41, 1285, (1980).

[27] (a) C. Destrade, P. Foucher, H. Esparoux, H. T. Nguyen, A. M. Levelut, J. Malthete, *Mol. Cryst. Liq. Cryst.*, 106, 121, (1984); (b) F. Morale, R.W. Date, D. Guillon, D. W. Bruce, R. L. Finn, C. Wilson, A. J. Black, M. Schroder, B. Donnio, *Chem. Eur. J.*, 9, 2484, (2003).

[28] B. Glusen, W. Heitz, A. Kettner, J. H. Wendorff, *Liq. Cryst*., 20, 627, (1996).

[29] (a) E. Fontes, P. A. Heiney, W. H. De Jeu, *Phys. Rev. Lett.*, 61, 1202, (1988) ; (b) P. A. Heiney, E. Fontes, W. H. De Jeu, A. Riera, P. Carroll, A. B. Smith III, *J. Phys. France*, 50, 461, (1989).

[30] (a) K. Ohta, H. Muroki, A. Takagi, K. I. Hatada, H. Ema, I. Yamamoto, K. Matsuzaki, *Mol. Cryst. Liq. Cryst*., 140, 131, (1986); (b) H. Sakashita, A. Nishitani, Y. Sumiya, H. Terauchi, K. Ohta, I. Yamamoto, *Mol. Cryst. Liq. Cryst*., 163, 211, (1988).

[31] T. Vlad-Bubulak, J. Buchs, A. Kohlmeier, M. Bruma, and D. Janietz, *Chem. Mater*., 19, 4460, (2007); (b) K. Ohta, T. Watanabe, H. Hasebe, Y. Morizumi, T. Fujimoto, I. Yamamoto, *Mol. Cryst. Liq. Cryst.*, 196, 13, (1991); (c) K. Hatsusaka, K. Ohta, I. Yamamoto, H. Shirai, *J. Mater. Chem*., 11, 423, (2001); (d) M. Ichihara, A. Suzuki, K. Hatsusaka and K. Ohta, *Liq. Cryst*., 34, 555, (2007); (e) K. Praefcke, P. Marquard, B. Kohne, W. Stephan, A. -M. Levelut, E. Watchtel, *Mol. Cryst. Liq. Cryst*., 203, 149, (1991).

[32] T. J. Philips, J.-C. Jones, *Liq. Cryst*., 16, 805 – 812 (1994).

[33] Zoulikha Belarbit , *The Journal of Physical Chemistry*, 94, 19, 7334-36 (1990).

[34] (a) N. Boden, B. Movaghar in *Handbook of Liquid Crystals*, Vol. 2B (Eds.: D. Demus, J. Goodby, G.W. Gray, H.-W. Spiess, V. Vill), Wiley-VCH, Weinheim, pp. 781 – 798 (1998); b) N. Boden, R. J. Bushby, J. Clements, B. Movaghar, *J. Mater. Chem*., 9, 2081 – 2086 (1999).

[35] Reviews: (a) C. Borchard-Tuch, *Chem. Unserer Zeit* 2004, 38, 58 – 59; b) K. Blankenbach, *Phys. Bl*., 55, 33 – 38 (1999); c) I. C. Sage in *Handbook of Liquid Crystals*, Vol. 1 (Eds.: D. Demus, J. Goodby, G.W. Gray, H.-W. Spiess, V. Vill), Wiley-VCH, Weinheim, pp. 731 – 762 (1998); d) T. Sergan, J. Kelly, O. Yaroshchuk, L.-C. Chien, *Mol. Cryst. Liq. Cryst.*, 409, 153 – 162 (2004).

[36] S.H. Lee, Y. Kim , Y. H. Lee, I. C. Park, B. G. Rho, H. G. Galabova, D. W. AllenderW. *Appl. Phys. Lett.* 73, 470, (1998).

[37] H. Eichhorn, D. W. Bruce, D. Wohrle, *Adv. Mater*., 10, 419, (1998).

[38] (a) S. Benning, H. –S. Kitzerow, H. Bock, M. –F. Achard, *Liq. Cryst*., 27, 901, (2000); (b) T. Hassheider, S. A. Benning, H. –S. Kitzerow, M. –F. Achard, H. Bock, *Angew. Chem.*, 113, 2119, (2001); (c) I. Seguy, P. Destruel, H. Bock, *Synth. Met*., 111, 15, (2000).

[39] W. Pisula, A. Menon, M. Stepputat, I. Lieberwirth, U. Kolb, A. Tracz, H. Sirringhaus, T. Pakula and K. Mullen, *Adv. Mater*, 17, 684, (2005).

[40] B. A. Gregg, M. A. Fox, A. J. Bard, *J. Phys. Chem*., 94, 1586, (1990).

[41] L. Schmidt-Mende, A. Fechtenkotter, K. Mullen, E. Moons, R. H. Friend, J. D. Mackenzie, *Science*, 293, 1119, (2001).

[42] (a) J. Jung, A. Rybak, A. Slazak, S. Bialecki, P. Miskiewicz, I. Glowacki, J. Ulanski, S. Rosselli, A. Yasuda, G. Nelles, Z. Tomovic, M. D. Watson and K. Mullen, *Synth. Met*., 155, 150, (2005) ; (b) J. P. Schmidtke, R. H. Friend, M. Kastler and K. Mullen, *J. Chem. Phys*., 124, 174704, (2006).

[43] (a) J. Clements, N. Boden, T. Gibson, R. Chandler, J. Hulbert and E. A. Ruck- Keene, Sens. Actuators, 47, 37, (1998); (b) N. Boden, R. J. Bushby and A. N. Cammidge, *J. Am. Chem. Soc*., 117, 924, (1995).

[44]. (a) L. Zhi, J. Wu, J. Li, U. Kolb and K. Mullen, *Angew. Chem. Int. Ed*., 44, 2120, (2005); (b) J. Wu, B. E. Hamaoui, J. Li, L. Zhi, U. Kolb and K. Mullen, *Small*, 1, 210, (2005); (c) L. Gherghe, C. Kubel, G. Lieser, H. -J. Rader and K. Mullen, *J. Am. Chem. Soc*., 124, 13130, (2002).

Chapter 2

Materials and Experimental Techniques

Abstract: This chapter provides information regarding the materials used in the present work. Also, it includes various characterization techniques employed for the study of discotic liquid crystal composite systems. The introduction, theory, and instrumentation of each characterization technique have been described in detail.

2.1 Selection of Discotic Liquid Crystal

To study electrical and optical properties of pure and dispersed DLC composite systems we have choosen “monomeric discotic liquid crystals” composed of anthraquinone (AQ) and triphenylene (TP) core. The majority of discotic liquid crystals belong to the class of monomeric DLCs. After the discovery of the first discotic liquid crystals derived from benzene core, most efforts are toward understanding the nature of the molecular parameters that favor the formation of discotic liquid crystals and control their transition temperatures. Accordingly, a large number of monomeric discotic liquid crystals have been designed, synthesized, and studied for their mesomorphism and to comprehend the chemical structure–physical property relationships. To date, the number of discotic liquid crystals derived from more than 60 different cores comes to about 3000. In next sections a general introduction of the AQ, TP and some other cores which are important from potential application point of view is given.

2.2 Triphenylene Core

The most studied core system in the field of DLCs is triphenylene (TP). TP is symmetrical fused aromatic hydrocarbon. It is known in the chemistry literature since more than a century. Schultz isolated this compound from the pyrolytic products of benzene and gave the name triphenylene [1]. It can be easily isolated from coal tar. Triphenylene as a novel core for DLCs was recognized by the French group in 1978 [2,3] just after a few months of the discovery of mesomorphism in disc-shaped molecules. Since then triphenylene has remained centre of attraction for liquid crystal scientists around the world. There are number of reasons; (a) its derivatives are thermally and chemically stable, (b) their chemistry is fairly accessible, (c) they show a variety of mesophases, and (d) their one-dimensional charge and

energy migration properties [4,5]. These properties offer tremendous potential applications. Many research groups are active in the synthesis of a variety of triphenylene-based DLCs. In addition to their importance as DLCs, triphenylene derivatives have also been recognized as interesting materials for molecular scale devices [5–9], molecular receptors [10–14], etc. More than 500 monomeric triphenylene derivatives have been prepared to investigate their mesomorphic properties.

2.3 Anthraquinone Core

Anthraquinone is one of the most widely occurring compounds in nature and are critical components to the development of a variety applications, such as the dye industry [15], drug synthesis [16], and organic materials [17,18]. Chemically related quinines are key components of both respiration and photosynthesis because of their inherent proton-coupled redox properties. A number of anthraquinone derivatives have been exploited extensively as eco-friendly natural colorants in food, cosmetics, and textiles [19,20], as dichroic dyes in host–guest displays [21], chemical sensors [22], organogelators [23], and anticancer drugs [24]. There are numerous reports of DLCs that are based on the AQ core. The 1,2,3,5,6,7-hexahydroxy-9,10-anthraquinone, commonly known as rufigallol, is one of the first compounds to be synthesized in the history of organic compounds by Robiquet in 1836 [25] and is a molecule of both biological and materials science interest. Rufigallol has been reported as a novel oxidant drug [26–28]. A remarkable synergistic antimalarial interaction between rufigallol and the structurally similar compound exifone has been described. It is believed that rufigallol acts in pro-oxidant fashion to produce oxygen radicals inside parasitized erythrocytes [26–28]. Rufigallol has also vitamin K activity [29]. These molecules have an elongated core with a twofold symmetry axis, they are colored, they

exhibit an important polymorphism, the core is electron-deficient in nature, they are thermally stable, and their chemistry is fairly easy. These properties make them interesting from chemical and physical point of view.

2.3 Other Cores

"Benzene" is the first discotic core and its hexaesters are the prototype discotic liquid crystalline materials discovered. Ever since the discovery, a large variety of benzene derivatives have been designed, synthesized, and studied for their mesomorphism and to comprehend the chemical structure–physical property relationships. "*Hexa-peri-hexabenzocoronene (HBC)"* is one of the largest and highly symmetrical *all-benzenoid* polycyclic aromatic hydrocarbons which acts as the core fragment of discotic liquid crystals. HBC derivatives are the discotic materials for which many of the proposed application potentials of discotic liquid crystals have been successfully demonstrated such as in field effect transistors, photovoltaic solar cells, etc. [30-33]. *"Phthalocyanine (Pc)"* is a two-dimensional symmetrical aromatic heterocyclic compound composed of four iminoisoindoline units with a cavity of sufficient size to accommodate various metal ions. In other words, phthalocyanines (*Pcs*) are macrocyclic compounds having an alternative nitrogen atom–carbon atom ring structure and act as a tetradentate ligand. Mesomorphic *Pcs* have been extensively studied for their various useful physical properties including charge migration, crystal structure, electron spin resonance, laser induced triplet excitons and energy migration, luminescence, electric and magnetic properties, nonlinear optical properties, etc.

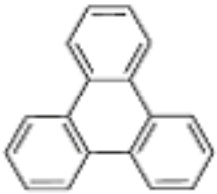

Triphenylene

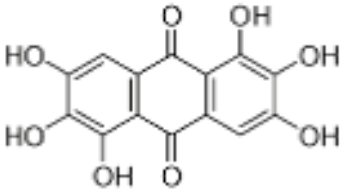

Rufigallol

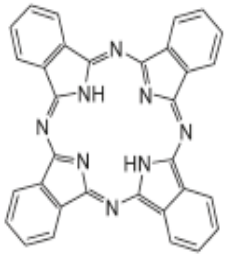

Phthalocyanine (Pc)

Hexa-peri-hexabenzocoronene (HBC)

Figure 2.1 Selected aromatic cores used in discotic mesogen.

Thermal behavior of some of the discotic mesogens under study is as follow:

(1) Triphenylene core

(i) Hexakis(nhexyloxy) triphenylene (HATn),

HAT4	Cr 88.6 Col_h 145.6 I
HAT5	Cr 69 Col_h 122 I
HAT6	Cr 68 Col_h 97 I
HAT10	Cr 58 Col_h 69 I

(ii) Mono-nitro triphenylene derivative (alkoxynitrotriphenylenes)

CnMNTP, n=4	Col_p 61.2 Col_h 141.3I
CnMNTP, n=5	Col_h 141.4 I

(iii) Hexahexylthiotriphenylene (HHTT for short),

HHTT	Cr 62 H 70 Col_h 93 I

(2) Rufigallol core

(i) Tetraaalkoxy-rufigallols

n=9 (branched tail)	Col_h 115.7 I
n=6 (linear chain)	Cr

Lattice parameter was measured for some of the discotic mesogens and tabulated as follow:

S.no	DLC compound	Lattice parameter (Å)
1.	HAT4	19.8
2.	HAT5	20.1
3.	HAT6	21.1
4.	HAT10	22.7
5.	C4MNTP	19.3
6.	C5MNTP	19.8
7.	Hexaalkoxyrufigallol (branched tail) n=9	18.9

*n is number of carbon atoms in alkyl chain

2.4 Dopant Material

2.4.1 Zinc Oxide Nanoparticles

ZnO is a wide band gap semiconductor that displays high optical transparency and luminescent properties in the near ultra violet and the visible regions. Due to these properties ZnO is a promising material for electronic and optoelectronic applications such as solar cells

(anti-reflecting coating and transparent conducting materials), gas sensors, liquid crystal displays, heat mirrors, surface acoustic wave devices etc [34-41]. ZnO nanoparticles are widely employed in fundamental research and potential applications, such as hydrogen-storage, field emitters, ultraviolet lasers and diodes, piezoelectric devices and photo catalysts fluorescence labels in medicine and biology, controlling units as UV photo detectors and as high-flame detectors in cosmetic industry and as a component of sun screens. The biggest advantages of ZnO NPs include their low price and non toxicity of ZnO NPs in small amounts ZnO NPs etc.

2.4.2 Gold Nanoparticles

The existence of gold nanoparticles has been known to people since ancient times and Colloidal gold nanoparticles have been utilized by artists due to the vibrant colors produced by their interaction with visible light. It was in 1850s that scientists focused their full attention on them. The main reasons behind this interest for gold nanoparticles are their extraordinary optical, electronic and molecular-recognition properties. More recently, these unique optical-electronics properties have been researched and utilized in high technology applications such as organic photovoltaics, sensory probes, therapeutic agents, drug delivery in biological and medical applications, electronic conductors and catalysis. The optical and electronic properties of gold nanoparticles are tunable by changing the size, shape, surface chemistry, or aggregation state [42].

2.4.3 2,4,7-Trinitrofluoren-9-one (TNF)

Trinitrofluorenone (TNF) is a trinitro derivative of fluorine that was used extensively as a toning agent in certain photocopy processes. TNF exists as pale yellow needles or crystals, has a melting point of 175-176°C, and a vapor pressure of 0 mmHg at 25°C. It is slightly

soluble in water and very soluble in acetone, benzene, and chloroform. TNF has been used widely in the transfer process in photocopiers and printers; it is the photoelectrically active ingredient of the coating mixture deposited on the photoconductor film on the exterior of the printing drum.

Due to three nitro groups attached to flat aromatic core, TNF molecule is highly electro negative. When mixed with suitable electron donor molecule, TNF forms strong charge transfer complex. This property of forming charge transfer complex with electron acceptor and donor molecules has been utilized to form charge transfer complexes of discotic liquid crystal.

Details of synthesis of ZnO nanoparticles and gold nanopatricles and their characterization have been discussed in chapter 3 and 4 respectively.

2.5 Experimental Techniques and Their Fundamentals

2.5.1 Polarized Optical Microscopy (POM)

POM is the most important technique for the identification of mesomorphic nature and morphology of liquid crystals. The principle of this is corresponding to the polarization of light. A polarizer is a filter that only permits the light oriented in a specific direction with its polarizing direction to pass through. There are two polarizers in a polarizing optical microscope (POM) and they are designed to be oriented at right angle to each other, which is termed as cross polar. The fundamental of cross polar is illustrated in Figure 2.2, the polarizing direction of the first polarizer is oriented vertically to the incident beam, so only the waves with vertical direction can pass through it. The passed wave is subsequently blocked by the second polarizer, since this polarizer is oriented horizontally to the incident wave. It utilizes the birefringence of LC materials – the ability to turn or change phase of

linearly polarized light. The textural observations and initial identification of the mesophase were carried out using polarizing light microscopy (Olympus BX51) combined with a heating stage (Mettler FP82HT) and a central processor (Mettler FP90). Heating stage makes it possible to investigate the phase behavior when heating or cooling the sample.

When a thin film of a material on a microscope slide is placed in between crossed polarizers, light travelling through the material gets affected by the birefringence of the material. When non birefringent media or isotropic media is present, the light will not get affected and the light will be blocked by the crossed polarizer and hence appears black. When there is birefringent media is present between the polarizer the light gets affected to varying degrees based upon the several factors e.g. the thickness of the sample, the magnitude of the birefringence, the orientation of the director and defects in the structure of the material. As the molecular orientation of each phase present in liquid crystal is unique, each phase can be recognized by its characteristic texture.

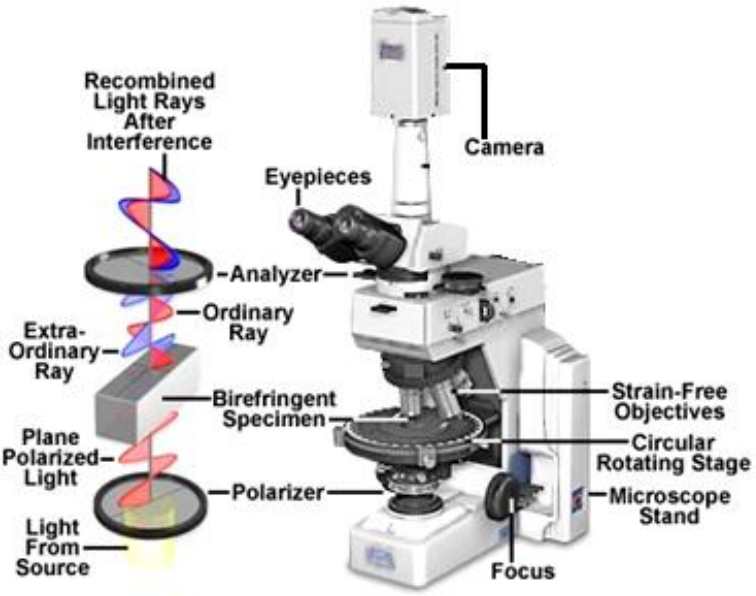

Figure 2.2 Polarizing Optical Microscope's configuration [Nikon Corporation].

2.5.2 Differential Scanning Calorimetry (DSC)

Differential Scanning Calorimetry (DSC) is a useful tool which complements optical methods in the study of liquid crystal phase transitions. Its utilization in determining the heat supplied or extracted during a process such as a phase transition. A phase change occurs when there is a change in the molecular ordering. Any changes in the molecular ordering have an associated change in enthalpy. DSC provides a convenient and moderately accurate method of measuring heat capacities and enthalpy changes. Commercial instruments provide a recorder output of the constant-pressure heat capacity:

$$C_P = \left(\frac{dq}{dT}\right)_P = \left(\frac{\partial H}{\partial T}\right)_P \qquad eq.(1)$$

as a function of temperature. The area under such a curve between any two temperature limits yields an enthalpy change:

$$\Delta H = \int_{T_1}^{T_2} \left(\frac{\partial H}{\partial T}\right)_P dT = \int_{T_1}^{T_2} C_P \, dT \qquad eq.(2)$$

The differential scanning calorimeter operates on the "null balance" principle. Within the assembly there are two small sample holders: one for the sample and the other to hold a reference material. Energy (as electrical work) is supplied to each sample holder independently, and the temperatures of each are monitored. Energy (as an associated heat) which is absorbed or evolved by the sample is compensated by increasing or decreasing the electrical energy delivered to the sample-holder heater. The temperatures are monitored by comparing the respective signals from platinum resistance thermometers in each of the sample holders. This adjustment of electrical input to the heating unit provides a varying electrical signal which is opposite but equivalent to the varying thermal behavior of the sample. For example, when a phase transition point is reached from lower temperatures, the

sample will absorb additional energy. Then additional electrical power must be supplied to the heater of this sample so that the reference and sample holders will be at the same temperature. When the transition is completed, the temperature of the sample will rise, and additional heat need no longer be supplied. The varying electrical signal thus provides a record of the thermal behavior of the sample.

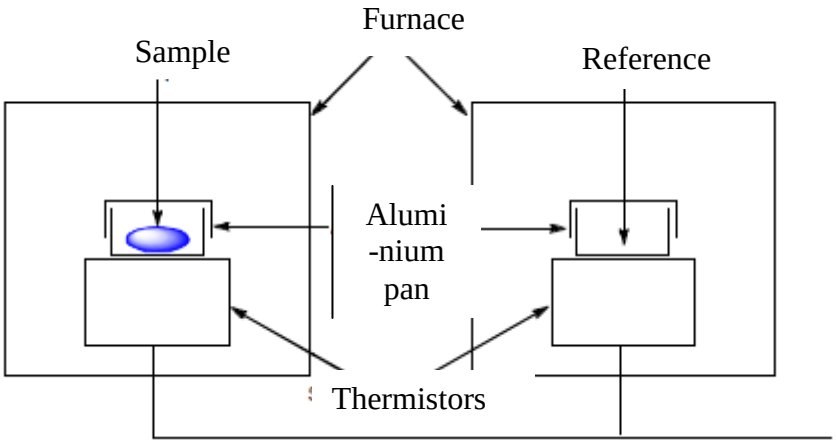

Figure 2.3 Schematic representation of operation of a DSC.

The change in the enthalpy corresponds to the difference in the level of the order of the material before and after the transition. However, this information is useful but it can't be used to identify the mesophase morphology of its own. DSC thermogram does give an excellent indication of the number of mesosphase that a compound exhibit and a precise measurement of their respective transition temperatures and associated enthalpies.

2.5.3 X-ray Diffraction (XRD)

X-ray diffraction (XRD) is a direct probe of electron density fluctuations, which occurs between atoms inside a condensed material. When X-rays hit the sample, they will scatter off the electron density differences. The diffraction of X-rays is strongest in crystalline solids, since the electron density difference is repeated many times at an identical distance. Crystals

are made up by unit cells – the smallest repeating unit which represents the crystalline material. Elastic Rayleigh scattering of the atoms in crystals can be thought of as scattering between different crystal planes in the atomic lattice. Depending on the phase shift between two scattered waves, constructive or destructive interference will occur. Constructive interference occurs when the phase shift is a multiple of 2π, which is expressed by Bragg's law,

$$2dsin\theta = n\lambda \qquad eq.3$$

where λ is the wavelength of the X-rays, d is the spacing between the crystal planes in the atomic lattice, θ is the angle between the incident ray and the scattering planes, and n is an integer which determines the order of the scattering.

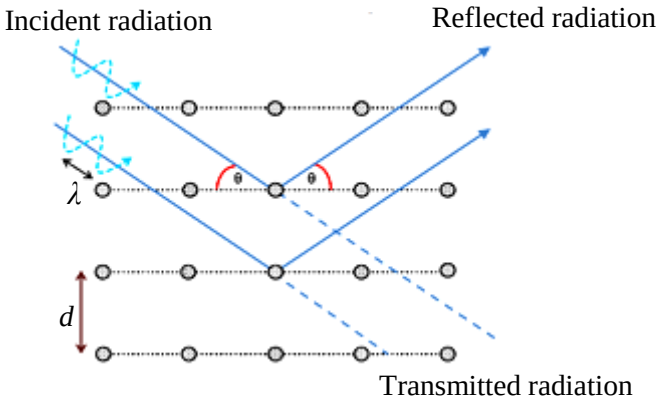

Figure 2.4 Schematic representation of the scattering of X-ray leading to the Bragg's law.

The distances in the unit cell obtained by XRD are connected to the miller indices (*h k l*). They are parameters of the reciprocal space, in which the interference pattern is directly observed. (100) represents the distance of the unit cell along the a-axis, (010) represents the distance of the unit cell along the b-axis, and (001) represents the distance of the unit cell along the c-axis. From Bragg's law it follows that when the distances between the scattering

atoms decrease, the scattered angle will increase, and, therefore, the miller indices also increase by an integer ($h\ k\ l$) representing the distance ($1/h\ 1/k\ 1/l$) inside the unit cell. It is also evident that higher order scattering ($n \geq 2$) of the atomic distances will also increase the scattering angle (2θ). Since higher order scattering occurs at the same place as the miller indices with higher numbers, it is usually represented by the miller indices within the field of liquid crystals, although their reciprocal distances do not represent the distances inside the unit cell.

Several types of XRD techniques exist: single-crystal XRD, powder XRD, wide-angle X-ray scattering (WAXS) and small-angle X-ray scattering (SAXS). WAXS and SAXS are used to determine the crystalline structure of polymers and liquid crystals, while single-crystal XRD and powder XRD are used for structural characterization of single crystals and powders and microcrystalline materials, respectively. WAXS and SAXS are principally the same technique, but they map different distances within the material, where the shorter angle is equivalent to a longer distance, in accordance with Bragg's law.

XRD is the ultimate technique in mesophase morphology identification as it provides accurate and direct information regarding molecular positioning and orientation. Careful analysis of XRD data permits the deduction of various important structural features which make it possible to determine the precise mesophase morphology and structure of liquid crystalline phase at a given temperature.

Since the thesis deals with discotic liquid crystal, next discussion will be devoted to structure of discotic mesogens.

2.5.3.1 Structures of Discotic Liquid Crystalline Phases

(i) The Hexagonal Columnar Mesophase (Col_h)

In the small-angle region, the columnar hexagonal phase generally exhibits four diffraction rings whose spacings are in the ratio 1:1/√3:1/√4:1/√7 along with two broad peaks in the wide-angle region. However, geometric considerations suggest that the Col_h phase can, in principle, display more reflections in the small-angle region. Out of the two wide-angle reflections, one corresponds to the liquid-like packing of flexible alkyl chains and the other one relatively narrow corresponds to the intracolumnar stacking of discotic cores.

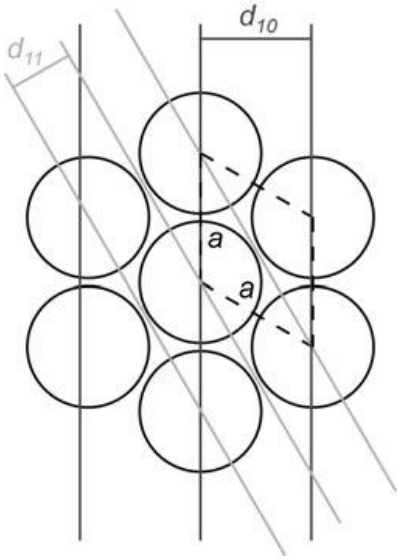

Figure 2.5 2D lattice planes corresponding to the (10) and (11) reflections, d_{10} and d_{11}, respectively for Col_h phase.

These two d spacings follow as:

$$d_{11} = \frac{d_{10}}{2cos30^o} = \frac{d_{10}}{\sqrt{3}} \qquad eq.4$$

Thus, the d spacings of the (10) and (11) reflections show the ratio 1:1/√3. More geometric considerations result in the characteristic ratios of 1:1/√3:1/√4:1/√7:√9:1/√12:1/√13 for the d

spacings of the (10), (11), (20), (21), (30), (22), and (31) reflections of a 2D hexagonal lattice in the small-angle regime. Also, the *d h k* spacings (in which h and k are the Miller indices of the associated reflection) are related to the lattice constant a according to Equation 5:

$$\frac{1}{d_{hk}^2} = \frac{4}{3}\frac{h^2 + hk + k^2}{a^2} \qquad eq.5$$

(ii) The Columnar Rectangular Mesophase (Col_r)

The 2D X-ray patterns resemble those of a columnar hexagonal mesophase with a diffuse halo in the wide-angle regime and sharp reflections in the small-angle regime. However, a closer look to the SAXS profiles reveals certain differences. The (10) peak of the Col_h mesophase splits in the (20) and (11) reflection of the Col_r phase lattice a rectangular unit cell with the lattice constants a′ and b′ is shown (Figure 2.6 (a)). Since $\delta=30^o$ in a hexagonal arrangement, $b'=a'/\sqrt{3}$, and thus $d_{11'}=d_{20'}$, since for a rectangular lattice, Equation (6) is valid.

$$\frac{1}{d_{hkl}^2} = \frac{h^2}{a^2} + \frac{k^2}{b^2} \qquad eq.6$$

As soon as the lattice deviates from perfect hexagonal symmetry, that is, $\delta \neq 30^o$ (Figure 2.6 (b)), the degeneracy of d_{11} and d_{20} is broken and two separate reflections appear in the small-angle regime.

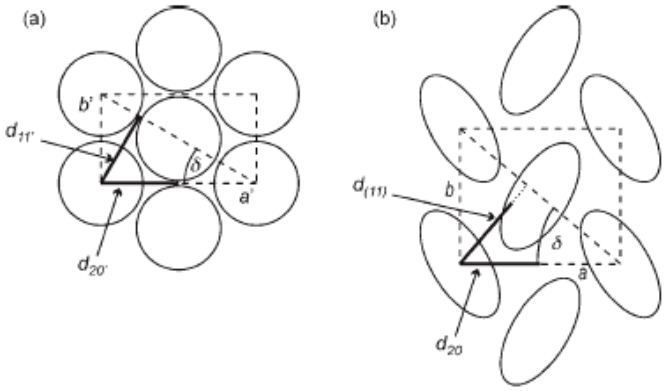

Figure 2.6 Symmetry breakdown at the transition from a hexagonal (a) to a rectangular columnar phase (b). For better clarification the rectangle in (b) is shown in a disproportionate way.

Normally the lattice of a rectangular mesophase is closer to that of a hexagonal columnar phase. The indexation of a columnar rectangular mesophase and the determination of the lattice structure (space group) are complex and often not completely unambiguous.

(iii) The Columnar Oblique Mesophase (Col_{ob})

Figure 2.6 shows the arrangement of the columns in a columnar oblique mesophase, in which the tilted columns are represented by elliptic cross sections. The symmetry of this 2D lattice corresponds to the space group P_1. Examples for columnar oblique mesophases are rare because strong core– core interactions are required. Since P_1 is a primitive planar space group, there are no reflection conditions and therefore all peaks (*h k*) are allowed.

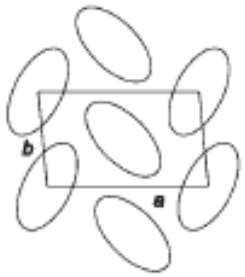

Figure 2.7 The arrangement of the columns in a columnar oblique mesophase

(iv) Columnar Lamellar Mesophase

The X-ray profile of this phase in the low angle region displays reflections whose spacings are in the ratio 1:2:3 suggesting the lamellar organization of the columns and there appears a wide angle reflection corresponding to a distance of intracolumnar separation suggesting columnar organization of molecules in the layers.

2.5.4 Dielectric Relaxation Spectroscopy

Dielectric relaxation spectroscopy is a robust and versatile measurement technique with numerous applications in both fundamental science and engineering applications. Amongst its main advantages are its wide frequency range, the (relative) simplicity of a measurement cell, and the flexibility in shape, size, and state of matter of the samples. Dielectric spectroscopy measures the time or frequency dependent response of current and voltage of a sample to a changing electric field. This response is that of the polarization inside the sample, thus related to the motion of free charge carriers or (permanent) dipoles. When molecular dipoles are present in the material, various relaxation modes reflecting the orientational dynamics of the polar species can be probed. These orientational dynamics can be non-cooperative, e.g. in gasses, or co-operative due to strong interactions between diploes. The outcome of an experiment is typically given in the form of a dimensionless quantity ε^*, the complex dielectric permittivity, which depends on parameters like frequency, temperature, and pressure.

2.5.4.1 Fundamentals

Any material can be polarized by an external electric field. Numerous mechanisms can contribute to the polarization, but they can be divided in three categories.

(i) Charge Displacement: The electric field moves the electric charges slightly away from their equilibrium positions, but without causing a real current although. This includes the displacement of the electron cloud relative to the core of an atom, movement of the core itself from its equilibrium position in a crystal, and shifts of bonding electron pairs. In this case a dipole moment is induced.

(ii) Orientational Polarization: Here dipoles move to new equilibrium orientations. Essentially molecules with an induced or permanent dipole moment, thus caused by some charge distribution in the molecule, reorient themselves to align their dipole moment with the electric field.

(iii) Redistribution of Free Charges: In a real material, conducting as well as non-conducting, there are always free charges present. These charges will also move through the material under influence of the field and accumulate at the edges of the material, or eventually at internal interfaces in heterogenous systems.

To contribute to the polarization, a dipole (and thus also the molecule or part of the molecule it belongs to) has to be able to reorient itself to align with applied electric field. This aligning serves of course the purpose of minimizing the energy of the dipole. The dipole has to overcome certain forces, like Van der Waals forces or hydrogen bond with neighbouring molecules and steric constraints, there has to be room for the new position. Thus it takes some typical time for a dipole to reorient, say τ, the relaxation time.

To carry out dielectric relaxation spectroscopy, LC cells are made with ITO coated glass plates. A circular pattern is etched on both plates to get active area with diameter of 8mm (Figure 2.8). We have used two types of treatment to get planar alignment (for calamatic LC). First method involves coating of thin layer of polyimide on etched ITO coated glass plates. Polyimide coated ITO glass plates were then cured at 250^{o}C for one and half hour. Then both plates were rubbed in a particular direction. Other method involves SiO vacuum coating on both sides of the plates at 32^{o}C grazing angle. Cells were made by placing two plates together ensuring that the active area overlaps. The separation is controlled by glass beads spacers with diameter 6 μm which are mixed with epoxy. The cells are cured at 150^{o}C

for one and half hours after glue was applied on the edges of the plates. Thickness of the empty cell is measured with $\pm 1\%$ accuracy by an interferometer using Ocean Optics spectrometer. The capacitance of empty cell was measured before filling the sample. Electrical connections made to apply external electric field and to measure the response. Material under investigations is now filled into the cell at isotropic temperature via capillary action.

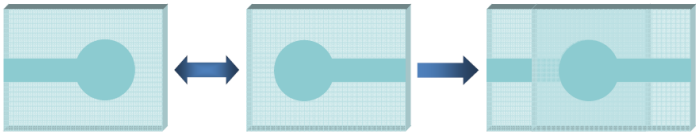

Figure 2.8 (a), (b). Top view of the two etched ITO glass plates. (c) Two are glued together to make LC cell.

This cell assembly can be considered as parallel plate capacitor having effective cell area A and thickness *d*. So the geometrical capacitance can be given as $C=\varepsilon_o A/d$ where ε_o is the electrical permittivity of vacuum. By using $C^*=C_o\varepsilon^*$, the complex dielectric constant $\varepsilon^*= \varepsilon'-\varepsilon''$, can be calculated where ε' is real part known as dielectric permittivity and imaginary part ε'' as dielectric loss.

Dielectric loss describes the dissipation of energy caused by molecular friction or by transport of real charge carriers. Although the dielectric constant can be measured both in the time and frequency domain, frequency domain spectroscopy is the most common technique as it directly yields the dielectric spectrum $\varepsilon^*(f)$. In practice the analysis of a dielectric spectrum is based on the determination of the (distribution of the) relaxation times of the processes that are seen in the spectrum. The models use to study the dielectric relaxations and it parameters are generally based on the Debye function, that has been extended empirically

to account for certain types of broadening of the spectra. Assuming an electrical circuit consisting of an ideal capacitor in parallel with an ideal resistor with alternating current and some basic calculations results into an equation known as *Debye relaxation function* [43]:

$$\varepsilon^*(\omega) = \varepsilon_\infty + \frac{\varepsilon - \varepsilon_\infty}{1 + i\omega\tau} \qquad eq.7$$

In practice a perfect Debye relaxation is rare. Loss curves obtained experimentally are usually broader than ideal Debye relaxation peaks. To account for asymmetric broadening of the peak Debye function has been modified into *The Cole–Cole function.* The Cole–Cole function is aimed at the description of a symmetric broadening of the peak [44] and equation 7 is modified as:

$$\varepsilon^*(\omega) = \varepsilon_\infty + \frac{\varepsilon - \varepsilon_\infty}{1 + (i\omega\tau)^\alpha} \qquad eq.8$$

The distribution or shape parameter α, which lies between 0 and 1, describes the broadening: $\alpha = 1$ corresponds to the situation of no broadening (the Debye function) and with decreasing α the peak becomes lower and broader.

When the relaxation peak is only broadened at the high frequency side, the *Cole–Davidson* function can be used [45,46]. In this case a shape parameter β is introduced, resulting in the expression:

$$\varepsilon^*(\omega) = \varepsilon_\infty + \frac{\varepsilon - \varepsilon_\infty}{(1 + i\omega\tau)^\beta} \qquad eq.9$$

For $\beta = 1$ this expression reduces to the Debye function. β lies values between 0 and 1. The *Havriliak–Negami function (HN function)* [47, 48] is the natural combination of the Cole–Cole and Cole– Davidson functions: It describes the combined symmetric and asymmetric broadening by two shape parameters α and β where, $0 < \alpha \leq 1$ and $0 < \beta \leq 1$.

$$\varepsilon^*(\omega) = \varepsilon_\infty + \frac{\varepsilon - \varepsilon_\infty}{(1 + (i\omega\tau)^\alpha)^\beta} \qquad eq.10$$

In low frequency region phenomenon of electrical conduction comes into picture. This simple movement of charge carriers leads typically to a response that is the same as of an ohmic conductor. It shows only in the imaginary part of the dielectric permittivity. When analyzing a dielectric spectrum, it is accounted for by a term of the form:

$$-\frac{i\sigma_o}{\varepsilon_o \omega^s} \qquad eq.11$$

σ_o is the DC electrical conductivity and the exponent s is a fitting parameter that has a value of 1 for pure ohmic conduction. So the modified HN function is as follow:

$$\varepsilon^*(\omega) = -\frac{i\sigma_o}{\varepsilon_o \omega^s} + \sum_j \frac{\Delta\varepsilon_j}{\left(1 + \left(i\omega\tau_j\right)^{\alpha_j}\right)^{\beta_j}} + \varepsilon_\infty \qquad eq.12$$

For a quantitative analysis of the relaxation spectra, ε'' is fitted with the corresponding expression of HN function, resulting relaxation times and relaxation strengths for each temperature dependent spectra. Generally two expressions are commonly used to express the temperature dependence of relaxation time. The first one is the Arrhenius equation (originally introduced to describe chemical reactions). The second one is the Vogel–Fulcher–Tamman (VFT) dependence, introduced to describe the non-Arrhenius dependence in many glass-forming systems.

The *Arrhenius equation* is usually given in the form:

$$\tau = Aexp\left(\frac{\Delta E}{RT}\right) \qquad eq.13$$

where A is a temperature independent factor and ΔE, the activation energy, does not depend on temperature either.

The VFT equation was introduced as a fitting function for the curved relaxation time behaviour

for glass-forming liquids. The VFT equation is usually given in the form:

$$\tau = \tau_{\infty} exp\left(\frac{B}{T - T_o}\right) \qquad eq.14$$

where τ_{∞} is the high temperature limit of the relaxation time, B is related to the fragility of the glass-former and T_o is the Vogel temperature. When T_o = 0, this equation reduces to the Arrhenius equation.

Dielectric measurements were carried out using Nova control Impedance analyzer in the frequency range 1 Hz to 10 MHz and the temperature of the sample was varied using Eurotherm temperature controller. Experiments were carried out in the temperature range 30^{o}C to 120^{o}C.

2.5.5 Ultraviolet/Visible Absorption Spectroscopy

Ultraviolet and visible (UV-Vis) absorption spectroscopy is the measurement of the attenuation of a beam of light after it passes through a sample or after reflection from a sample surface. Absorption measurements can be at a single wavelength or over an extended spectral range. Ultraviolet and visible light are energetic enough to promote outer electrons to higher energy levels, and UV-Vis spectroscopy is usually applied to molecules or inorganic complexes in solution. The UV-Vis spectra have broad features that are of limited use for sample identification but are very useful for quantitative measurements. The first absorption peak gives valuable information about the optical band gap:

$$E_g^{opt} = h\nu_{abs} = \frac{hc}{\lambda_{abs}} \qquad eq.15$$

where h is the Planck constant, ν_{abs} is the frequency of the absorbed light, c is the speed of light in vacuum, and λ_{abs} is the wavelength of the absorbed light. The optical band gap can be related to the valence and conduction bands of a molecule in a condensed state or the highest

occupied molecular orbital (HOMO) and the lowest unoccupied molecular orbital (LUMO) of an isolated molecule.

In solution, the UV/Vis absorption of a chromophore at low concentrations follows Lambert-Beer's law,

$$T = \frac{I}{I_o} = 10^{-A} = 10^{-\varepsilon lc} \qquad eq.16$$

where T is the transmissivity, I is the light intensity passed through the sample, I_o is the incident light intensity, A is the absorbance, ε is the molar absorptivity of the chromophore, l is the length of the sample which the light passes through, and c is the concentration of the sample. The molar absorptivity of the chromophore is a measure of how strongly each molecule absorbs the UV/Vis radiation.

In thin films, UV/Vis absorption spectroscopy contains information about the intermolecular interactions inside the self-assembled structures. The absorption peaks can shift due to aggregation, but are usually just broadened.

For our experimental studies, absorbance spectra in solution were taken using Perkin Elmer, Lambda 35 UV/VIS spectrometer and for thin films Ocean Optics 2000 spectrometer along with Olympus BX 51 POM was used.

2.5.6 Infrared Spectroscopy

Infrared (IR) spectroscopy focuses on the absorbance of electromagnetic waves in the IR region of the electromagnetic spectrum. The absorbance of IR radiation depends on the vibrational and rotational transitions within the molecule, making it possible to connect specific bonds or functional groups with the absorbing frequencies. This can be used as a trace of a successful synthesis, or more specifically, as a proof of functional groups present in the sample.

We have utilized infra-red dichroic technique to measured orientational order parameter (*S*) of DLCs and composite materials. Isolated and pronounced bands available in the infrared spectra of the compounds can be used for this purpose if the orientation of the related transition moment with respect to the molecular geometry is known.

Our studies are concerned with the temperature variation of the order parameter. Hence it is required to confine the liquid crystal samples in suitable cells in which temperature could be varied. We used CaF_2 plates for this purpose because they possess good transmission in the required frequency range, they have good mechanical and thermal strength. For the experiment, smooth and scratch free surface of the plates were obtained by polishing the plate surfaces on velvet sheet. To obtain homeotropic alignment of sample CaF_2 plates were coated with thin layer of nylon 6/9. Cell thickness was maintained with mylar spacer. Sample was filled into the cell at isotropic temperature. On slow cooling homeotropic alignment was obtain which was checked under POM. To obtain IR spectra at different temperature, cell was placed in homemade heater whose temperature was varied by varying the voltage.

The spectra were recorded in the isotropic phase and at various temperatures in mesophase using infrared spectrophotometer (FTIR-8400 from Shimadzu). Order parameter of different systems was plotted as function of temperature.

References

[1] C. M. Buess, D. D. Lawson, *Chem. Rev*. 60, 313–330, (1960).

[2] J. Billard, J. C. Dubois, N. H. Tinh, and A. Zann, *J. Chim*. 2, 535–540, (1978).

[3] C. Destrade, M. C. Mondon, J. and Malthete, *J. Phys. Colloque*. 40, C3–17–21, (1979).

[4] S. Kumar, S. *Liq. Cryst*. 32, 1089–1113, (2005).

[5] J. D. Badjic, V. Balzani, A. Credi, J. N. Lowe, S. Silvi, and J. F. Stoddart, *Chem. Eur. J.* 10, 1926–1935, (2004).

[6] F. Cardullo, D. Giuffrida, F. H. Kohnke, F. M. Raymo, J. F. Stoddart, and D. J. Williams, *Angew. Chem. Int. Ed*. 35, 339–341, (1996).

[7] M. C. T. Fyfe, J. N. Lowe, J. F. Stoddart, and D. J. Williams, *Org. Lett*. 2, 1221–1224, (2000).

[8] V. Balzani, M. C. Leon, A. Credi, J. N. Lowe, J. D. Badjic, J. F. Stoddart, and D. J. Williams, *Chem. Eur. J*. 9, 5348–5360, (2003).

[9] J. D. Badjic, V. Balzani, A. Credi, S. Silvi, and J. F. Stoddart, *Science* 303, 1845–1849, (2004).

[10] S. R. Waldvogel, A. R. Wartini, P. H. Rasmussen, and Jr. J Rebek Jr, *Tetrahedron Lett*. 40, 3515–3518, (1999).

[11] M. C. Schopohl, A. Faust, D. Mirk, R. Frohlich, O. Kataeva, and S. R. Waldvogel, *Eur. J. Org. Chem*. 2987–2999, (2005).

[12] S. R. Waldvogel, and D. Mirk, *Tetrahedron Lett*. 41, 4769–4772, (2000).

[13] C. Siering, H. Kerschbaumer, M. Nieger, and S. R. Waldvogel, *Org. Lett*. 8, 1471–1474, (2006).

[14] C. Siering, B. Beermann, and S.R. Waldvogel, *Supramol. Chem*. 18, 23–27, (2006).

[15] E. S. B Ferreira, A. N. Hulme, H. McNab, A. Quye, *Chem. Soc. Rev.*, 33, 329–336 (2004). [16] M. E. Maier, F. Bosse, A. J. Niestroj, *Eur. J. Org. Chem.* 1999, 1–13 (1999).

[17] M. Catellani, S. Luzzati, N.-O. Lupsac, R. Mendichi, R. Consonni, A. Famulari, S. V. Meille, F. Giacalone, J. L. Segura, N. J. Martin, *Mater. Chem.* 14, 67–74 (2004).

[18] M. Mamada, J.-i. Nishida, S. Tokito, Y. Yamashita, Y. *Chem. Commun*., 2177–2179 (2009).

[19] R. H. Thomson, *Naturally Occurring Quinones*, Chapman and Hall, New York, (1987).

[20] R. M.Christie, *Colour Chemistry*, RSC, Cambridge, U.K., (2001).

[21] A. V. Ivashchenko, *Dichroic Dyes for Liquid Crystal Displays*, CRC, Boca Raton, FL, (1994).

[22] B. Kampmann, Y. Lian, K. L. Klinkel, P. A. Vecchi, H. L. Quiring, C. C. Soh, C and A. G. Sykes, *J. Org. Chem*. 67, 3878–3883, (2002).

[23] P. Terech, and R. G. Weiss, *Chem. Rev*. 97, 3133–3160, (1997).

[24] L. F. Tietze, K. M. Gericke, and I. Schuberth, I. *Eur. J. Org. Chem*. 4563–4577, (2007).

[25] J. Grimshaw, J. and R. D. Haworth, *J. Chem. Soc*. 56, 4225–4232, (1956).

[26] M. V. Ignatushchenko, R. W. Winter, and M. Riscoe, M. *Am. J. Trop. Med. Hyg*. 62, 77–81, (2000).

[27] J. Ziegler, R. Linck, and D. W. Wright, *Curr. Med. Chem*. 8, 171–189, (2001).

[28] R. W. Winter, K. A. Cornell, L. L. Johnson, L. M. Isabelle, D. J. Hinrichs, and M. K. Riscoe, *Bioorg. Med. Chem. Lett*. 5, 1927–1932, (1995).

[29] G. J. Martin, C. F. and Lischer, *J. Biol. Chem*. 137, 169–171, (1941.

[30] J. Li, M. Kastler, W. Pisula, J. W. F. Robertson, D. Wasserfallen, A. C. Grimsdale, J. Wu, and K. Mullen, *Adv. Funct. Mater*. 17, 2528–2533, (2007).

[31] W. Pisual, A. Menon, M. Stepputat, I. Lieberwirth, U. Kolb, A. Tracz, H. Sirringhaus, T. Pakula, and Mullen, *Adv. Mater*. 17, 684–689, (2005).

[32] I. O. Shklyarevskiy, P. Jonkheijm, N. Stutzman, D. Wasserberg, H. J. Wondergem, P. C. M. Christianen, A. P. H. J. Schenning, D. M. de Leeuw, Z. Tomovic, J. Wu, K. Mullen, K., and J. C. Maan, *J. Am. Chem. Soc*. 127, 16233–16237, (2005).

[33] A. M. Van de Craats, N. Stutzmann, O. Bunk, M. M. Nielsen, M. Watson, K. Mullen, H. D. Chanzy, H. Sirringhaus, and R. H. Friend, *Adv. Mater*. 15, 495–499, (2003).

[34] O'Regan B and Graetzel M, *Nature* 353 737–40, (1990).

[35] M. K. Nazeeruddin, A. Kay, I. Rodicio, R. Humphry-Baker, E. Mueller, P. Liska N. Vlachopoulos and M. Graetzel , *J. Am. Chem. Soc.* 115, 6382–90, (1993).

[36] V. Thavasi, R. Jose, and S. Ramakrishna , *Mater. Sci. Eng.* R at press doi:10.1016/j.mser.2008.09.001(2008).

[37] S. A. Haque, S. Koops, N. Tokmoldin, J. R. Durrant, J. Huang J, D. D. C. Bradley and E. Palomares, *Adv. Mater.* 19, 683–7, (2007).

[38] R. Cinnsealach, G. Boschloo, S. N. Rao and D. Fitzmaurice D *Sol. Energy Mater. Sol. Cells* 55, 215–23, (1998).

[39] C. G. Granqvist, *Sol. Energy Mater. Sol. Cells*, 60, 201–62, (2000).

[40] M. S. Arnold, P. Avouris, Z. W. Pan and Z. L. Wang, *J. Phys. Chem.* B, 107, 659–63, (2003).

[41] M. Law, H. Kind, B. Messer, F. Kim and P. Yang, *Angew. Chem. Int. Edn Engl.* 41, 2405–8, (2002).

[42] M.-C. Daniel and D. Astruc, *Chem. Rev.***,** 104, 293-346, (2004).

[43] G.Williams and D. K. Thomas, *Phenomenological and molecular theories of dielectric and electrical relaxation of materials*, Novocontrol Application Note Dielectrics nr. 3 (1998).

[44] K. S. Cole and R. H. Cole, *J. Chem. Phys*., 9, 341, (1941).

[45] D. W. Davidson and R. H. Cole, *J. Chem. Phys*., 18, 1417, (1950).

[46] D. W. Davidson and R. H. Cole, *J. Chem. Phys.,* 19, 1484, (1950).

[47] S. Havriliak and S. Negami, *J. Polymer Sci.*, C14, 99, (1966).

[48] S. Havriliak and S. Negami, *Polymer,* 8, 101, (1967).

Chapter 3

Chararterisation of Pure and ZnO Nanoparticles Dispersed Rufigallol Based Discotic Liquid Crystal

Abstract: Chapter 3 is divided into two parts. Part (1) deals with temperature-dependent dielectric spectroscopy of pure discotic liquid crystal with rufigallol core having wide temperature range hexagonal columnar (Col_h) mesophase in frequency range 1 Hz to 10 MHz. The mesophase and its transition temperature have been determined by using polarizing optical microscopy and differential scanning calorimeter. SAXS showed the existence of hexagonal columnar phase. We studied the molecular dynamics of rufigallol core in liquid crystalline and isotropic phase. Part (2) is an experimental characterization of dispersions of ZnO nanoparticles (NPs) in the columnar matrix of a discotic liquid crystal. Thermophysical properties were investigated by absorbance spectroscopy, differential scanning calorimetry, polarizing optical microscopy, dielectric measurements, dc conductivity, x-ray diffraction and infrared (IR) dichroism technique. The experimental results show that inclusion of ZnO NPs into the columnar matrix enhances the orientational order in the columnar phase and does not affect the two dimensional hexagonal lattice. The alignment in homeotropic samples is also found to be better with the addition of the NPs. The real (ε') and imaginary parts (ε'') of the permittivity increase by a small amount in the dispersions and a new loss process appears in the isotropic phase. The order parameter measured using the IR dichroism technique in the face on geometry (homeotropic alignment) shows an enhancement for the composite system. The dc conductivity is also found to increase by an order of magnitude by addition of the NPs. These results suggest an improved

stacking of the disc-like molecules within the columns by the insertion of the ZnO NPs possessing high electron mobility. Such composite systems would be highly beneficial for potential applications like organic conductors.

Part (1)

3.1 Dielectric Studies and Other Thermo-physical Properties of Rufigallol Based Discotic Liquid Crystal

3.1.1 Introduction

In discotic liquid crystals (DLC) [1], the self organization of disc like molecules results into unique nanostructure in which one disc is stacked on the top of the other to form columns. A typical discotic mesogen is compromises of a planar aromatic core with several long alkyl chains attached to it. These aliphatic chains that surround the central core insulate one column from the neighboring column with the effective distance of separation of usually 2-4 nm. And, these flexible peripheral chains promote the formation thermotropic mesophases, solubility and processability of DLC. $\pi - \pi$ interactions, van der waals forces, hydrogen bonds and other various non covalent forces results in the interaction between discotic molecules leading to their self assembly in supramolecular structures. Because of their self assembly behavior, DLCs exhibit advantageous properties of self healing, ease of processing, high charge carrier mobility and high solubility in organic solvents. Hence, DLCs find potential applications in electronic devices. At the same time, the supramolecular structure of discotics plays very important role in the molecular design and their performance in devices [2-12]. Therefore, the knowledge about the structure and associated dynamics is very important.

Because of the high intracolumnar and intercolumnar order, the dynamics of molecular mesophases are expected to deliver some unique features. The dynamics of DLCs are obviously expected due to the rotation of the discs around the column axis and collective orientation of the peripheral chains around the aromatic core within the plane of the core.

DLCs with triphenylene, benzene, and HBC cores have been studied extensively by dielectric spectroscopy [13-18]. The dielectric studies of the rufigallol based DLC which is similar to the present compound under study, has also been carried out [19]. Rufigallol belongs to earliest systems which showed columnar mesophase. Because of their easy synthesis, existence of hexagonal columnar mesophase at room temperature, electron deficiency of the core, thermal stability, color, redox reaction reversibility etc, they provide promising future applications in devices having long term stability [9].

Therefore, the combined studies of dielectric spectroscopy, differential scanning calorimetry, small angle x ray scattering and optical polarizing microscopy help to create an insight into both structure and dynamics of rufigallol based DLC.

3.1.2 Results and Discussion

Hydroxyl groups functionalized rufigallol derivative 2,3,6,7-tetrakis(3,7-dimethyloctyloxy)-1,5-dihydroxyanthracene-9,10-dione (compound **1**) was synthesized as reported [20]. Molecular structure of the compound under investigations is shown in Figure 3.1. The thermal behavior of the compound was studied by DSC (DSC; Perkin Elmer, Model Pyres 1D) at 5^{o}C/min both on heating and cooling. The scans revealed that the DLC exhibit only one mesophase and is a room temperature DLC. SAXS was carried out on the sample which was held in sealed Lindemann capillary tubes (0.7 mm diameter) and the diffraction pattern was recorded on a two dimensional image plate. Textural studies of aligned and unaligned samples were carried out using POM. Dielectric measurements were done at atmospheric pressure conditions as function of frequency in range from 1 Hz to 10 MHz and at constant frequency as function of temperature in range 30^{o}C to 120^{o}C.

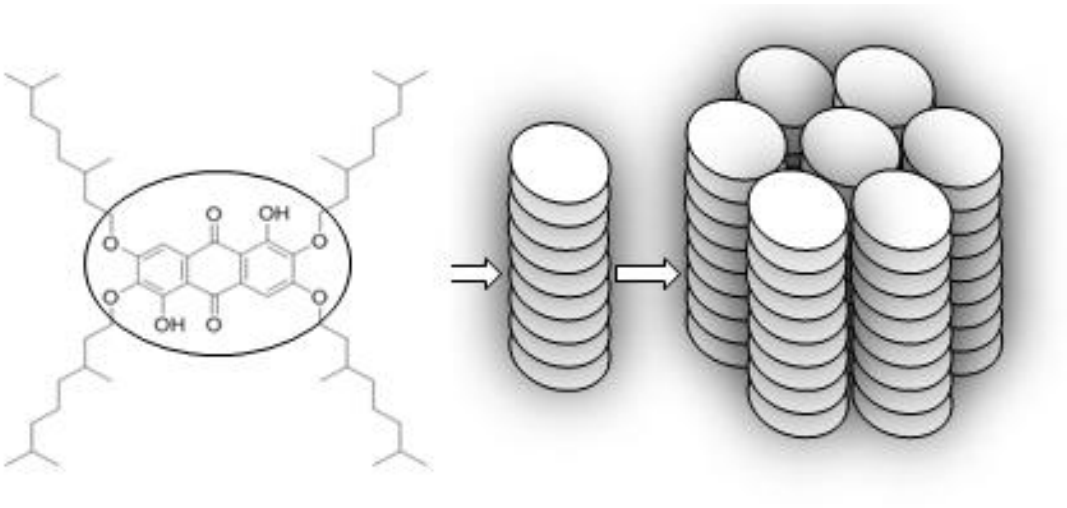

Figure 3.1 Structure of 2,3,6,7-tetrakis(3,7-dimethyloctyloxy)-1,5-dihydroxyanthracene-9,10-dione molecule and schematic representation of arrangement of disc molecules into one dimensional column and self assembly of columns into two dimensional hexagonal columnar pattern.

3.1.2.1 Mesomorphic Behavior

The phase transition temperatures of the compound **1** was initially established from the polarizing optical microscopy (POM) and then measured accurately by differential scanning calorimetry (DSC). In a thin (5μm) aligned cell compound **1** forms large homeotropic domains when cooled from the isotropic state as shown in Figure 3.2 (a). The slow cooling of the material from isotropic phase initiates the formation of homeotropic alignment. Homeotropic alignment generally occurs for columnar mesophase. Thus the molecules are arranged on the surface acts as nucleation site at which one disc stacks on the top of the other and self assemble in form of columns. Moreover the self alignment of discs was strongly dependent on the film thickness as shown in Figure 3.2(a) and (b). In the case of thick samples (125 μm), we get optical texture shown in Figure 3.2(b) due to random orientation of

molecules. Compound **1** possesses sufficient mobility at room temperature so that they can be easily sheared.

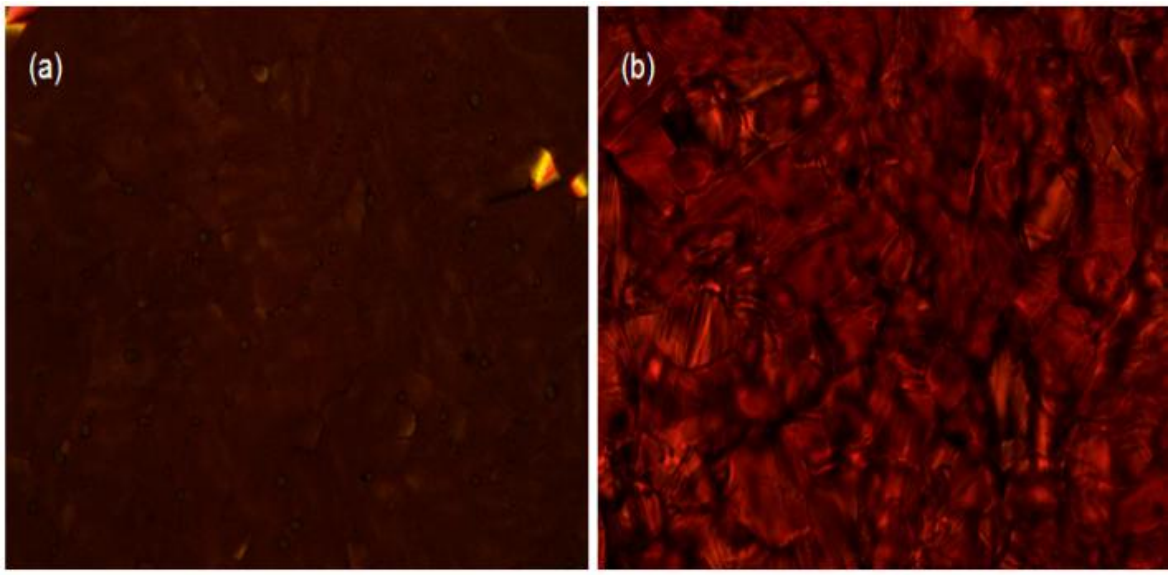

Figure 3.2 POM images of DLC at room temperature (a) Homeotropic alignment for 5 µm cell. (b) Random alignment for 125 µm cell.

This compound shows only one transition Col–I at 115.7^{o}C while heating and I–Col transition at 114.1^{o}C while cooling, which is the widest mesophase range amongst all the rufigallol derivatives known to date [8] and it does not crystallizes even after cooling to temperature of -30^{o}C. (A typical example the DSC thermogram of compound **1** is shown in Figure 3.12 in section 3.2.2.1)

3.1.2.2 X-Ray Diffraction Study

In order to reveal the mesophase structure and hence the supramolecular organization of these compounds, X-ray diffraction experiments were carried out using unoriented samples taken in glass capillaries at room-temperature. The X-ray diffraction patterns of the mesophase exhibited by compound **1** belong to discotic hexagonal columnar arrangement. As

a typical example, the X-ray diffraction pattern of compound **1** and the intensity vs. theta (θ) plot derived from the pattern at room temperature are shown in Figure 3.3. Four sharp rings, one strong (d_{10}) and three weak reflections are seen in the pattern as well as in the plot in the small-angle region. The d-spacings of these four rings are in the ratio 1: 1/√3: 1/√4 and they can be indexed as 10, 11, 20, reflections of a two-dimensional hexagonal lattice. Additionally, a fairly narrow diffraction ring corresponding to a spacing of 3.7 Å, matching the interdisc (intracolumnar = d_{01}) spacing within a column, and a broad diffuse reflection at ~4.6 Å suggesting a liquid like structure of the alkyl chains, are also seen in the wide angle region. So the discotic molecules stack one on top of the other to form the columns and these columns in turn arrange themselves in two dimensional hexagonal fashion with the intra-columnar core–core separation of 3.43Å. In the columns the insulating alkyl chains surround the conducting aromatic cores with the intercolumnar distances which varies from 20–26 Å. The compound possesses high intracolumnar order which could be due to the added intermolecular interactions by two additional hydrogen bonded rings in the molecular core.

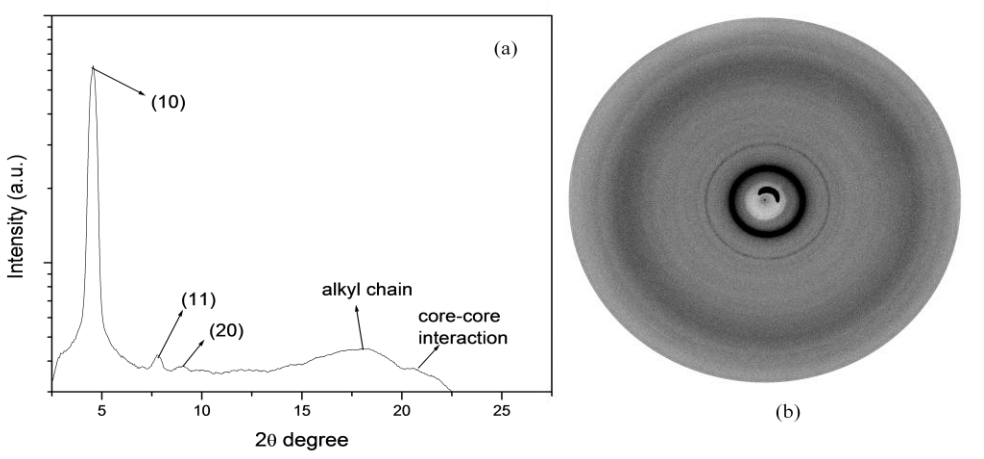

Figure 3.3 (a) One dimensional intensity *vs* 2θ plot (b) XRD pattern for pure compound **1** at room temperature.

3.1.2.3 Dielectric Spectroscopy

The dielectric studies of discotic materials are rare. There have been previous studies on different types of relaxation processes present in discotic material [22-29]. Temperature-dependent dielectric spectroscopy of the homologous series of rufigallol hexa-n-alkoxylates discotic compounds which have a structure closely related with the compound used in the present study has not shown evidence for any relaxation phenomenon in the frequency range of 10 Hz to 10 MHz [28].

The complex dielectric permittivity $\varepsilon^* = \varepsilon' - i\varepsilon''$ where ε' is the real part and ε'' is the imaginary part, is a function of frequency ω, and temperature T. Dielectric measurements have been performed in a cell with thickness of 5 μm. As discussed in the previous section, slow cooling of sample from isotropic phase results in good homeotropic alignment. The dielectric data was collected in the cooling cycle and the dielectric measurement under this condition yields dielectric permittivity parallel to the column axis ($\varepsilon'_{\parallel}$).The real ε' and imaginary parts ε'' of the complex permittivity ε^* were measured as a function of temperature at a fixed frequency and also as a function of frequency at a given temperature T. The value of real part of permittivity ε' shows monotonous increase in the value with lowering of temperature at 1 KHz (Figure 3.4). Also, we were able to detect the phase transition between hexagonal columnar phase to isotropic phase as there sudden drop in the value of ε' at isotropic temperature. Again, this temperature scan of real part of dielectric permittivity ε' shows the presence of single mesophase in the DLC. The increase in the value of ε' can be explained on the basis that as the temperature is lowered the system becomes more ordered and order increases the value of ε'. Effect of different frequencies on value of ε' as a function of temperature was also studied and is shown in Figure 3.4. At frequency higher than the

relaxation frequency (~100 Hz), all the dipole moment associated with the DLC molecules reorient and align in direction of applied electric field hence contribute to polarization. If frequency higher than 1 kHz is applied no molecules can follow the electric field anymore and the contribution of this dipole motion to the polarization decreases and consequently the real part of the permittivity decreases. Therefore we observed that at frequency 100 kHz, the permittivity is lower in mesophase than in the permittivity values at 1 kHz.

Since the dielectric measurements are carried out in homeotropically aligned cell (5μm thick), the dielectric scan yields the dielectric permittivity parallel to the column axis ($\varepsilon'_{\parallel}$). In case of thick sample (125 μm) the molecules orient randomly yielding average value of the dielectric permittivity (ε'_{av}) (Figure 3.3 (b)). The perpendicular component of dielectric permittivity (ε') can be easily calculated from the formula [30]:

$$\varepsilon'_{av} = \frac{2\varepsilon'_{\perp} + \varepsilon'_{\parallel}}{3} \qquad eq.1$$

In general at isotropic temperature (and above), $\Delta\varepsilon$ ($\varepsilon'_{\parallel} - \varepsilon'_{\perp}$) i.e dielectric anisotropy should be zero. But in our case, we observed that the value of $\Delta\varepsilon \neq 0$ as shown in Figure 3.5.

During the transition from Col_h to isotropic phase, the two dimensional hexagonal lattice is broken but columns continue to exist in isotropic fluid forming a biphasic mixture even 10^{o}C above isotropic temperature due to strong π-π interations between cores. The existence of columns in isotropic liquid was also confirmed by the appearance of new loss process in isotropic phase (Figure 3.6) [22].

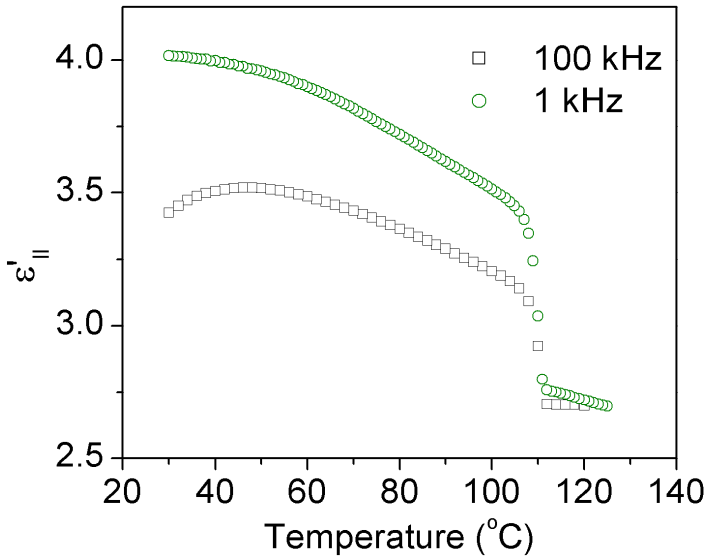

Figure 3.4 Real part of permittivity $\varepsilon_{\parallel}^{'}$ vs temperature at 1 kHz and 100 kHz.

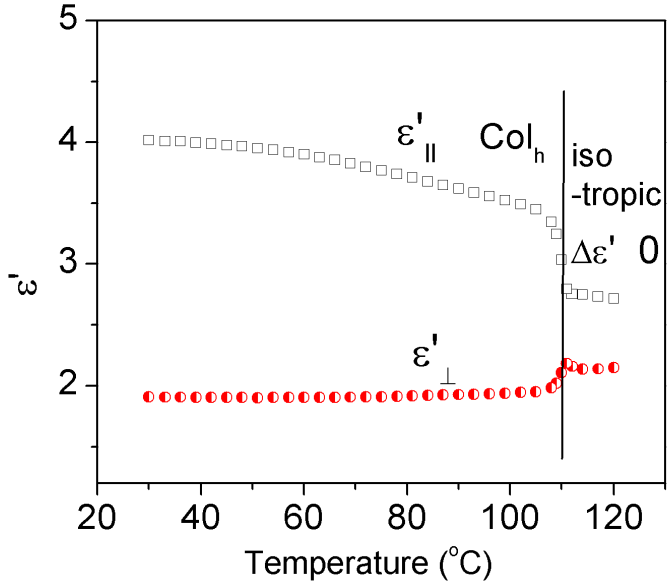

Figure 3.5 Plot of real part of permittivity $\varepsilon_{\parallel}^{'}$ and $\varepsilon_{\perp}^{'}$.

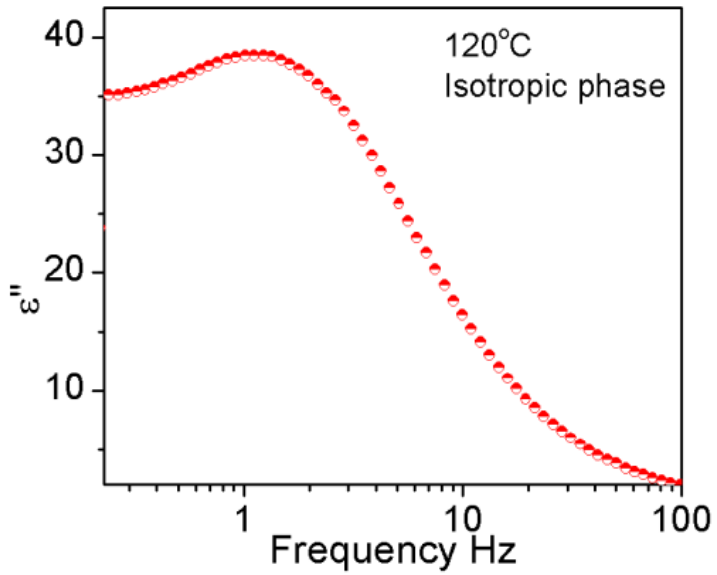

Figure 3.6 Dielectric loss ε" vs frequency at 120°C.

Relaxation curves observed at different temperatures are asymmetric in shape and are broader than ideal debye relaxation curves as shown in Figure 3.7.

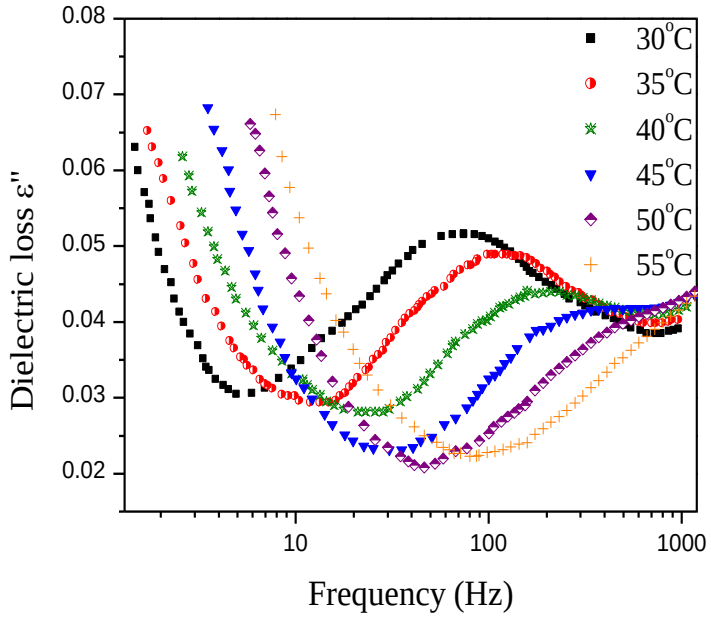

Figure 3.7 Dielectric loss (ε″) verses frequency at different temperatures for pure DLC.

Hence, frequency dependent experiments were analysed by using emphirical equation of Havrilaik and Negami (HN) to extract relaxation parameters:

$$\varepsilon^*(T,\omega,t)=\varepsilon_\infty(T,t)+\frac{\Delta\varepsilon(T,t)}{[1+(i\omega\tau_{HN}(T,t))^{\alpha(t)}]^{\beta(t)}}+\frac{\sigma_{dc}(T,t)}{i\varepsilon_f\omega} \qquad eq.2$$

Here τ_{HN} $(T,\ t)$ is the characteristic relaxation time, $\Delta\varepsilon\ (T,\ t)= \varepsilon_0\ (T,t)- \ \varepsilon_\infty(T,t)$ is the relaxation strength of the process under investigation, α, β (with limits $0<\alpha$, $\alpha\beta\leq1$) describe, respectively, the symmetrical and asymmetrical broadening of the distribution of relaxation times, σ_{dc} is the dc conductivity, and ε_f is the permittivity of free space. After fitting dielectric data using HN function, we calculated relaxation time at different temperatures. The temperature dependence of relaxation times $\tau(T)$, is shown in Figure 3.8 in the usual Arrhenius representation as a function of temperature. The data fits well to Arrhenius equation:

$$\tau = \tau_o log\left(\frac{E_a}{k_b T}\right) \qquad eq.3$$

The low temperature α process is a weak process and has Arrhenius temperature dependence. The activation energy was found to be ~ 46 kJ/mol. This process is ascribed to the local librational motion of the side chain involving the hydroxyl group of the linkage.

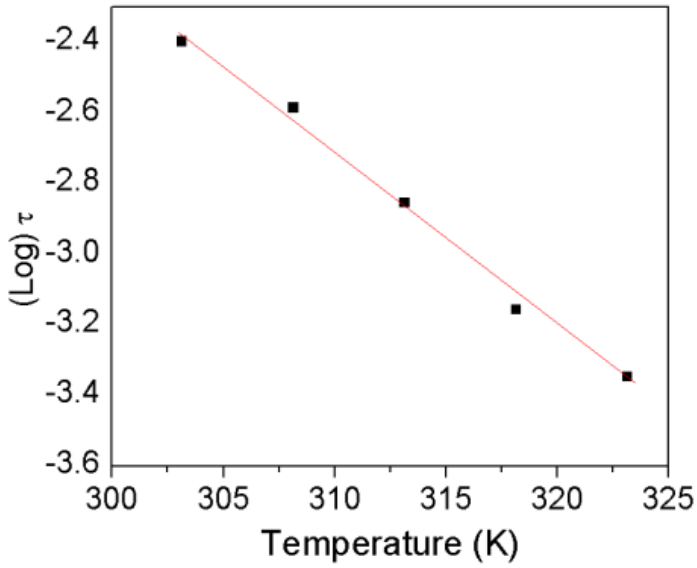

Figure 3.8 Arrhenius plot for pure DLC. Symbol (■) is experimental data and solid line is Arrhenius fit.

Effect of dc voltage on the dielectric permittivity for pure DLC was also studied upto 10 V. However no effect of dc bias field on pure DLC was observed as shown in figure 3.9.

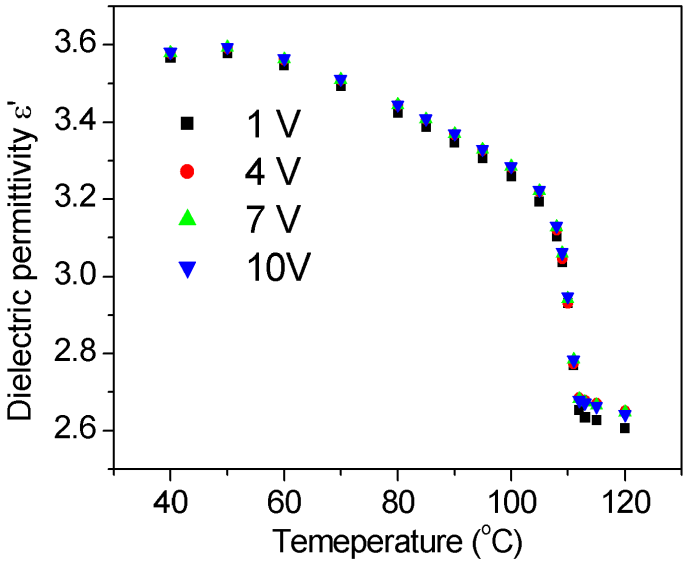

Figure 3.9 Effect of dc voltage on the dielectric permittivity ($\varepsilon'_{\parallel}$) for pure DLC.

3.1.3 Conclusions

To conclude, the compound under present study is room temperature DLC with columnar hexagonal mesophase. Homeotropic alignment was achieved in thin aligned cell yielding dielectric permittivity parallel to the column axis ($\varepsilon'_{\parallel}$). We also calculated ($\varepsilon'_{\perp}$)and found out that $\Delta\varepsilon$ was non zero. This shows that some columns still exist in isotropic fluid which was also confirmed by the new relaxation process in isotropic phase. The α-process shows Arrhenius-like temperature dependence with activation energy of 46 kJ/mol. This process is ascribed to a local librational motion of side chains. The intrinsic disc mobility can influence the charge carrier mobility. Considering the potential application of DLCs as self-healing active semiconductors, knowledge about structural disorder in DLCs in terms of their associated dynamics is essential and thus needs to be explored in detail.

Part (2)

3.2 Insertion of ZnO nanoparticles in Columanr Matrix of Discotic Liquid Crystal Based on Rufigallol Core.

Over the past several years, immense research is being carried out to improve upon the properties of liquid crystals. One technique that is being investigated a great deal currently, is the doping of NPs into liquid crystals. The inclusion of NPs into the columnar matrix of DLCs can result in novel functional materials that combine the special properties of both these materials. S. Kumar and *et. al* has previously studied the dispersion of various NPs, such as gold NPs, quantum dots and carbon nanotubes in the supramolecular order of the DLCs [31-34]. Earlier studies on doping ZnO NPs into liquid crystals have been tried out only on ferroelectric (FLC) and nematic (NLC) liquid crystals made of rod-like molecules. It has been found that the addition of ZnO NPs in FLCs, improves the optical contrast and

primarily reduces the threshold voltage of the liquid crystal display devices [35-37]. A physical model describing an interaction of ZnO NPs with the surrounding FLC molecules was given by Li and Huang [38]. Doping of ZnO NPs in surface stabilized FLCs (SSFLCs) was found to improve the alignment of the FLC molecules and a field induced reorientation process was also observed [39]. Miranda et al. investigated the role that order plays in the transfer of charge in the ZnO NPs and nematic liquid crystal system, which is considered for photovoltaic applications [40]. However, the effect of ZnO NPs on the orientational order, dielectric and other thermophysical properties of DLCs has not yet been reported. In this paper we report, for the first time, detailed experimental investigations on these properties, based on UV-Vis spectroscopy, differential scanning calorimetry, polarizing optical microscopy, dielectric measurements, infrared dichroism measurements, dc conductivity and x-ray diffraction of rufigallol based DLC doped with ZnO NPs.

3.2.1 Experimental Procedure

a) Synthesis of Pure ZnO:

The ZnO NPs used in the present study were synthesized in an alcoholic medium at room temperature by using zinc acetate and sodium hydroxide. In order to achieve first objective samples of pure Zinc Oxide has been prepared by base catalyzed reaction using co-precipitation method. Zinc Acetate (Loba Chemie, purity 98.0%), Ethanol (Merck, purity 99.9%) and Sodium Hydroxide (Loba Chemie, purity 98.0%) were the materials used as a precursor, solvent and base for the synthesis of ZnO. All the materials were used as received without any purification.

For the synthesis of ZnO NPs, 0.01 mole of Zinc Acetate [$Zn(CH_3CO_2)_2.2H_2O$] was dissolved in 100 ml of ethanol. Temperature of the reaction was maintained at 70^oC along

with continuous stirring for two hours. After that about 0.02 mole of NaOH added in the solution to adjust pH in basic region (10.82).The solution turned milky and the reaction mixture was then stirred for another two hours. The precipitate thus obtained were filtered out and washed with ethanol several times. Finally, the obtained product was heated in the oven at 90^{o}C for four hours to remove the excess solvent and other residue material. The dried product was collected and grinded to make fine powder and finally characterized with many techniques. For more details on the synthesis and characterization of ZnO NPs see reference [41]. The characteristic size of synthesized ZnO NPs was estimated by TEM (Figure 3.10). TEM images were recorded with Hitachi H-7500 Electron microscope. For imaging the NPs, freshly ultrasonicated very dilute solution of NPs in ethanol was drop cast on carbon coated copper grid. ZnO NPs possess high surface energy and therefore have a tendency to agglomerate. TEM image (Figure 3.10) therefore shows some agglomeration of the NPs. The average particle size was found to be ~ 6nm.

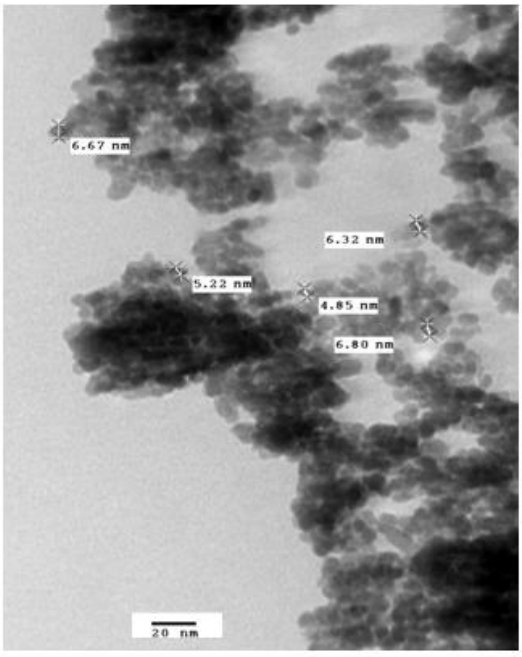

Figure 3.10 TEM image of ZnO NPs

(b) Preparation of Dispersion of ZnO NPs in DLC Columnar Matrix

The DLC material chosen for the present study is 2, 3, 6, 7-tetrakis (3, 7-dimethyloctyloxy)-1, 5-dihydroxyanthracene-9,10-dione, was synthesized as reported earlier [42]. It is a room temperature hexagonal columnar DLC. The structure of the molecule is shown in Figure 3.1.

To disperse ZnO NPs in DLC, first DLC was dissolved in chloroform and sonicated with optimized weight ratio of ZnO NPs for two hours to obtain uniform mixtures and slow evaporation of the solvent resulted in the formation of a dispersion. We prepared samples with three different compositions for the purpose of comparison, using 0.125%, 0.25% and 0.4% by weight of ZnO NPs with the DLC.

3.2.2 Characterizations

The composites were characterized using polarizing optical microscopy (POM), small-angle X-ray scattering (SAXS), differential scanning calorimetry (DSC), Visible absorbance spectroscopy, dielectric spectroscopy, infrared (IR) dichroism technique and electrical conductivity measurements.

The transition temperature and associated enthalpy values were determined using DSC (DSC; Perkin Elmer, Model Pyres 1D), which was operated at a scanning rate of 5^{o}Cmin-1 both on cooling and heating. The apparatus was initially calibrated using indium (156.5^{o}C) as a standard. The textural observations of the mesophase were carried out using polarizing light microscopy (Olympus BX51) combined with a heating stage (Mettler FP82HT) and a central processor (Mettler FP90). Small angle X-ray diffraction (SAXS) was carried out on powder samples using Cu-Kα (λ=1.54Å) radiation from a Rigaku ultrax 18 rotating anode generator (4Kw) monochromator with a graphite crystal. The samples were held in sealed Lindemann capillary tubes (0.7mm diameter). Absorbance spectra were taken using Perkin Elmer,

Lambda 35 UV/VIS spectrometer. IR dichroism measurements were carried out using the IR spectrophotometer FTIR-8400 from Shimadzu. The sample was taken between CaF_2 substrates which had been coated with a thin film of nylon 6/9. A 12 μm mylar spacer was used to maintain a uniform thickness of the sample. Slow cooling of the sample from the isotropic phase yielded good homeotropic alignment. The spectra were obtained first in the isotropic phase and at various temperatures in the columnar phase. The dichroic ratio was calculated using the integrated absorption intensities corresponding to the C-C stretching mode and the corresponding order parameters obtained as a function of temperature in both the pure DLC and the composite with 0.4% of ZnO NPs. Dielectric measurements were carried out using Nova control Impedance analyzer in the frequency range 1 Hz to 10 MHz and the temperature of the sample was varied using Eurotherm temperature controller. Experiments were carried out in the temperature range 30^{o}C to 120^{o}C. Dielectric isotherm spectra were measured every 5^{o}C. Before each frequency scan, the temperature was kept constant to within ~0.1^{o}C. The dc conductivity studies were carried out in ITO-coated glass sandwich cells (8mm×8mm) with thickness of 10 μm. The samples were introduced via capillary action by heating to the isotropic phase. Current measurements were carried out using a Keithley picoammeter (model 480) along with a constant voltage source and a temperature controller. The resistance values were based on the measured current at different temperatures.

3.2.3 Results and Discussion

3.2.3.1 Mesomorphic Behaviour

POM and DSC are complementary techniques to confirm the liquid crystalline nature of the sample. POM and DSC results show that the composite systems are mesomorphic in nature.

Generally in pure discotic liquid crystals (DLC), there can be two possibilities to align the disc-like molecules. If the column axis is in the plane of the electrode, the alignment is called planar alignment (or edge on) and when the disc column axis is perpendicular to electrode surface, it is called homeotropic alignment (or face on) [43-45]. In the present case when the sample was taken in a thin (5μm) cell homeotropic alignment was obtained on slow cooling from isotropic phase and the alignment thus obtained is stable throughout the mesophase range as confirmed by the dark field view under crossed polarizers at different temperature (Figure 3.11).

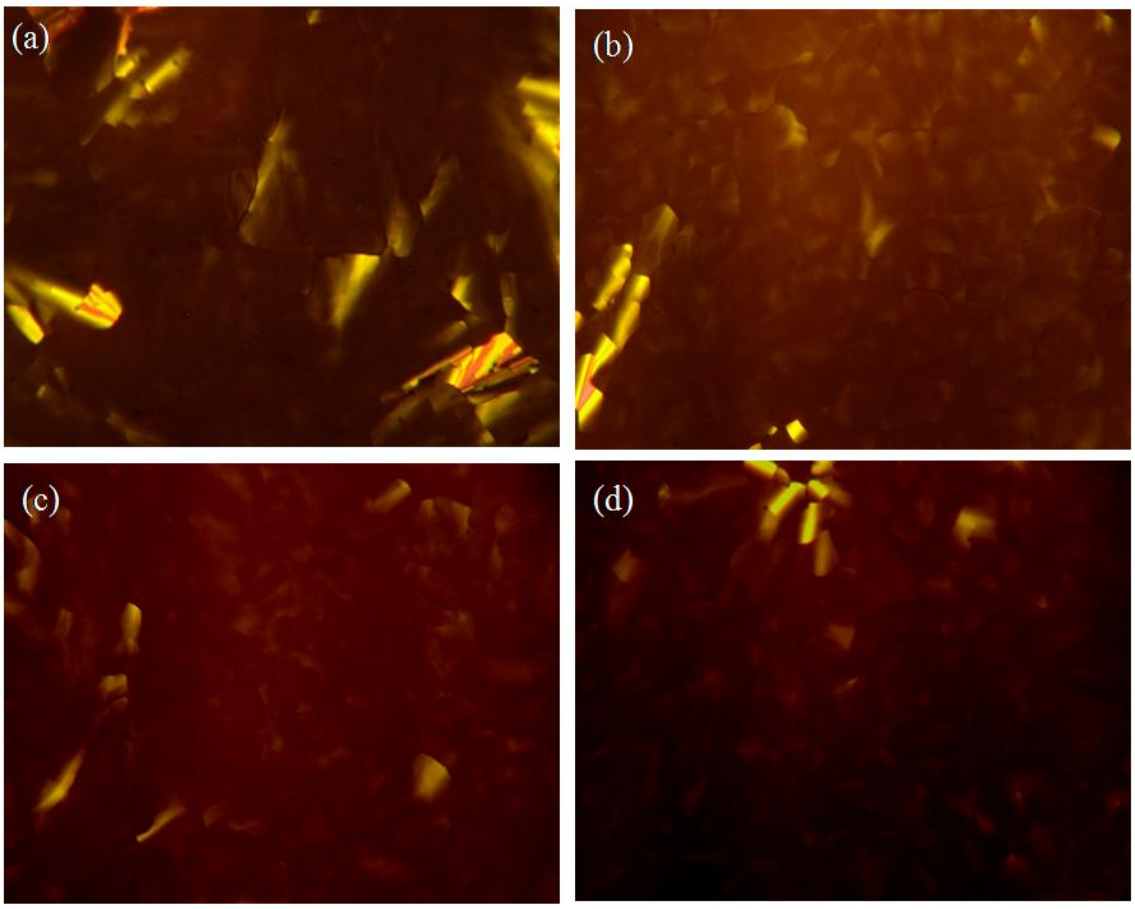

Figure 3. 11 POM images of (a) pure discotic liquid crystal, (b) 0.125%, (c) 0.25% and (d) 0.4% ZnO nanoparticles in columnar matrix at 30^{o}C.

POM images clearly show that the ZnO NPs are well dispersed in columnar phase as there is no evidence for any aggregation, while the homeotropic alignment is preserved. In fact the homeotropic alignment appears to be better with the addition of the NPs, as the defects are fewer in number.

Figure 3.12 shows the DSC data for the pure and the composite systems. It is clear, from the scans that phase transition profiles are not significantly changed even after the addition of NPs at low concentrations and the isotropic phase transition temperature of composites is not significantly altered. The increase of ~ 1^0C in the columnar to isotropic phase transition temperature for the composite with 0.4% of ZnO NPs indicates that the range of the columnar phase is slightly increased. This shows that the columnar phase is not destabilized by the addition of the NPs.

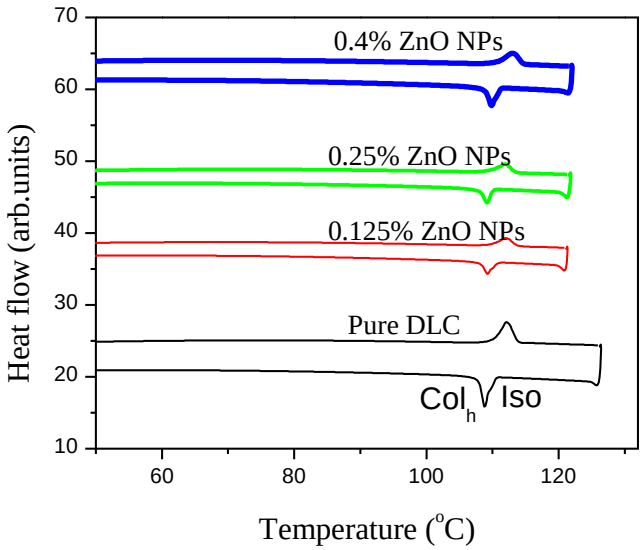

Figure 3.12 DSC thermogram of pure DLC and composite systems.

3.2.3.2 SAXS

The X-ray diffraction patterns were recorded for the pure DLC and the composite system under the same conditions in the columnar phase. The sample was cooled from the isotropic phase and the diffraction patterns obtained at 95^{o}C and at room temperature. The diffraction patterns obtained at 95^{o}C and room temperature are almost similar. The variation of the scattering intensity as a function of scattering angle 2θ for the composite system having 0.4% of ZnO NPs at 95^{o}C is shown in Figure 3.13.

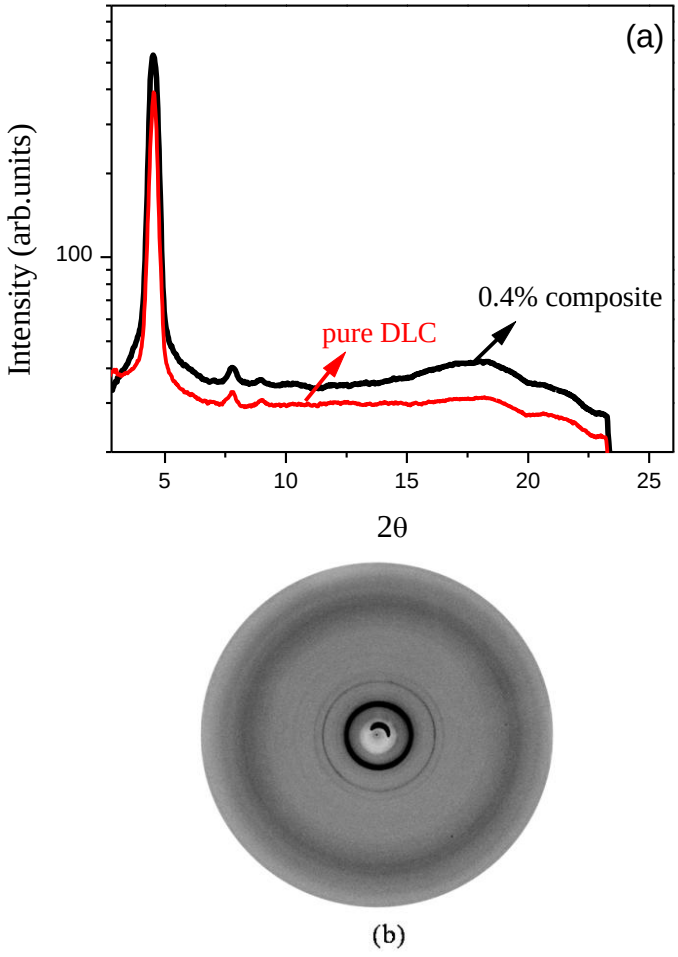

Figure 3.13 (a) One dimensional intensity *vs* 2θ for pure DLC and 0.4% composite system (b) XRD pattern of 0.4% composite system at 95^{o}C.

The overall features observed in all cases are in good agreement with two dimensional columnar hexagonal phase. Periodicities within the hexagonal lattice give rise to sharp low angle peaks corresponding to (10), (11) and (20) Bragg's peaks with d-spacing of 19 Å. In contrast, two broad peaks appear in the wide angle region, one corresponding to the liquid like character of highly disordered alkyl chains and the other to core-core correlation. The obtained values for the composite systems are almost similar to the pure DLC [42]. This is because the concentration of the ZnO NPs is too small in the composites to cause any major changes to the hexagonal lattice of the DLC. Similar results were found with insertion of CdSe quantum dots and gold NPs in the columnar matrix.

3.2.3.3 Absorbance Studies

Absorbance spectral studies in the visible region were carried out on the DLC, ZnO NPs and the composite in chloroform medium using pure chloroform as reference. Figure 3.14 shows the absorbance spectra of pure DLC and the composite systems. The pure ZnO NPs show a peak ~ 370 nm as seen in the inset of Figure 3.14.

In the case of the composites, in addition to the peak exhibited by the pure DLC ~ 290nm, another peak which becomes more prominent with increasing concentration of the NPs can be observed in the wavelength region 275-285 nm. It can be attributed to the presence of the ZnO NPs in the composite systems. However the peak shows a blue shift of the wavelength which most likely arises from the formation of weak charge transfer complexes between electron deficient core of the disc-like molecules and ZnO NPs.

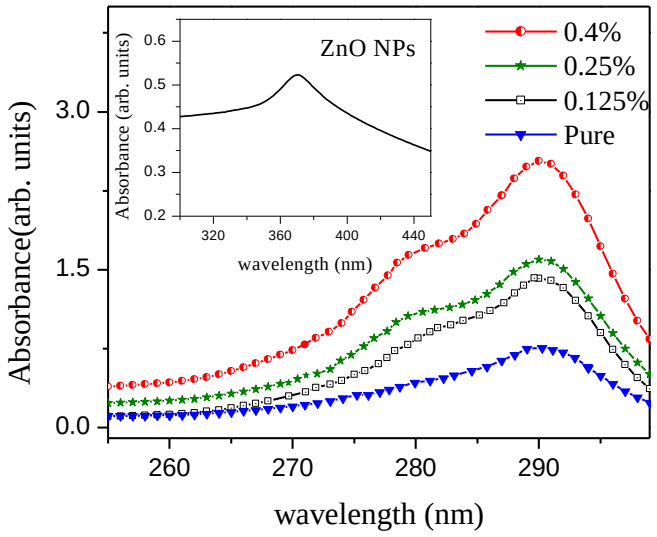

Figure 3.14 Visible absorbance spectra of pure DLC and composite systems. Inset of figure shows the absorbance in the visible region for pure ZnO NPs.

3.2.2.4 IR Dischroic Technique

The infrared (IR) dichroism technique can be used to measure the orientational order parameter (S) in a liquid crystal. In the case of a discotic LC [43]

$$S = \tfrac{1}{2}(3\cos^2 \Phi - 1) \qquad eq.4$$

where Φ is the angle made by the local director and the column axis (Figure 3.15 (a)) and δ is the angle between the transition dipole moment p_i and the normal to the core [44]. When unpolarized IR radiation is used, the dichroic ratio is given by $R = {}^{I_{DLC}}/_{I_{Iso}}$ where I_{DLC} and I_{Iso} are the integrated absorption intensities in the liquid crystalline and isotropic phases respectively. In the case of the C-C in plane stretching vibration, $\delta = 90^o$ and

$$S = 2(R-1) \qquad eq.\ 5$$

and for the out of plane vibrations corresponding to C-H, $\delta = 0^o$ and

$$S = 1\text{-}R. \qquad \text{eq. 6}$$

Figure 3. 13 (a) shows the schematic representation of the interaction of the IR beam with a discotic molecule in the face on alignment geometry. In DLC, the IR band near 1600 cm^{-1} corresponding to C-C aromatic stretching vibration has been found to be a sensitive indicator of ordering [46]. The IR dichroism technique is a convenient method which can be used to measure the molecular order parameter corresponding to the disc-like molecules in both the pure DLC and in the composites with ZnO NPs by using IR bands exclusively present in the disc –like molecules. In the present study the order parameter corresponding to the disc-like molecules was measured using the IR band 1617cm^{-1} in both the pure DLC and in the composite with 0.4% ZnO NPs as the sample was cooled from the isotropic phase.

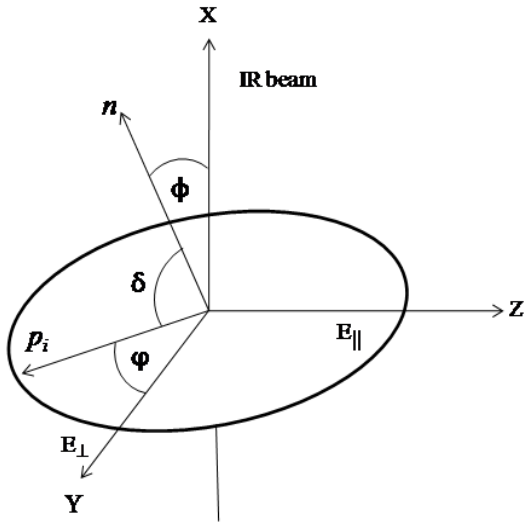

(a)

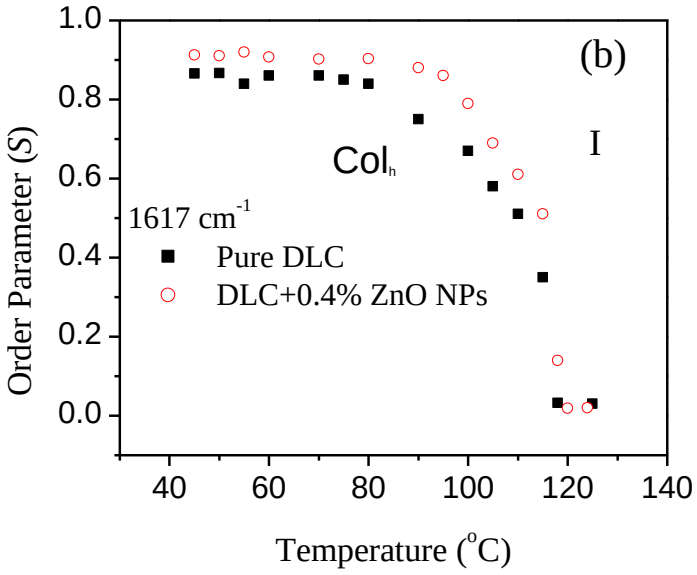

Figure 3.15 (a) Schematic representation of the interaction of the IR beam with a disc-like molecule for homeotropic alignment (b) Plot of order parameter versus temperature showing enhancement of order parameter corresponding to the disc-like molecules in the composite with 0.4% ZnO NPs for C-O-C symmetric vibrations at 1617 cm^{-1}.

A plot of *S* versus temperature [Figure 3.15(b)] shows enhancement of *S* for the composite with 0.4% ZnO NPs. The increase in the measured order parameter corresponding to the disc-like molecules, in the composite as compared to that in the pure DLC, implies that the orientation of the individual columns along the director also improves, which results in a better homeotropic alignment.

3.2.2.5 Dielectric Spectroscopy

Dielectric spectroscopy is widely used to study the molecular dynamics and phase behavior of thermotropic liquid crystals. As the dielectric properties are sensitive to the local electric

field distribution in the sample, measurements of temperature and frequency dependent dielectric constants and loss can yield information about structural changes.

The real ε' and imaginary parts ε'' of the complex permittivity ε^* of pure and composite systems were measured as a function of temperature at a fixed frequency and also as a function of frequency at a given temperature T. The isotropic to columnar phase transition was manifested as a step in the variation of $\varepsilon'_{\parallel}$ with temperature as shown in Figure 3.16.

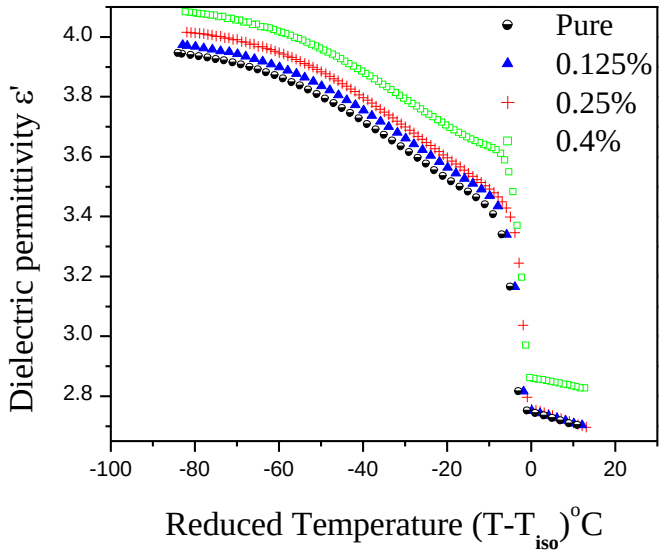

Figure 3.16 Dielectric permittivity ε' as function of reduced temperatures for pure and composite systems.

With the increase in the concentration of NPs, the value of dielectric permittivity ε' increases. As indicated by the increase in the orientational order parameter measured using IR dichroism an improved stacking of the discs within the columns is obtained. It can therefore be expected that the component of the dielectric permittivity measured parallel to the column axis in the homeotropic sample also increases.

As discussed in section 3.1.2.3 we observed that a weak relaxation peak starts appearing at a temperature of 50°C in the frequency range 4 Hz to 900 Hz for pure DLC and the peak shifts to lower frequency with decrease in temperature. However, measured dielectric data above 1 MHz is mainly affected by ITO resistance from the cell [47].

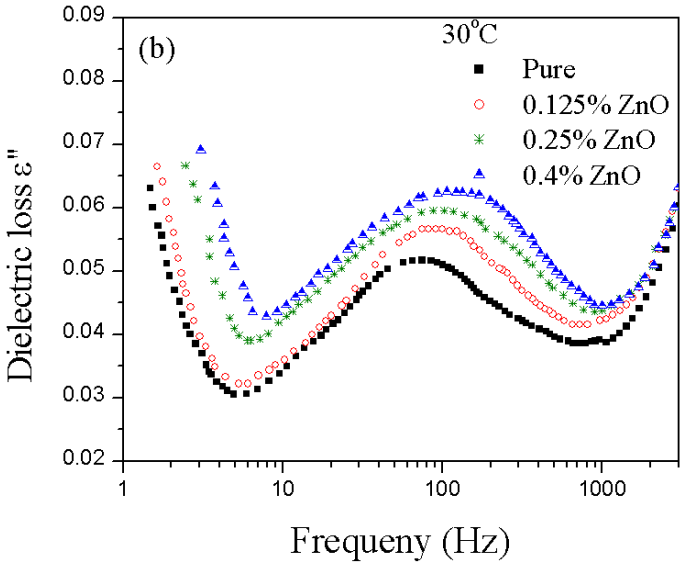

Figure 3.17 Dielectric loss ε'' as a function of frequency for composite systems at 30°C in frequency range of 4 Hz to 900 Hz.

Figure 3.17 shows ε'' as a function of frequency for the pure DLC and composite systems at 30°C in frequency range of 4 Hz to 900 Hz. It is evident that the composite systems show a nearly identical frequency response to that of the pure DLC. This shows that the molecular motions related with the DLC molecules are not affected by the insertion of the NPs.

These loss curves are broader than the ideal Debye relaxation. As the sample is cooled slowly from isotropic phase, the molecules start aligning along the column axis. We found that with increase in the concentration of ZnO NPs, there is slight increase in the value of imaginary

part ε″ of the permittivity and the relaxation peak shifts to higher frequency with increasing concentration of NPs.

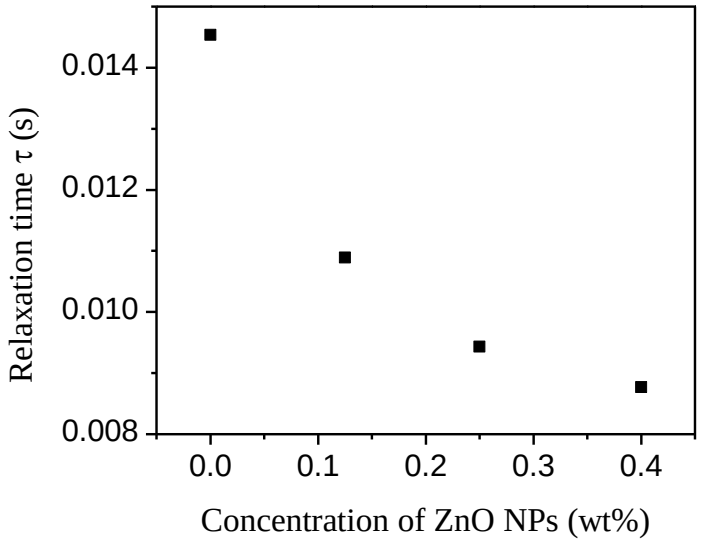

Figure 3.18 Variation of dielectric relaxation time with concentration of ZnO NPs at 30^{o}C.

As the composite consisting of the DLC and the ZnO NPs is a heterogeneous medium, the dielectric dispersion can be described by the Maxwell-Wagner (M-W) theory [48,49]. This theory gives the relationship between the complex dielectric constant of the host medium, the embedded NPs and the volume occupation factor of the NPs. Kobayashi et al. [50,51] have extended this theory to LCs doped with NPs, by considering an equivalent circuit model. In the present system the increase in the imaginary part of the dielectric permittivity and the shift of the relaxation frequency to higher frequencies is in accordance with this model. The dependence of relaxation time (τ) on the concentration of ZnO NPs as shown in Figure 3.18 is in agreement with this theory.

Effect of dc voltage on the dielectric permittivity for pure and composite systems was also studied upto 10 V. However no effect of dc bias field on either the pure or composite systems was observed.

3.2.2.6 dc Conductivity

Generally in discotic materials, doping with NPs increases the conductivity [31-34,52]. A similar effect could be observed by doping the present DLCs with ZnO NPs. The dc conductivity of the empty cell was first measured and found to be very negligible. Measurements were then carried out on the pure DLC and the composite systems as a function of temperature. An increment was found in the conductivity of the dispersed system and the increase was found to be dependent on the concentration of NPs. Figure 3.19 shows the dc conductivity plot of pure and composite systems. The dc conductivity of the pure DLC sample is very low and is of the order of 10^{-10}-10^{-11} Sm^{-1}.

With 0.4% of NPs, the conductivity increases by ten times at 80^{o}C. This can be explained as due to the charge transport that takes place after the addition of NPs. Precise interpretations of electron mobility within the columns along with the conductivity of ZnO NPs needs time of flight (TOF) measurements which will be taken up in future.

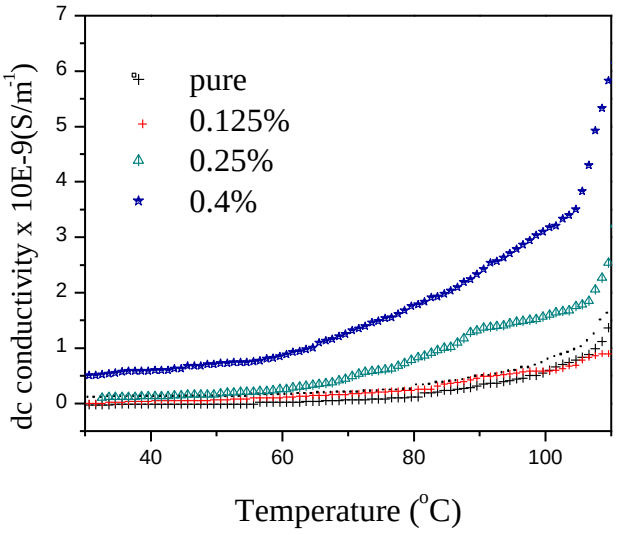

Figure 3.19 Temperature variation of dc conductivity of pure and composite systems.

3.2.3 Conclusions

The sample under the present study 2,3,6,7-tetrakis(3,7-di-methyloctyloxy)-1,5-dihydroxyanthracene -9,10-dioneis a room temperature discotic liquid crystal (DLC) with a wide range of the hexagonal columnar mesophase. ZnO NPs were dispersed in pure DLC matrix in different (wt/wt%) ratios. Dielectric and other thermophysical studies were carried out for pure and dispersed systems. POM, DSC and SAXS results showed the uniform inclusion of NPs in the discotic liquid crystalline matrix. Insertion of NPs brought order and stability in DLC matrix, which was confirmed by DSC, POM, dielectric and IR dichroism measurements. However, the hexagonal columnar structure of DLC is not affected by the NPs as confirmed by XRD and POM results. There is increase in the value of real part and imaginary part of permittivity and the dielectric loss peak shifts to higher frequency with increasing concentration of NPs. The variation of the relaxation time with concentration of

NPs is in accordance with the theory of heterogeneous dielectrics. The increase in the permittivity measured parallel to the column axis with the addition of the NPs also implies that the stacking of the discs within the columns improves, leading to better homeotropic alignment. IR dichroism measurements showed increase in the order parameter of DLC with 0.4% of ZnO NPs. Conductivity measurements showed that there is increase in conductivity by one order of magnitude with 0.4% of ZnO NPs. The reports of DLCs with potentially attractive properties are extensive. However, very less work for the optimization of their properties has been done. These inorganic-organic liquid crystal hybrid systems may be extremely important for many device applications such as photovoltaic solar cell, photoconduction, light emitting diodes, thin film transistors etc.

References

[1] S. Chandrasekhar, B. K. Sadashiva and K. A. Suresh, *Pramana*, 9, 47, (1977).

[2] S. Kumar; *Chem. Soc. Rev*., 35, 83, (2006).

[3] S. Kumar; *Liq. Cryst.*, 32, 1089, (2005).

[4] S. Kumar; *Liq. Cryst.*, 31, 1037, (2004).

[5] B. Donnio, D. Guillion, R. Deschenaux, D. W. Bruce; *Comp. Coord. Chem*., 7, 357, (2003).

[6] C. Tschierske, Annu. Rep. Prog. Chem., Sect. C, 97, 191, (2001).

[7] R. J. Bushby, O. R. Lozman; *Curr. Opin. Colloid Interface Sci.*, 7, 343, (2002).

[8] D. Demus, J. Goodby, G. W Gray, H.W. Spiess, V. Vill (Eds.). *Handbook of Liquid Crystals, Wiley-VCH: Weinheim*, Germany, Vol. 2B (1998).

[9] S. Kumar; *Chemistry of Discotic Liquid Crystals: From Monomers to Polymers*, CRC Press, Boca Raton, FL, (2011).

[10] S. Sergeyev, W. Pisula, Y. H. Geerts; *Chem. Soc. Rev*., 36, 1902, (2007).

[11] B. R. Kaafarani; *Chem. Mater*., 23, 378, (2011).

[12]. R. J. Bushby, K. Kawata; *Liq. Cryst.*, 38, 11, 1415, (2011)

[13] N. Tasios, C. Grigoriadis, M. R. Hansen, H. Wonneberger, C. Li, H. W. Spiess, K. Mullen, G. Floudas, *J. Am. Chem. Soc.*, 132, 7878, (2010).

[14] J. Leisen, M. Werth, C. Boeffel, H. W. Spiess, *J. Chem. Phys.* 97, 3749, (1992).

[15] S. U. Vallerien, M. Werth, F. Kremer, H. W. Spiess, *Liq. Cryst.*, 8, 889, (1990).

[16] M. M. Elmahdy, G. Floudas, M. Kastler, K. Mullen, *J. Phys. C*, 20, 244105, (2008).

[17] M. M. Elmahdy, G. Floudas, M. Mondeshki, H. W. Spiess, X. Dou, K. Mullen, *Phys. Rev. Lett*., 100, 107801, (2008).

[18] M. M. Elmahdy, X. Dou, M. Mondeshki, G. Floudas, H-J Butt, H. W Spiess, K. Mullen, *J. Am. Chem. Soc.*, 130, 5311, (2008).

[19] R. Dhar, S. Kumar, M. Gupta, V.K. Agrawal, *J. Mol. Liq.*, 141, 19, (2008).

[20] H. K. Bisoyi and S. Kumar, *Tet. Lett*., 48, 4399, (2007).

[21] Supreet, S. Kumar , K.K. Raina, R. Pratibha *Liq. Cryst.*, 40, 2, 228, (2013).

[22] H. Groothues, F. Kremer, D. M. Collard, and C. P. Lillya, *Liq. Cryst.*, 18, 117, (1995).

[23] W. Haase, D. Kilian, M. A. Athanassopoulo, D. Knawby, T. M. Swager, S. Wrobel. *Liq Cryst*., 29,133, (2002).

[24] H. Zheng, P. J. Carroll, T. M. Swager. *Liq Cryst*.,14,1421, (1993).

[25] U. Dahn, C. Erdelen, H. Ringsdorf, R. Festag, J. H. Wendorff, P. A. Heiney, N. C. Maliszewskyj, *Liq Cryst*.,19, 759, (1995).

[26] B. Glusen, W. Heitz, A. Kettner, J. H. Wendorff, *Liq Cryst*., 20, 627, (1996).

[27] B. Palacios, M. R. De La Fuente, M. A. P Jubindo, R. Iglesias, J. L. Serrano, T. Sierra, *Liq Cryst*., 25, 481 (1998).

[28] R. Dhar, M. Gupta, V. K. Agrawal, S. Kumar, *Phase Transitions*. 81, 459, (2008).

[29] M. M. Elmahdy, G. Floudas, M. Mondeshki, H. W. Spiess, X. Dou, and K. Mullen, PRL, 100, 107801, (2008) and references there in.

[30] Shri Singh. *Liquid Crystals: Fundamentals. World Scientific, Science*; 2002.

[31] S. Kumar, V. Lakshminarayanan, *Chem Commun*. 14, 1600 (2004).

[32] S. Kumar, H. K. Bisoyi, *Angew Chem. Int. Ed.*, 46, 1501, (2007).

[33] H. K. Bisoyi, S. Kumar, *J. Mater. Chem.* 18, 3032, (2008).

[34] S. Kumar, L. K. Sagar, *Chem Commun.*, 47, 12182, (2011).

[35] H. Jiang, N. Toshima, *Chem. Lett*., 38, 566 (2009).

[36] T. Joshi, A. Kumar, J. Prakash, A. M. Biradar, *Appl Phys Lett.*, 96, 253109, (2010).

[37] A. Malik, A. Choudhary, P. Silotia, A. M. Biradar, *J. Apl. Phys*., 110, 064111 (2011).

[38] L. S. Li, J. Y. Huang, *J Phys D Appl Phys.*, 42, 125413 (2009).

[39] J. Y. Huang, L. S. Li, M. C. Chen, *J Phys Chem C.*, 112, 5410 (2008).

[40] L. J. Martinez-Miranda, K. M. Traister, I. Melendez- Rodriguez, Salamanca-Riba, *Appl Phys Lett.*, 97,223301 (2010).

[41] Z. L.S. Seow, A. W. Wong, V. Thavasi, R. Jose, S. Ramakrishna, G. W. Ho, Nanotechnology, 20, 045604 (2009).

[42] H. K. Bisoyi, S. Kumar, *Tetrahedron Lett.*, 48, 4399, (2007).

[43] J. K. Vij, T. S. Perova, A. Kocot, *Mol Cryst Liq Cryst.*, 397, 531 (2003).

[44] T. S. Perova, J. K. Vij,. *Adv Mater.*, 7, 919 (1995).

[45] T. S. Perova, A. Kocot, J. K. Vij, *EPL*., 44, 198 (1998).

[46] G. Kruk, A. Kocot, R. Wrzalik, J. K. Vij, O. Karthaus, H. Ringsdorf, *Liq Cryst.* 14, 807, (1993)

[47] P. Perkowski, *Phase Transitions,* 83, 836 (2010).

[48] J. C. Maxwell, Treatise on electricity and magnetism, vol 1. New York, Dover, (1945).

[49] K. W. Wagner, *Erkl Arch Electrorech*., 2, 371, (1914).

[50] J. Thisayukta, H. Shiraki, Y. Sakai, T. Masumi, S. Kundu, Y. Shiraishi, N. Toshima, S. Kobayashi, *Jap J Appl Phys*., 43, 5430 (2004).

[51] S. Kobayashi, T. Miyama, N. Nishida, Y. Sakai, H. Shiraki, Y. Shiraishi, N. Toshima, *J Display Tech.* 2, 121 (2006).

[52] L. A. Holt, R. J. Bushby, S. D. Evans, A. Burgess, G. Seeley G. *J Appl Phys*., 103, 063712 (2008).

Chapter 4

Dispersion of Gold Nanoparticles in Discotic Liquid Crystals Comprise of Triphenylene Core

Abstract: Chapter 4 discusses the synthesis of hexanethiolate-stabilized gold nanoparticles (GNPs) and their dispersion in hexaalkyloxytriphenylene H10T (compound **1**) and mono nitro substituted triphenylene based discotic liquid (MNTP4) (compound **2**). Compound **1** is a room temperature crystalline material and shows wide range of columnar hexagonal mesophase (Col_h). Whereas, compound **2** shows columnar plastic phase along with columnar hexagonal phase at higher temperature before going to isotropic phase. This chapter is also divided into two part. Part (1) deals with the dispersion of GNPs in symmetrically substituted hexaalkyloxytriphenylene (HATn), n=10. POM, DSC and dielectric results show that GNPs are well dispersed into the columnar matrix without affecting the hexagonal arrangements of columns of DLC. Part (2) deals with the dispersion of GNPs in mono nitro substituted triphenylene based discotic liquid (MNTP4) (compound **2**). DSC, POM, XRD, IR-dichroic technique, dielectric spectroscopy results show the inclusion of GNPs in DLC matrix. The nature of mesophases is not altered by GNPs but a shift in transition temperature was observed. Though there is decrease in order parameter and the disc motion about the column axis is hindered, dc conductivity increases with GNPs. These GNP-DLC composite systems may be important for many device applications such as photovoltaic solar cell, photoconduction, light emitting diodes, thin film transistors etc.

4.1 Introduction and Background

Gold has always been the topic of interest from ancient times. With advancement in the technology, there is exponential increase in the nanoscience and nanotechnology with gold nanoparticles (GNPs). When the nanoparticle size ranges between 1-10nm, the resulting physical properties are quite different from those of bulk materials and GNPs of 1-2 nm become semiconducting [1]. Moreover when GNPs are protected by organic shells, they become stable and find numerous applications towards biology, catalysis, sensors, nanotechnology etc. [2-4].

On the other hand, as discussed in chapter 1 liquid crystals are very fascinating materials because of the unique properties they possess such as long range order, co-operative effects and anisotropic nature in optical and electronic properties based on the self organizing nature in a certain temperature range with fluidity. In discotic liquid crystals (DLCs), the self-assembly of disc-shaped molecules results in one-dimensional columns, and these columns then generally self-assemble to form two-dimensional hexagonal lattices. The columns are well insulated from the neighbouring columns by insulating alkyl chains attached to the discotic core and form quasi one-dimensional molecular conducting wires [5–9]. The most widely studied core system in the field of DLCs is triphenylene (TP) [10]. The inclusion of gold nanoparticles in discotic liquid crystals is a very fascinating from the point of the view that it provides material that possess the metallic properties of nanoparticles as well as the self assembly, self healing(dynamics), ease of processing, high charge carrier mobility of DLCs [11-13] which may be useful for many device applications.

There are some previous reports on intercalation of GNPs in DLCs. Kumar *et al*. reported the synthesis and thermal studies on hexanethiol stabilized gold nanoparticles (GNPs) included

into the discotic liquid crystal namely hexahexylthiotriphenylene (HHTT) [14]. They observed that increasing the amount of GNPs in this discotic liquid crystal decreases the isotropic transition temperatures but have negligible effect on the crystal to mesophase or mesophase to mesophase temperatures. Based on this, it was suggested that the GNPs might have been included between the aromatic cores of the discotic liquid crystal and the π-π interactions of aromatic cores are primarily responsible for holding the nanoparticles in the column. They also prepared several mixtures of hexanethiolate capped gold nanoparticles and discotic liquid crystals. Further, preliminary results on GNPs:HHTT (1:1 wt%) showed that the conductivity is 250 times enhanced with respect to that of the pure HHTT [15]. Mikio Miyake *et al.* synthesized gold nanoparticles fully coated with discotic liquid crystalline molecules of hexaalkoxy-substituted triphenylene (Au–TP), the self-assembled structure of which could be controlled (hexagonal or 1D nanochain) just by altering the ratio of methanol to toluene in the solvent[16]. Kumar *et al*. synthesized gold nanoparticles fully covered with triphenylene-based discotic liquid crystals (DLCs) and dispersed them in a columnar matrix. The presence of the gold nanoparticles in the triphenylene-based DLCs did not disturb the nature of the mesophase other than altering the transition temperatures. They proposed that the gold nanoparticles were distributed between the domain gaps of the DLCs in random disordered manner. Interestingly the DC conductivity measurements showed an enhancement of the electrical conductivity by more than a million times upon doping of the discotic liquid crystals with the triphenylene-capped nanoparticles under ambient conditions [17]. Holt *et al.* also reported a 10^6-fold enhancement in the conductivity of hexakis(hexyloxy)triphenylene doped with 1% methylbenzene thiol-coated gold nanoparticles .This increase in conductivity was attributed to the formation of chains of gold

nanoparticles upon applying a DC field [18]. Vijayaraghavan *et al.* carried out SAXS, magnetic susceptibility and DC conductivity studies on hexanethiol covered gold nanoparticles-HHTT composites. TEM image showed the nanoparticles are predominantly of size 1.2 nm. However, there were few GNPs with sizes 2.6nm and 4.6 nm. They inferred from SAX studies that the smaller 1.2nm GNPs were randomly distributed in the liquid crystal matrix within the discotic columns as well as between the columns and strains the hexagonal lattice of the liquid crystal. The nanoparticles between the columns in the composite shifted the SAXS pattern to the low q region indicating an increase in the intercolumnar spacing. The bigger 2.6 and 4.6nm particles independently formed 2D intercalated hexagonal lattices with the disc molecules of HHTT. These intercalated hexagonal lattices co-exist with the HHTT lattice. They believed that the 1.2nm GNPs within the discotic columns were held between the aromatic cores of the disc molecules due to π-π interactions between the aromatic cores. The magnetic susceptibility increases with decrease in temperature in both the pure HHTT and 1:4 composite. We have related the temperature dependence of magnetic susceptibility to the ordering of the triphenylene cores along the columns. We found a marked increase in the susceptibility and about three orders of magnitude increase in the conductivity in the crystalline phase of the GNPs:HHTT (1:4 wt%) composite. They proposed that large enhancement in the core-core ordering along the column axis in the crystalline phase of the composite with respect to its high temperature phases may be responsible for this behavior [19]. Also, dispersion of gold nanoparticles in rod-like systems is studied well [20–22].

4. 2 Experimental Procedure

(a) Synthesis of Thiol Coated Gold Nanoparticles

Gold nanoparticles (GNPs) covered with hexanethiolate monolayer were synthesised by following the literature method [14, 15 23, 24]. In brief, a solution of tetraoctylammonium bromide (1.1 g) in toluene (65 mL) was added with stirring to a solution of 158 mg of $HAuCl_4.3H_2O$. This solution was stirred for 20 min and mixed with n-hexanethiol (142 mg) with further stirring for 10 min. A solution of 450 mg of NaBH4 dissolved in 5 mL of water was added to the above mixture. The reaction mixture was stirred at room temperature for 24 h. The organic phase was separated, evaporated to about 2-3 mL in a rotary evaporator under vacuum at room temperature, mixed with 50 mL of ethanol and centrifuged at 5000 rpm for 1 h. The supernatant liquid was removed and the resulting hexanethiol-protected gold nanoparticles were dissolved in about 1 mL of dichloromethane and precipitated with ethanol. The centrifugation and re-dispersal process was repeated several times to ensure the complete removal of noncovalently bound organic material. Removal of the solvent afforded 60 mg of hexanethiol-capped gold nanoparticles (C_6GNP). It has been shown that this procedure results in the formation of GNPs with an average composition of $Au_{140}[S(CH_2)_5\text{-}CH_3]_{53}$ [23].

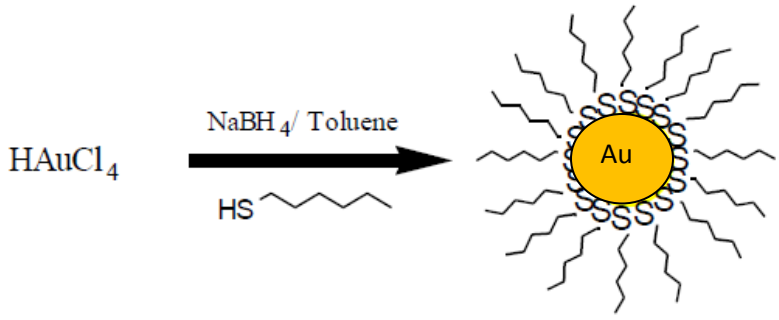

Figure 4. 1 Scheme of preparation of hexanethiolate-covered gold nanoparticles.

(b) Preparation of Dispersion of GNPs in DLC Columnar Matrix

The DLC materials chosen for the present study are symmetrically substituted hexaalkyloxytriphenylene (HATn), n=10 (**1)** and mono nitro substituted 1-nitro-2, 3, 6, 7, 10, 11-hexabutaoxyltriphenylene (MNTP4) (**2**), were synthesized as reported earlier [25].

To disperse GNPs in DLC, first DLC was dissolved in chloroform and sonicated with optimized weight ratio of GNPs for two hours to obtain uniform mixtures and slow evaporation of the solvent resulted in the formation of a dispersion. We prepared samples with different compositions by weight of GNPs in the DLC for the purpose of comparison.

4.3 Characterization of GNPs

There are varieties of techniques to characterize the metal nanoparticles intended for a particular use, including spectroscopic methods (UV-visible absorption, Raman scattering) or microscopy (transmission electron microscopy, scanning atomic force microscopy) etc. In our case we have used scanning transmission electron microscope (STEM), scanning electron microscope (SEM) and UV-Vis spectroscopy.

Nanoparticles have optical properties that are sensitive to size, shape, concentration, agglomeration state, and refractive index near the nanoparticle surface, which makes UV/Vis/ IR spectroscopy a valuable tool for identifying, characterizing, and studying these materials. GNPs interaction with light is strongly dictated by their environment, size and physical dimensions. Oscillating electric fields of a light ray propagating near a colloidal nanoparticle interact with the free electrons causing a concerted oscillation of electron charge that is in resonance with the frequency of visible light. These resonant oscillations are known as surface plasmons. The surface plasmon resonance is observed at specific frequencies of incident light and depends on the particle size, shape, dielectric constant of metal and the

medium around nanoparticles. The typical frequency of plasmon resonance for spherical gold nanoparticles varies from 520 nm to 530 nm. In our case the formation of GNPs was confirmed by UV/VIS spectroscopy at a wavelength close to 520 nm (Figure 4.2). For small particle size (1.2-2nm) the peak observed is damped due to reduced mean free path of the electrons.

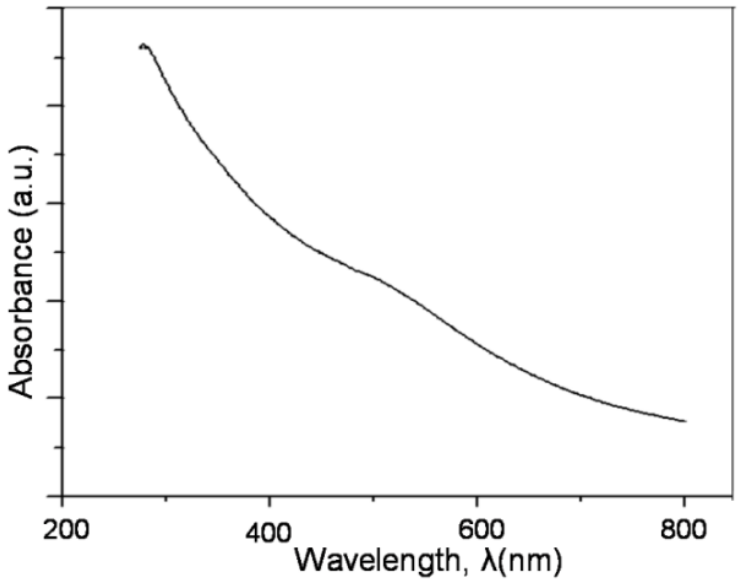

Figure 4.2 Surface plasmon absorption spectra of gold nanoparticles.

To study the particle size and morphology, the nanoparticles were dispersed over an ITO coated glass plate**.** We took scanning transmission electron microscope (STEM) and scanning electron microscope (SEM) images. The images were analyzed using Scanning Probe Image Processor software (SPIP, Image Metrology, Denmark). From the STEM and SEM studies, as shown in Figure 4.3 and Figure 4.4, we found that majority of GNPs have core diameter in range 1.2–2 nm.

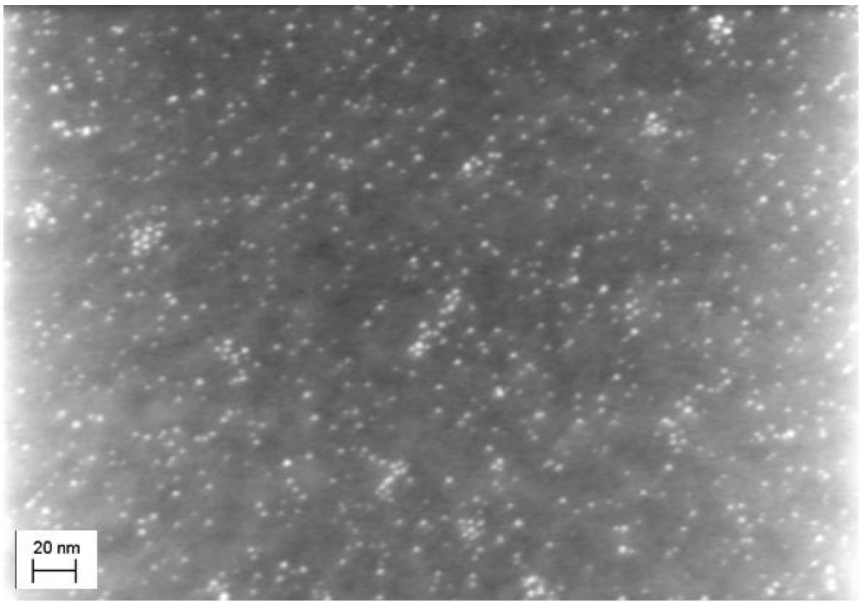

Figure 4.3 STEM image of GNPs in dark field mode at EHT voltage 20 kV.

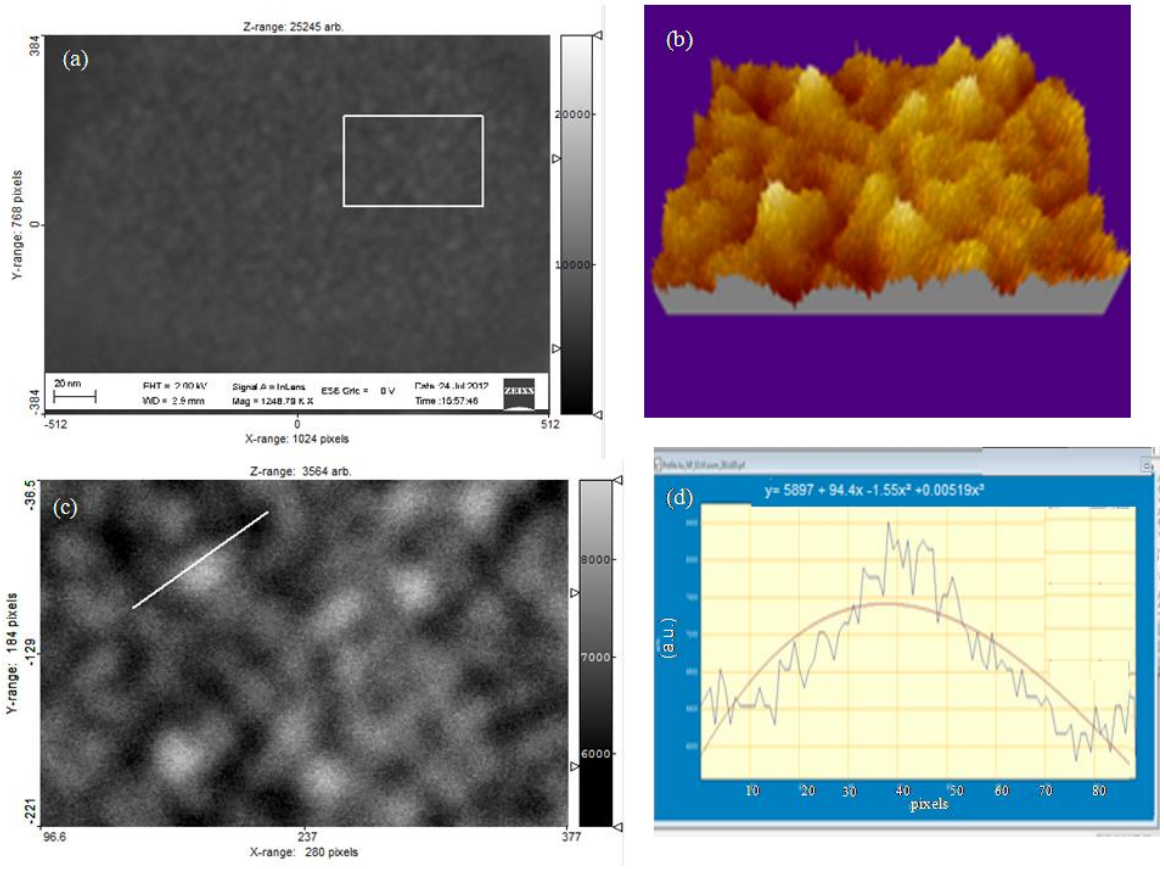

Figure 4.4 (a) Scanning electron microscopic image of the hexanethiol capped gold nanoparticle. (b) 3-D image of GNPs. (c) zoomed SEM image. (d) line profile for the image.

Part (1)

4.4 Dispersion of GNP in Symmetrically Substituted Hexaalkyloxytriphenylene (HATn), n=10

DLC used in the present study is hexadecyloxytriphenylene (HATn), n=10 (where n is the number of carbon in aliphatic chain. This discostic liquid crsytal shows wide temperature range of hexagonal columnar (Col_h) phase.

4.4.1 Results and Discussions

4.4.1.1 Mesomorphic Behaviour

All the GNP-HAT_{10} composites were found to be liquid crystalline in nature. They show classical textures of columnar mesophase upon cooling from isotropic phase. DLC molecules possibly align in two ways, one is planar alignment (or edge on) when the column axis is in the plane of the electrode and other is homeotropic alignment (or face on) when the disc column axis is perpendicular to electrode surface. In case of thin aligned sample (5µm), this disc like molecules gives homeotropic alignment on slow cooling from isotropic phase which is confirmed by the dark field view under crossed polarizer. POM images (Figure 4.5 (a-c)) for 0.5% and 1% GNPs show uniform dispersion of GNPs in columnar matrix without the separation of phases.

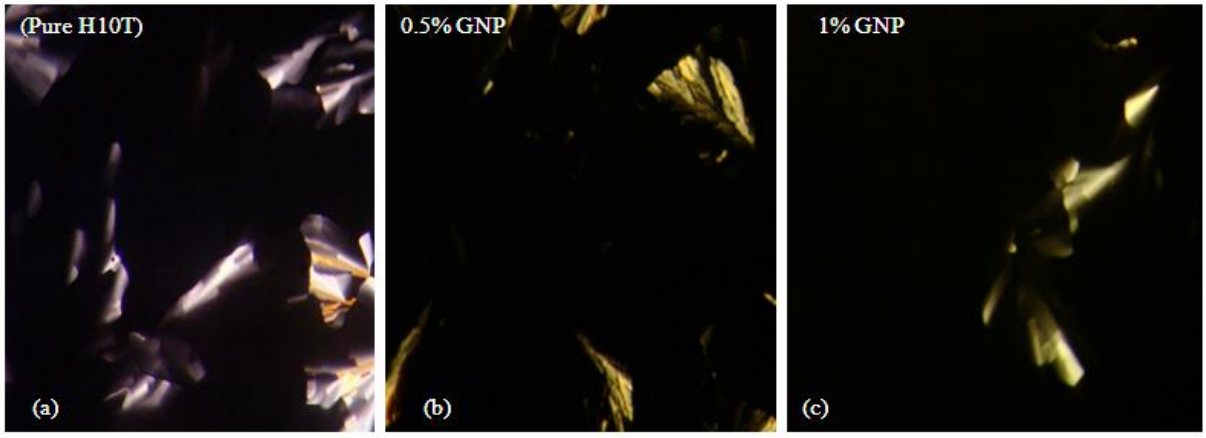

Figure 4.5 POM images of (a) pure DLC and composite systems with (b) 0.5% GNPs, (c) 1% GNPs.

DSC scans were taken on both heating and cooling cycles. Figure 4.6 shows DSC scan of pure and composite systems on cooling cycle GNPs are expected to be present between the aromatic cores and among the columns [19], therefore disturbing π-π interactions between the cores and columns. As seen from the data with the increasing amount of GNPs mesophase to crystal temperature decreases. However there is not much decrease in the mesophase to isotropic temperature. Even so the columnar phase is not destabilized by the addition of the NPs.

4.4.1.2 Dielectric Spectroscopy

The complex dielectric permittivity $\varepsilon^*=\varepsilon'-i\varepsilon''$ where ε' is the real part and ε'' is the imaginary part, is a function of frequency ω, and temperature T. The dielectric data of homeotropic aligned DLC was collected in the cooling cycle and the measurement condition yields dielectric permittivity parallel to the column axis ($\varepsilon'_{\parallel}$).The real ε' and imaginary parts ε'' of the complex permittivity ε^* were measured as a function of temperature at a fixed frequency 10kHz. The isotropic to columnar phase transition and columnar to crystalline phase

transition was manifested as a step in the variation of $\varepsilon'_{\parallel}$ with temperature (Figure 4.7), which is in accordance with DSC results. With the increase of NPs, ε' increases. In the applied electric field, the GNPs get aligned in the direction of column axis and contribute to the polarization of DLC.

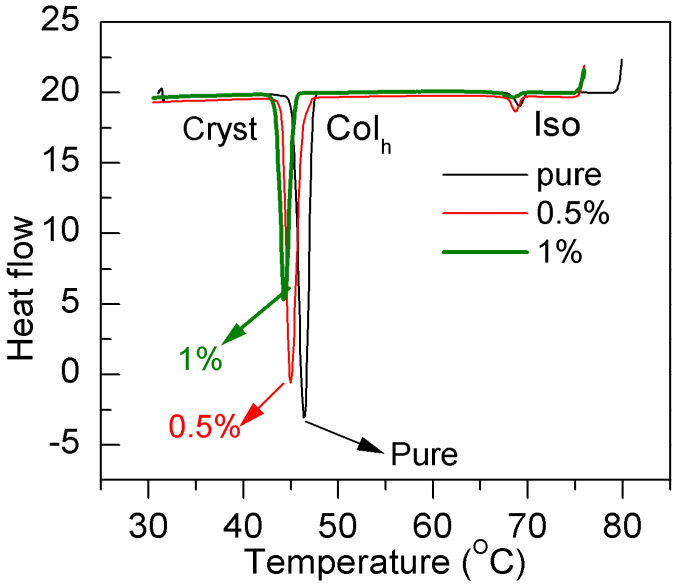

Figure 4.6 DSC scans of pure and GNPs composite systems.

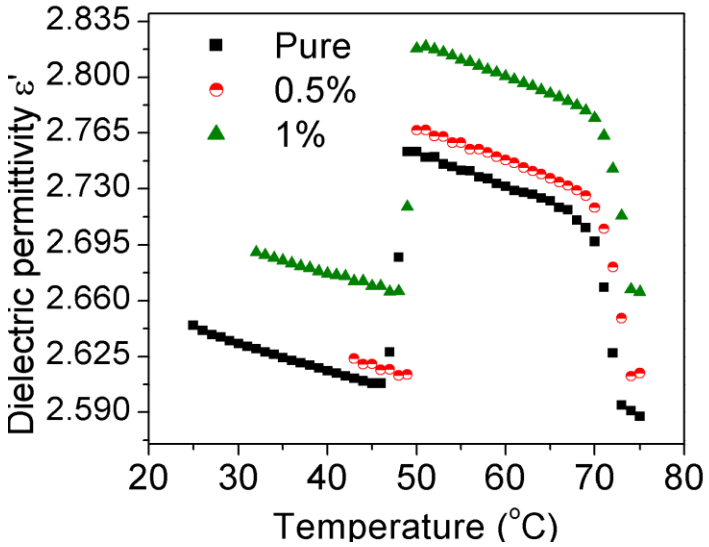

Figure 4.7 Dielectric permittivity as function of temperature for pure and composite systems.

4.4.2 Conclusions

We successfully synthesized GNPs having diameter 1-2nm. POM, DSC and dielectric results show that GNPs are well dispersed into the columnar matrix without affecting the hexagonal arrangements of columns of DLC. This approach of crossing of the field of nanotechnology with DLC may lead to novel materials with interesting properties that are useful for many device applications.

Part (2)

4.5 Effect of Dispersion of Gold Nanoparticles on the Optical and Electrical Properties of Discotic Liquid Crystal

4.5.1 Material Used

The DLC used in the present study is 1-nitro-2, 3, 6, 7, 10, 11-hexabutaoxyltriphenylene (MNTP4) **1** which shows unique columnar plastic phase at low temperature and columnar hexagonal phase at high temperature. Details of synthesis of this compound is reported somewhere else [16].

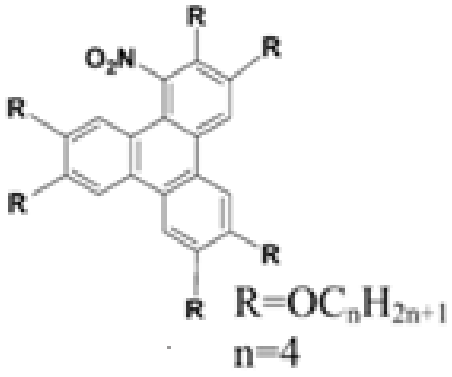

Figure 4.8 Chemical structures of DLC under present study.

Dispersions of GNPs in MNTP4 were prepared in different (wt/wt) % of 0.25% **1(a)**, 0.5% **1(b)**, 1% GNPs **1(c)** in DLC by sonicating these two components in dichloromethane followed by removal of solvent and drying.

The composites thus prepared were analyzed by Differential Scanning Calorimetry (DSC), Polarizing Optical Microscopy (POM), X-ray Diffraction, dielectric spectroscopy, visible absorbance spectroscopy and IR-dichroism technique.

4.5.2 Results and Discussion

4.5.2.1 Mesomorphic Behaviour

POM and DSC were used to characterise these materials for their liquid crystalline nature. A combined study of POM and DSC showed that all three GNP-MNTP4 compositions show liquid crystalline nature. Pure and composite systems were taken between glass slides, and textures were taken on cooling from isotropic phase. Figure 4.9 shows the POM images of different systems under study at room temperature. We observed that on slow cooling from isotropic phase, homeotropic alignment is obtained for pure DLC and homeotropic alignment seems to be disturbed to some extend by GNPs.

Detail analysis of POM at magnification ×500 images show small amounts of aggregates of GNPs in composite system (Figure 4.10). However, no phase separation was observed for composite systems.

The phase transition temperatures of all the compounds were initially established from the polarizing optical microscopy and then measured accurately by differential scanning calorimetry. We observed that the columnar plastic phase is maintained even with 1% GNPs, though the range of columnar plastic phase decreases with concentration of GNPs.

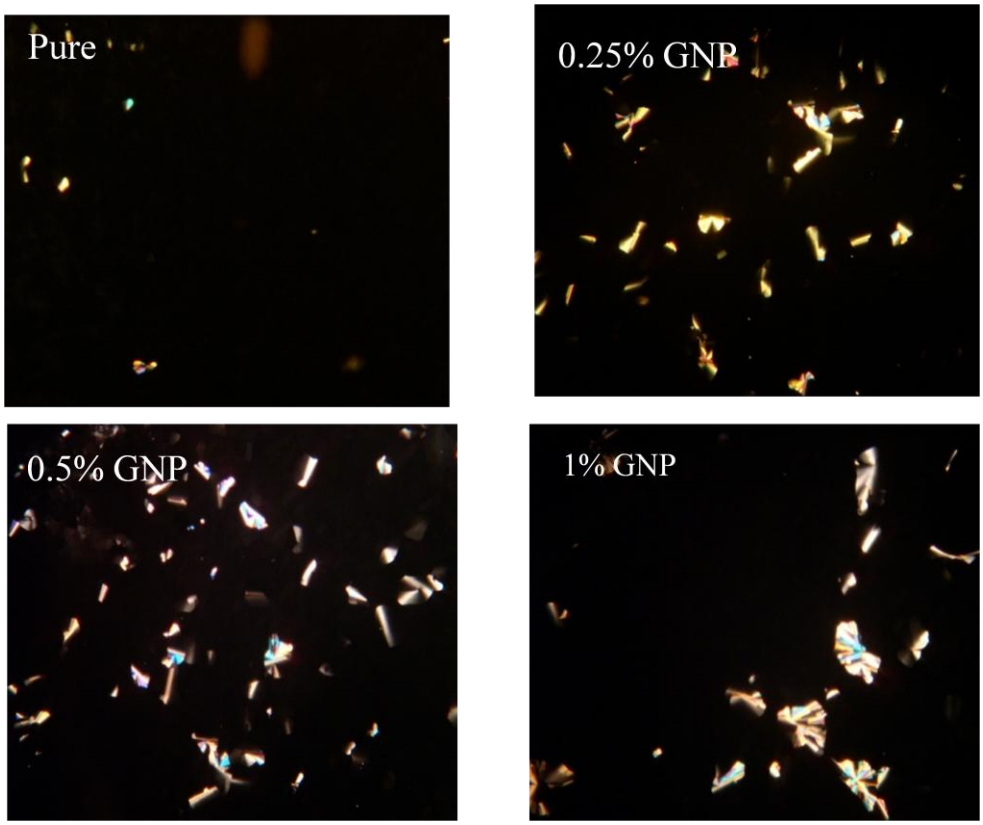

Figure 4.9 POM images of pure and composite system at room temperature at magnification ×100.

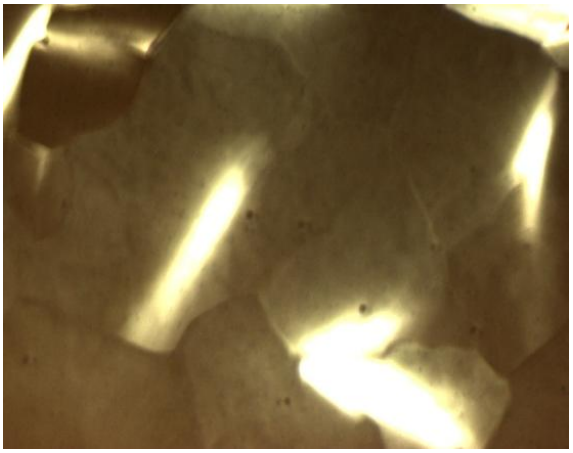

Figure 4.10 POM image of 1% GNP-DLC composite system in Col_p phase at room temperature (magnification X 500). The small black "spots" visible in the POM image are aggregates of GNPs.

Typical thermograms of pure and composite systems are shown in Figure 4.11. DSC data obtained for pure and other composite systems is tabulated in Table 1. Results show that the mesophase isotropic temperature decreases slightly by 1°C with GNPs. However there is noticeable decrease in mesophase to mesophase transition temperature (columnar hexagonal to columnar plastic phase). This is expected as the GNPs are expected to insert in columns and domain boundaries [19] thereby disturbing packing of molecules of the highly columnar plastic phase.

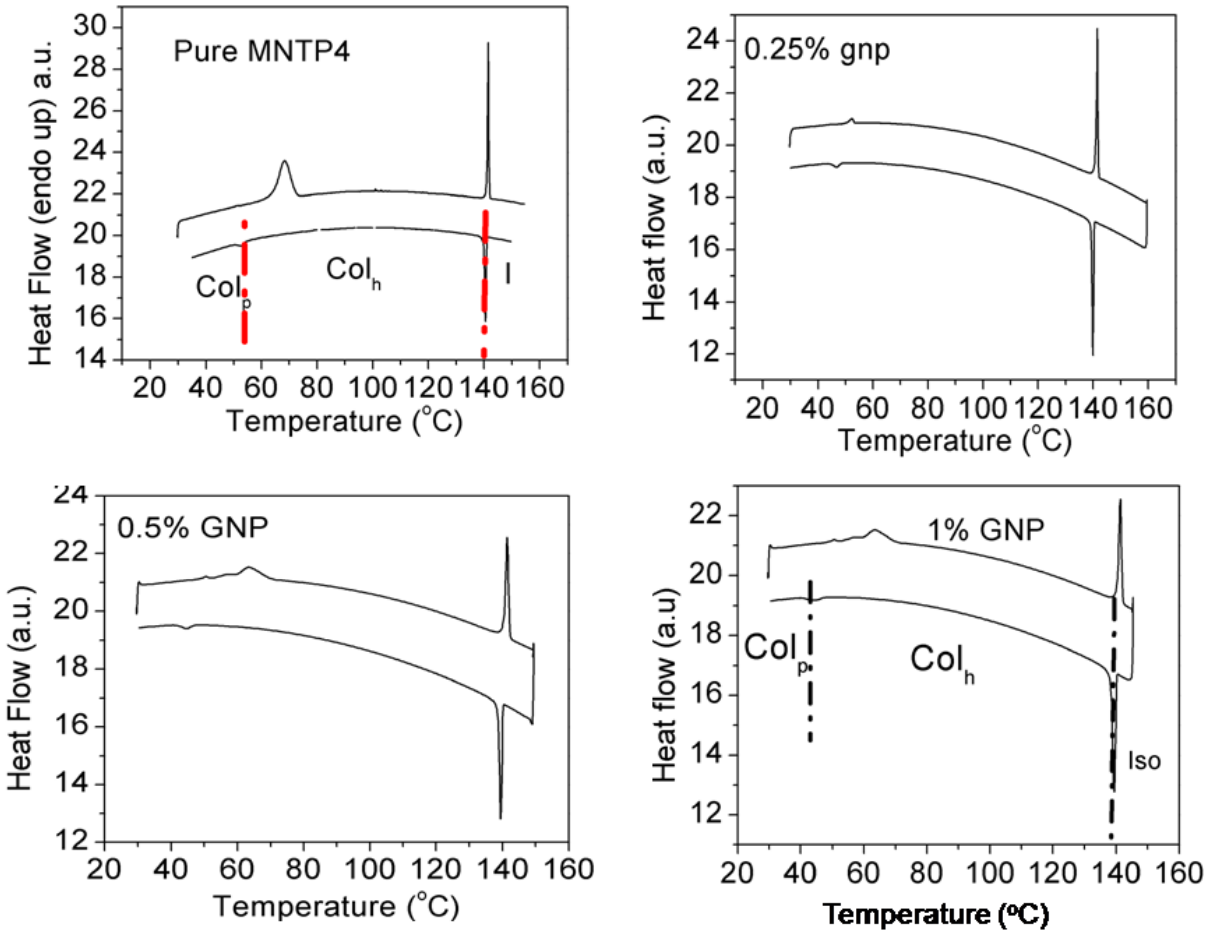

Figure 4.11 DSC thermograms of pure and composite systems.

Table 4.1 DSC results of pure and GNP-DLC composites; Col_p = columnar plastic phase, Col_h=columnar hexagonal phase and I=isotropic phase.

Composites	Thermal Transitions	
	Heating scan	Cooling scan
1	Col_p68.28Col_h141.56 I	I140.54Col_h47.51Col_p
1(a)	Col_p63.25Col_h141.55 I	I139.97Colh46.68Col_p
1(b)	Colp63.23Colh141.25 I	I139.46Col_h44.31Col_p
1(c)	Col_p63.18Col_h141.16 I	I 139.324Col_h44.14Col_p

4.5.2.2 X-ray Diffraction

For the better understanding of liquid crystalline phase of composite system typical powder x-ray diffraction patterns for pure and composite systems were recorded at same condition and the variation of the scattering intensity as a function of scattering angle 2θ is shown in Figure 4.12 Results show that even with inclusion of 1% GNP, columnar plastic phase [26] is still maintained by DLC and the intercolumnar separation is not significantly altered by inclusion of GNPs. Table 2 shows the X-ray diffraction data for pure and composite systems. But, the Bragg's reflection peaks for alkyl chains and core-core correlation become broader and intensity of the peaks decreases. Previous studies showed that smaller 1-2nm NPs are randomly distributed in liquid crystal matrix within the columns and as well as between the columns [19]. The inclusion of GNPs in DLC matrix strain the highly ordered columnar plastic phase.

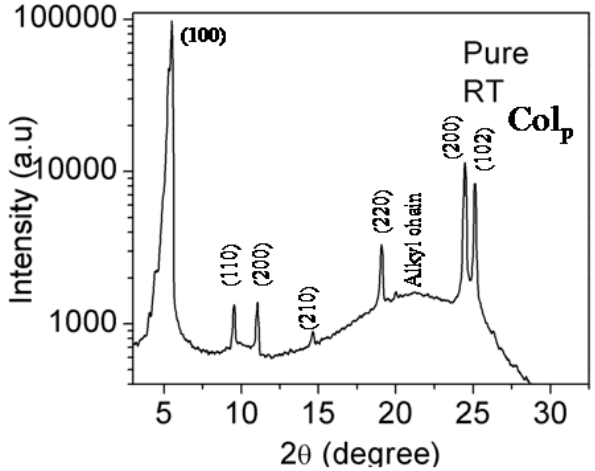
Pure
RT
Col$_p$
(100)
(110)
(200)
(210)
(220)
Alkyl chain
(200)
(102)
Intensity (a.u)
2θ (degree)

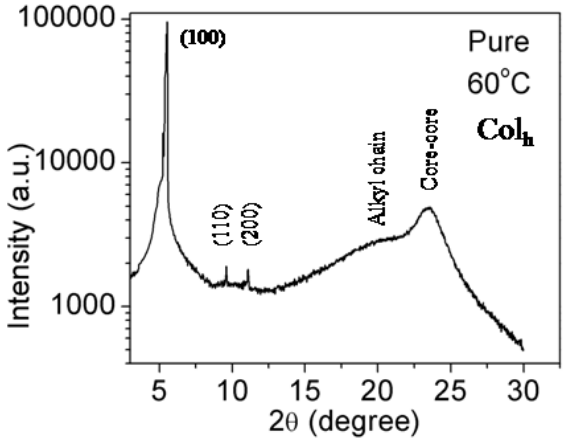
Pure
60°C
Col$_h$
(100)
(110)
(200)
Alkyl chain
Core-core
Intensity (a.u.)
2θ (degree)

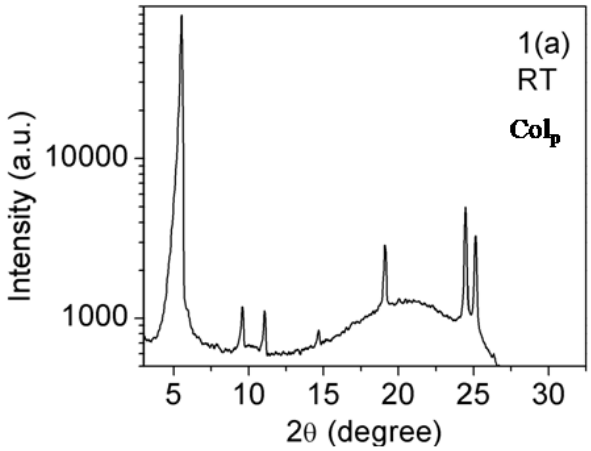
1(a)
RT
Col$_p$
Intensity (a.u.)
2θ (degree)

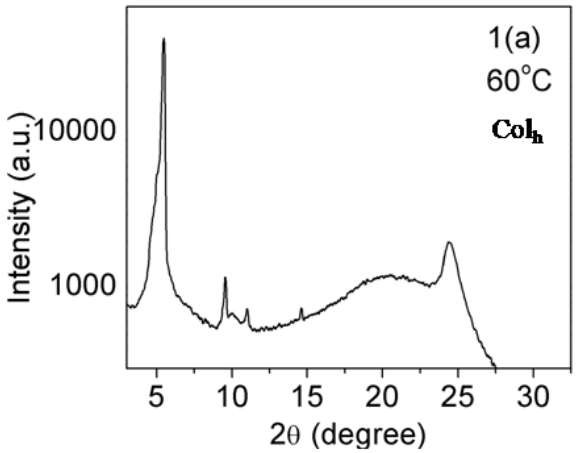
1(a)
60°C
Col$_h$
Intensity (a.u.)
2θ (degree)

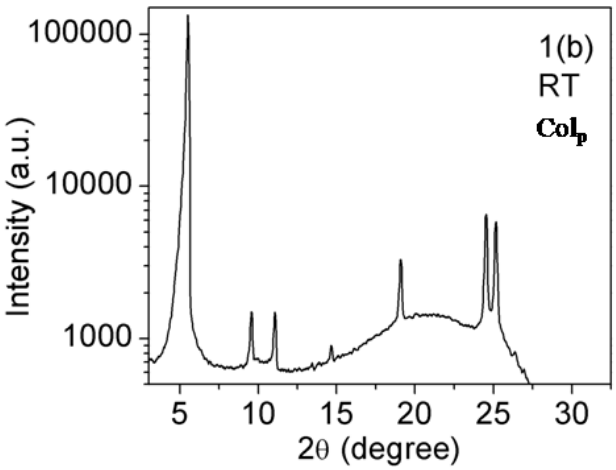
1(b)
RT
Col$_p$
Intensity (a.u.)
2θ (degree)

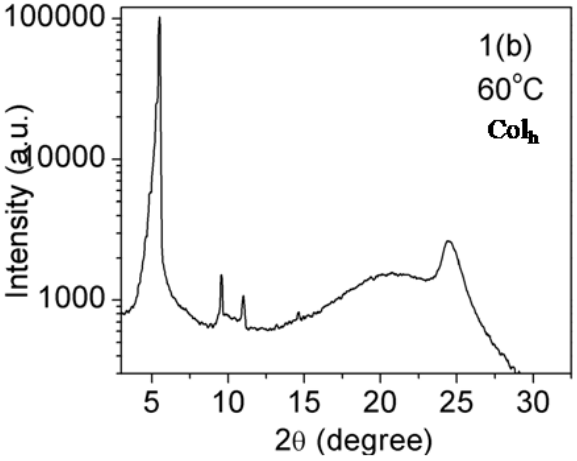
1(b)
60°C
Col$_h$
Intensity (a.u.)
2θ (degree)

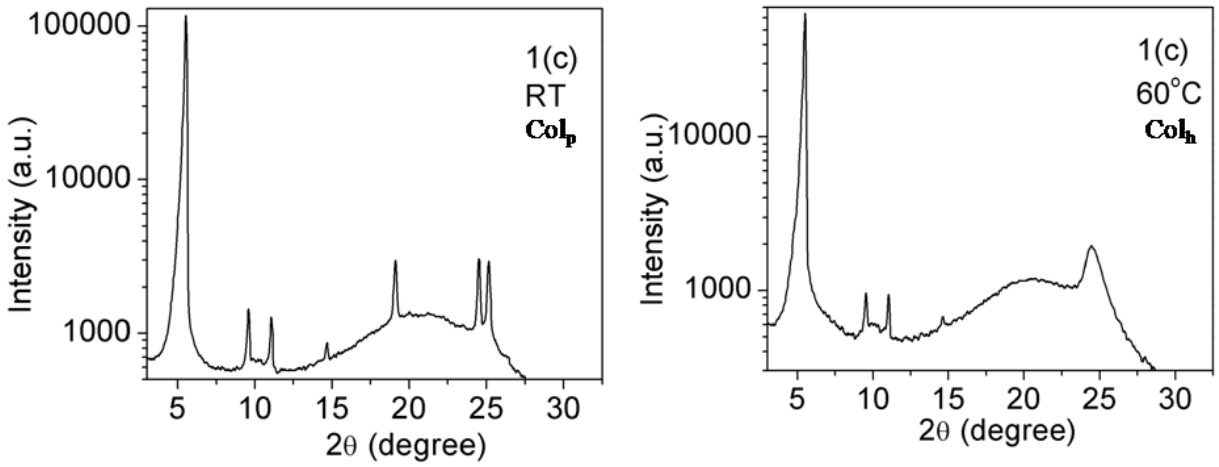

Figure 4.12 Intensity vs 2θ profile of pure and composite systems taken on cooling from isotropic phase in Col_p and Col_h phase.

Table 4.2 X-ray diffraction data for pure and composite systems at room temperature (Col_p).

Peak position (Å)						
Compound	**(10)**	**(11)**	**(20)**	**(21)**	**Core-core**	**Alkyl chain**
1	16.12	9.41	8.04	6.034	3.64	4.26
1(a)	16.01	9.40	8.03	6.033	3.63	4.25
1(b)	15.99	9.37	8.03	6.031	3.65	4.21
1(c)	15.98	9.34	8.025	6.027	3.65	4.19

* RT= room temperature

4.5.2.3 Dielectric Spectroscopy

To study the effect of GNPs on the motion of disc about the column axis, we carried out dielectric relaxation spectroscopy. The relaxation curves observed at different temperatures

for pure and composite systems are asymmetric in shape and are broader than ideal debye relaxation curves. Hence, the frequency dependent experiments were analysed by using emphirical equation of Havrilaik and Negami (HN) to extract relaxation parameters:

$$\varepsilon^*(T,\omega,t)=\varepsilon_\infty(T,t)+\frac{\Delta\varepsilon(T,t)}{[1+(i\omega\tau_{HN}(T,t))^{\alpha(t)}]^{\beta(t)}}+\frac{\sigma_{dc}(T,t)}{i\varepsilon_f\omega} \qquad eq.\ 1$$

Here τ_{HN} $(T,\ t)$ is the characteristic relaxation time, $\Delta\epsilon\ (T,\ t)= \epsilon_0\ (T,t)- \epsilon_\infty(T,t)$ is the relaxation strength of the process under investigation, α, β (with limits $0<\alpha$, $\alpha\beta\leq1$) describe, respectively, the symmetrical and asymmetrical broadening of the distribution of relaxation times, σ_{dc} is the dc conductivity, and ϵ_f is the permittivity of free space. We did HN function fitting for all systems at different temperature.

After fitting dielectric data using HN function, we calculated relaxation time at different temperatures. The temperature dependence of relaxation times $\tau(T)$, is shown in figure 4.14 in the usual Arrhenius representation as a function of temperature. The data fits well to Arrhenius equation:

$$\tau = \tau_o log\left(\frac{E_a}{k_b T}\right) \qquad eq.2$$

The low temperature α process is a weak process and has Arrhenius temperature dependence. As discussed earlier, GNPs are expected to present randomly within the columns as well as between the columns, the GNPs hinder the disc motion about the column axis.

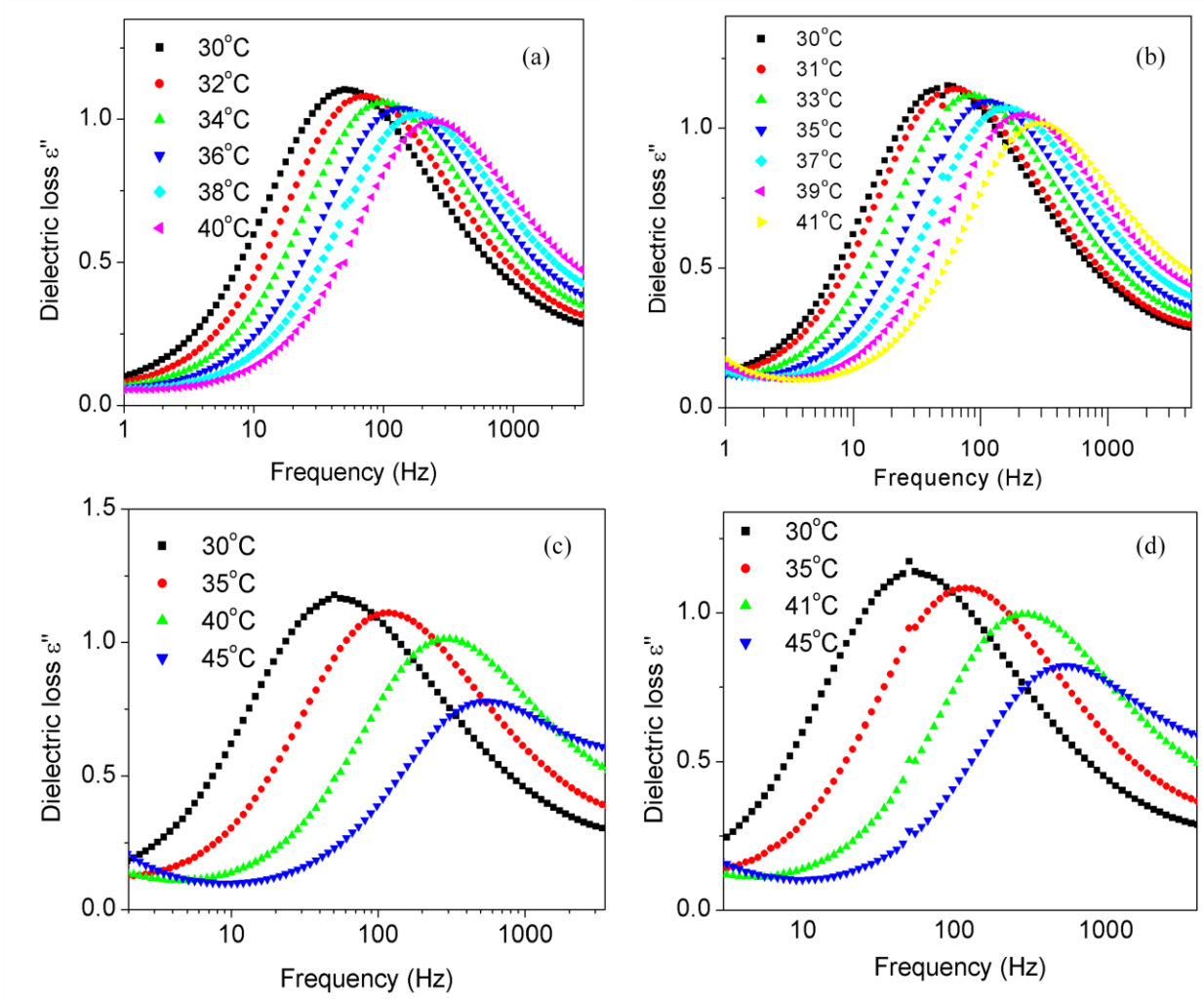

Figure 4.13 Relaxation curves (a) pure, (b) 0.25% GNP, (c) 0.5% GNP and (d) 1% at different temperatures.

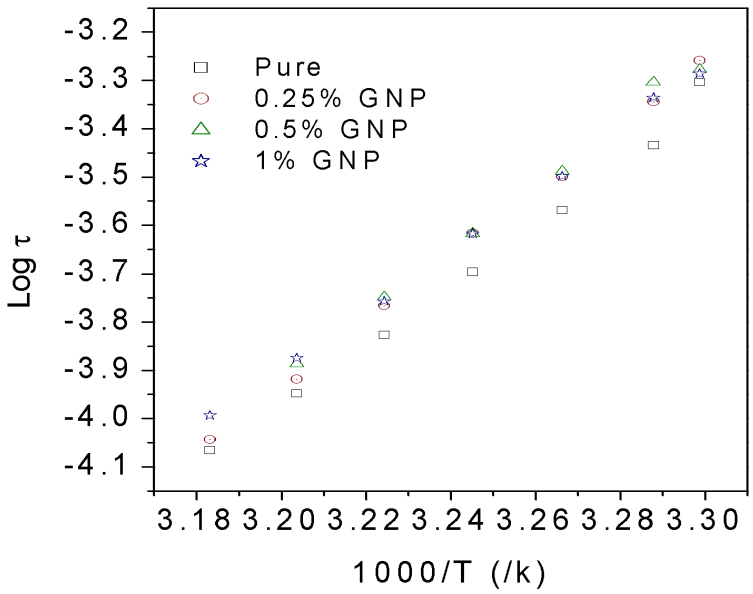

Figure 4.14 Variation of Relaxation time with temperature for pure and composite systems.

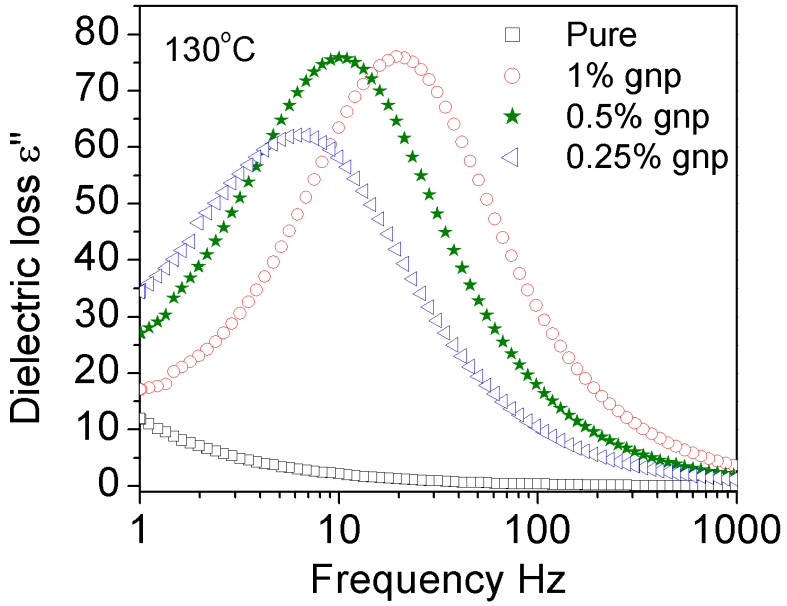

Figure 4.15 Dielectric loss ε″ as function of frequency at 130°C for pure and composite systems.

At higher temperature (Figure 4.15) and in isotropic phase extra relaxation peak appears for all composite systems which arise from conductivity of GNPs.

We have also studied the effect of frequency on real part of dielectric permittivity (ε′). If an oscillating field is applied with a frequency that is substantially larger than 1/τ all dipoles can reorient themselves and contribute to the polarization. This changes if the field frequency raises to a level similar as 1/τ not all molecules can contributed any more, thus the polarization and consequently the (real part of the) dielectric permittivity decreases. This is the step in ε′ and the peak in ε″. Finally, when the field frequency rises above 1/ τ no molecules can catch up with the electric field any more and the contribution of this dipole motion to the polarization ceases to exist. ε′ is flat again and ε″ has returned to zero. However, measured dielectric data above 1 MHz are mainly affected by ITO resistance from the cell [22].

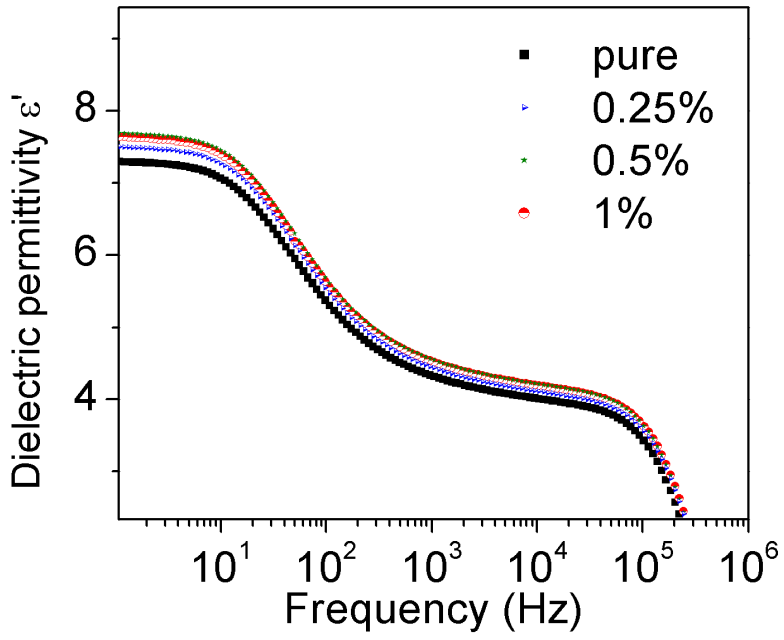

Figure 4.16 Dielectric permittivity ε′ as function of frequency for pure and composite systems.

4.5.2.4 Visible Spectroscopy of Thin Films

Visible absorption studies of pure and composite films were carried out on glass substrate. Figure 4.17 shows spectra of pure and composite films. Uniform film thickness of 5 μm between two quartz plates was maintained by mylar spacer. All the systems show significant absorbance band in visible region of the spectrum. Spectra clearly show absence of surface plasmon resonance band in composite systems which is expected as GNP size is very small (1-2nm).

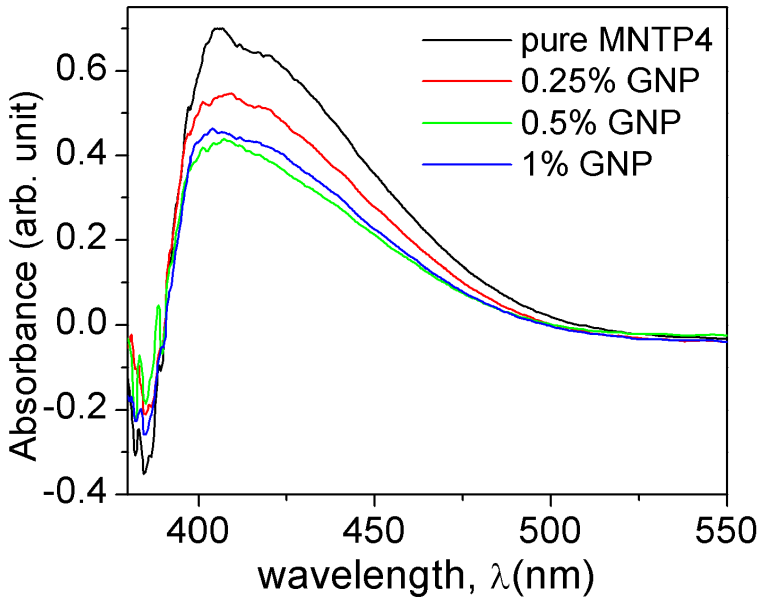

Figure 4.17 Visible absorbance spectra of pure and composite film in glass substrate.

4.5.2.5 IR Dichroic Measurements

We measured order parameter for pure and composite systems using IR-dichroism technique [28-31]. Unpolarised IR beam was incident on homeotropic aligned samples between CaF_2 plates separated by 16 μm mylar spacer. Dichroic ratio which is given by $R = {}^{I_{DLC}}/_{I_{Iso}}$ where

I_{DLC} and I_{Iso} are the integrated absorption intensities in the liquid crystalline and isotropic phases respectively, was calculated. Order parameter (*S*) corresponding to C-C inplane stretching vibrations was calculated as follow:

$$S = 2(R-1) \qquad eq.\ 3$$

Order parameter (S) as a function of temperature for pure and 1% GNP composite system is shown in figure 4.18.

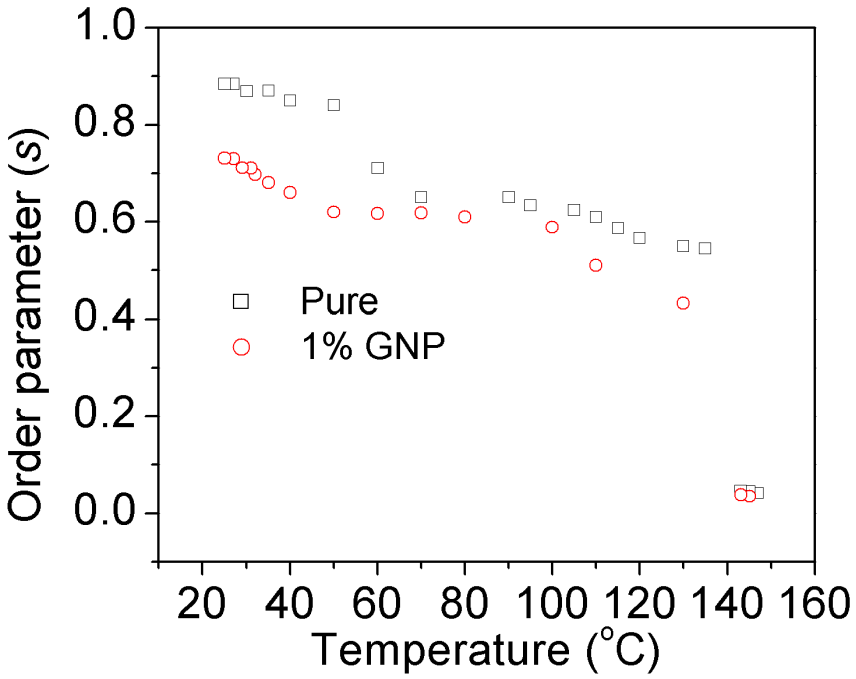

Figure 4.18 Plot of order parameter versus temperature showing decrease of order parameter of DLC with 1% GNPs for the C-C aromatic stretching vibration near 1617 cm^{-1}.

The calculated value of *S* corresponding to the C-C aromatic stretching vibrational band is ≅ 0.848 (Figure 4.18) for pure DlC. This large value of *S* indicates the discotic cores are almost perfectly aligned by self organizations of discotic molecules. In general triphenylene based DLC have almost planar core and due to intense π-π interactions between the cores

causing TP cores to be almost normal to the column's axis. We observed that there is about 15% decrease in value of orientational order parameter in columnar plastic phase for 1% GNPs system. Though there is decrease in order parameter for composite systems but interestingly dc conductivity increases with GNPs. A plot of *S* for C-O-C asymmetric stretching vibration near 1175 cm^{-1} for pure and composite 1(**c**) is shown in Figure 4.19. We also calculated *S* for C-O-C symmetric stretching near 1100 cm^{-1}. The plot of *S* as function of temperature for this band is shown in Figure 4.20. If we look at structure of DLC molecule Figure 4.8, we observed that C-O-C bonds are directly attached to the central core. But the direction of dipole moments associated with these vibrations is not exactly parallel to the plane of the core. Also they change with the change of the conformation of the molecule [32]. Therefore the observed value of *S* for C-O-C band is much lesser than that for the C-C aromatic stretching vibration near 1617 cm^{-1}.

Trend followed for pure and composite system is almost same but the value of *S* for different significant bonds in DLC is different. We observed that the value of *S* for C-O-C symmetric stretching vibrational band is greater than that calculated for C-O-C asymmetric stretching vibrational band. This shows that the associated dipole moment for C-O-C symmetric vibrations are aligned more towards the direction parallel to the plane of the core as compared to the C-O-C asymmetric vibrations.

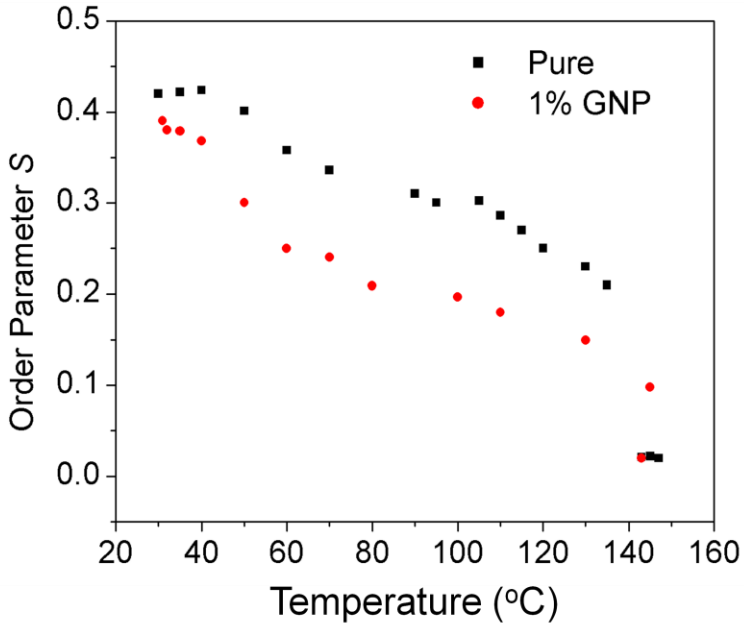

Figure 4.19 Plot of order parameter versus temperature showing decrease of order parameter of DLC with 1% GNPs for the C-O-C stretching asymmetric vibration near 1175 cm^{-1}.

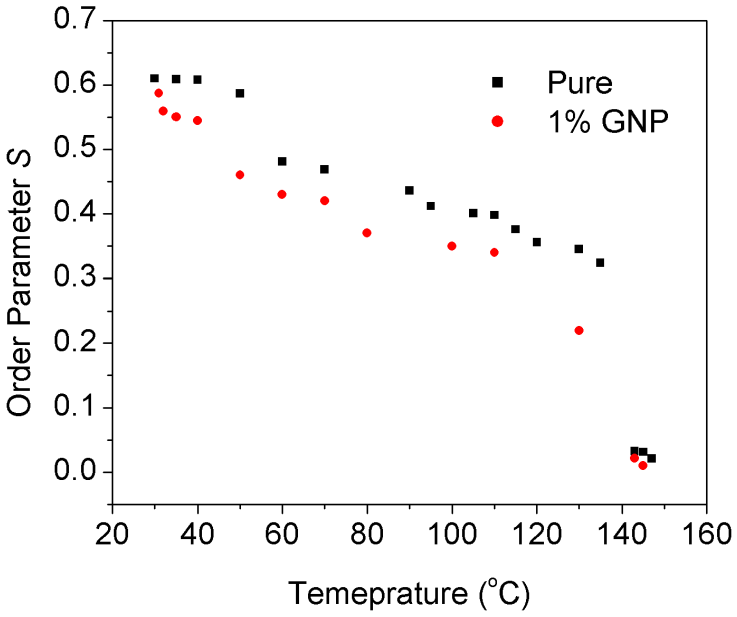

Figure 4.20 Plot of order parameter versus temperature showing decrease of order parameter of DLC with 1% GNPs for the C-O-C stretching symmetric vibration near 1100 cm^{-1}.

4.5.2.6 dc Conductivity

Figure 4.21 shows temperature dependence of dc conductivity for pure and composite systems during cooling from isotropic phase. It can be seen from the plots that conductivity increases by about 5% in columnar phase and about order of two in columnar hexagonal phase and we can also see change in conductivity at respective phase transition temperatures. Expected reasons for increase in conductivity are the hopping between localised sites involving both the GNPs and the discoid aromatic cores. Also limiting the molecular rotation within the column leads to a decrease in the degree of freedom within the mesophase, and therefore the charge carrier mobility of columns increases. Sometimes ionic conduction also contributes to enhancement of conductivity.

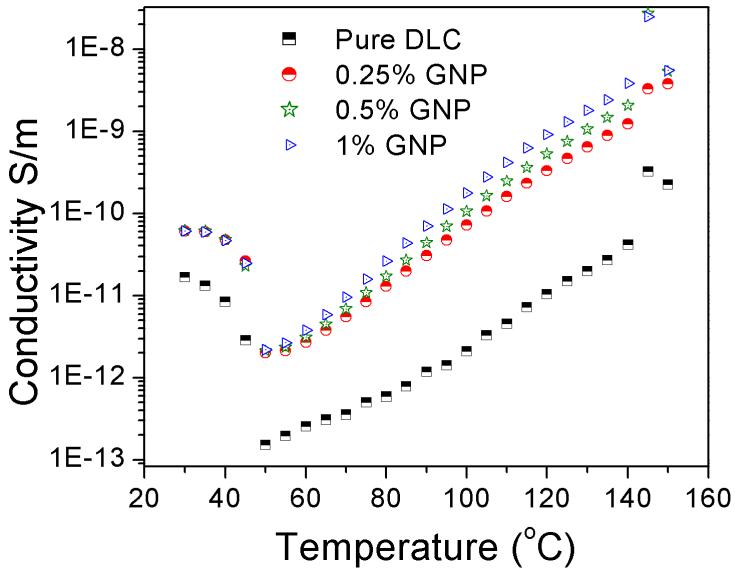

Figure 4.21 Temperature variation of dc conductivity of pure and composite systems.

4. 5. 3 Conclusions

In conclusion, DSC, POM, XRD, IR-dichroic technique, dielectric spectroscopy results show the inclusion of GNPs in DLC matrix. The nature of mesophases is not altered by GNPs but a

shift in transition temperature was observed. Though there is decrease in order parameter and the disc motion about the column axis is hindered, dc conductivity increases with GNPs. These inorganic-organic liquid crystal hybrid systems may be extremely important for many device applications such as photovoltaic solar cell, photoconduction, light emitting diodes, thin film transistors etc.

References

[1] P. Schwerdtfeger, *Angew Chem. Int. Ed*., 42, 1892, (2003).

[2] R. Elghanian, J. J. Storhoff, R. C. Mucic, R. L. Letsinger, C. A. Mikkin, *Science*, 277, 1078, (1997).

[3] D. A. Giljohann, D. S. Seferos, W. L. Daniel, M. D. Massich, P.C. Patel, C. A, Mirkin, *Angew Chem. Int. Ed.*, 49, 3280, (2010).

[4] M. C. Daniel, D. Astruc, *Chem. Rev*., 104, 293, (2004).

[5] S. Chandrasekhar, B. K. Sadashiva, K. A. Suresh, *Pramana*, 9, 471 (1977).

[6] S. Kumar, Chemistry of discotic liquid crystals: from monomers to polymers. Boca Raton (FL), CRC Press, (2011).

[7] N. Boden, R. L. Bushby, J. Clements, B. Movaghar, *J. Mater. Chem.*, 9, 2081, (1999).

[8] R. J. Bushby, K. Kawata, *Liq. Cryst*., 38, 1415, (2011).

[9] S. Laschat, A. Baro, N. Steinke, F. Giesselmann, C. Hägele, G. Scalia, R. Judele, E. Kapatsina, S. Sauer, A. Schreivogel, M. Tosoni, *Angew Chem. Int. Ed*., 46, 4832 (2007).

[10] S. K. Pal, S. Setia, B. S. Avinash, S. Kumar, *Liq. Cryst*., 40, 1769 (2013).

[11] S. Sergeyev, W. Pisula, Y. H. Geerts, *Chem. So.c Rev*., 36, 1902 (2007).

[12] J. Hanna, *Opto Electron Rev.*, 13, 259, (2005).

[13] B. L. Kaafarani, *Chem. Mater*., 23, 378 (2011).

[14] S. Kumar, S. K. Pal, V. Lakshminarayanan, *Mol. Cryst. Liq. Cryst.,* 434, 251, (2005)

[15] S. Kumar, V. Lakshminarayanan, *Chem. Commun.*, 14, 1600, (2004).

[16] M. Yamada, Z. Shen, M. Miyake, *Chem. Commun*., 2569, (2006).

[17] S. Kumar, S. K. Pal, P. S. Kumar, V. Lakshminarayanan, *Soft Matter*, 3, 896, (2007).

[18] L. A. Holt, R. J. Bushby, S. D. Evans, A. Burgess, G. A. Seeley, *J. Appl. Phys*., 103, 063712, (2008).

[19] D. Vijayaraghavan, S. Kumar, *Mol. Cryst. Liq. Cryst.,* 508, 101 (2009).

[20] S. Tripathi, J. Prakash, A. Chandran, T. Joshi, A. Kumar, R. Dhar, A. M. Biradar, *Liq. Cryst*., 40, 1255, (2013).

[21] K. K. Vardanyan, D. M. Sita, R. D. Walton, I. S. Gurfinkiel, W. M. Saidel, *Liq. Cryst.*, 39, 1083, (2012).

[22] K. K. Vardanyan, D. M. Sita, R. D. Walton, I. S. Gurfinkiel, W. M. Saidel, *Liq. Cryst.*, 39, 595, (2012).

[23] Y. Song, T. Huang, R. W. Murray, *J. Am. Chem. Soc*., 125, 11694 (2003).

[24] M. Brust, M. Walker, D. Bethell, D. J. Schriffin, R. Whyman, *J. Chem. Soc. Chem. Commun.*, 801, 801, (1994).

[25] (a) C. Destrade, M. C. Mondon, J. Malthete, *J. Phys. Colloque*. 40, C3‑17, (1979).

(b) S. Kumar, M. Manickam, *Mol. Cryst. Liq. Cryst*., 309, 291, (1998).

[26] S. K. Prasad, D. S. Shankar Rao, S. Chandrasekhar, S. Kumar, *Mol. Cryst. Liq. Cryst*., 396, 121, (2003).

[27] P. Perkowski, *Phase Trans*., 83, 836, (2010).

[28] Supreet, S. Kumar, K. K. Raina, R. Pratibha, *Liq. Cryst.*, 40, 228, (2013).

[29] J. K. Vij, A. Kocot, T. S. Perova, *Mo.l Cryst. Liq. Cryst*., 397, 231, (2003).

[30] T. S. Perora, J. K. Vij, *Adv. Mater*., 7, 919, (1995).

[31]T. S. Perova, J. K. Vij, A. Kocot, *EPL*., 44, 198, (1998).

[32] G. Kruk, A. Kocot, R. Wrzalik, J. K. Vij, O. Karthaus, H. Ringsdorf, *Liq. Cryst.*, 14, 807, (1993).

Chapter 5

Induction, Variation, and Stabilization of Mesomorphic Properties of Disc-Like Molecules in Binary Systems via Charge Transfer

Abstract: The ability of some discotic liquid crystals (DLC) to form columns has made them attractive candidates for conductive devices. The π-π orbital overlap of the aromatic-core carbon atoms forms a one-dimensional (1D) path for charge carriers to travel along the column direction. Many potential mesogenic DLC species have extended aromatic cores and are electron-rich. They are, therefore, excellent candidates for forming charge-transfer complexes with flat electron-deficient molecules, such as non-liquid-crystalline electron acceptor 2,4,7-trinitrofluorenone (TNF). It has been found that charge-transfer inter action has a profound effect on the induction and stabilization of mesophases.

Chapter 5 is divided into two parts. Part (1) deals with the CT complexes of triphenylene based DLC with 2,4,7-trinitrofluoren-9-one (TNF). Part (2) deals with induction of mesomorphism in non mesogenic disc like molecules via CT complexes with TNF. The thermotropic mesomorphic behavior of the CT complexes was studied by differential scanning calorimetry (DSC), polarizing optical microscopy (POM), and X-ray diffraction (XRD) measurement. This approach to achieve molecular orientation without crystallization via a charge-transfer complex process involving derivatives of triphenylene could prove particularly useful and versatile in organic optoelectronic device applications.

Part (1)

5.1 Charge Transfer Complexes of Discotic Liquid Crystals

5.1.1 Abstract

DLCs derived from triphenylene core formed a donor–acceptor charge-transfer complex with 2, 4, 7-trinitrofluorenone (TNF). The resulting CT complex has been investigated using visible absorbance spectroscopy, polarized optical microscopy, thermal analysis, and X-ray diffraction. A columnar mesophase with hexagonal symmetry was found. More interestingly, this charge-transfer complex can be easily aligned on a glass surface in a homeotropic orientation, which is stable at room temperature (RT) and over a wide temperature range.

5.1.2 Introduction

CT interactions are especially relevant for binary or multi-component systems in the context of mesophase induction or variation and stability. These terms denominate a significant change in the mesomorphic self-aggregation in the mixture compared to those of its constituting components, for example, the occurrence of a new mesophase; we also include here the stabilization of a mesophase of one of the compounds [1-3]. This approach for columnar mesogens was first realized by Ringsdorf et al. charge-transfer induced nematic columnar (N_{col}) phases exhibited by mixtures of amorphous sidechain polymers carrying 2,3,6,7,10,11- hexasubstituted triphenylene moieties with TNF and TNF-induced columnar hexagonal (Col_h,) phases of related main-chain polymers [4]. 2,3,6,7,10,11- Hexaethers of triphenylene, for example, forming columnar hexagonal mesophases with intracolumnar stacking order (Col_h) [5] show a stabilization of the existing columnar structures and an extension of the mesomorphic range on addition of TNF due to CT interactions [6-8]. The

clearing temperature steadily increases with the TNF concentration and maximum stabilization is observed for the 6 : 4 electron donor acceptor ratio. The TNF-CT complexes of the triphenylene hexaethers with this composition behave like a single compound, showing a sharp transition from the Col_h to the isotropic phase; higher or lower acceptor concentrations in such mixtures lead to biphasic ranges. The same type of mesophase stabilization is also observed in mixtures of 2,3,6,7,10,11-hexaester derivatives of triphenylene with TNF, while analogous nonliquid crystalline hexaethers with polyethyleneoxy chains show the induction of a Col_h, phase instead, even with TNF contents of only about 15 mol% [6].

Although pure DLCs generally show a poor absorption in the visible spectral domain, mixtures of the electron donating discoids with non-discogenic electron acceptors could exhibit absorption bands in the visible due to the formation of a charge transfer (CT) complex [9-11]. Despite these favorable properties it is still unclear to what extent DLC-CT compounds can be attractive for application in a photovoltaic device. For good performance of a photovoltaic device the donor and acceptor molecules must form separate columns, *i.e.* enable charge separation and subsequent charge transport along the columnar wires. The position of the electron acceptors within the columnar mesophases is still controversial [12]. Acceptor molecules such as TNF have been reported to be "sandwiched" between discotic molecules within the same column,[9, 1, 13-15] but also "intercolumnar", i.e. between the columns within the aliphatic tails of the discotic molecules [1, 4,16-18]. Only the intercolumnar juxtaposition could provide a morphology with separate continuous columns for electron and hole transport. The addition of electron acceptors such as TNF has been shown to increase the conductivity of DLCs [19, 16, 20, 21]. On the other hand, it has been

proposed that recombination processes limit the hole photocurrent in DLC-CT compounds [22]. Charge carriers in CT compounds are supposed to be trapped and readily annihilated through rapid, phonon-assisted relaxation and recombination processes [22-24].

5. 1. 3 Materials and Experimental

The DLCs under study are derivatives of triphenylene (TP):, hexahexylthiotriphenylene (HHTT) (**1**), mononitro derivative of hexabutyloxytriphenylene; 1-nitro-2,3,6,7,10,11-hexabutyloxy triphenylene (C_4MNTP) (**2**).

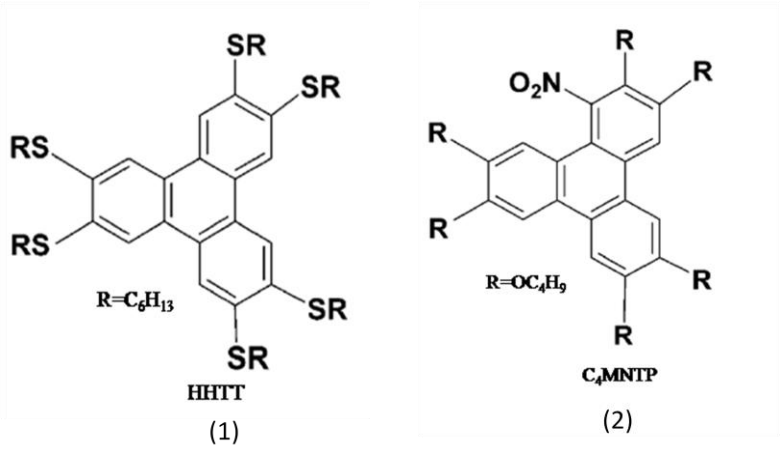

Figure 5.1 Molecular structures of the discotic liquid crystals studied.

CT complexes were prepared by dissolving the DLC compounds and with different weight ratio of TNF in chloroform (1%, 5% and 10% TNF in HHTT **1(a)**, **1(b),** 1**(c)** respectively and 10% TNF in C_4MNTP **2(a)**) , sonicating for two hours, evaporating the solvent, and drying the residues in a vacuum. The TP compounds and TNF were pale yellow powders. When they were dissolved in chloroform, the color of the solutions changed to deep red. Initial evidence to support the formation of a charge-transfer complex was therefore their changes in color. The complexes thus prepared were analyzed by differential scanning calorimetry

(DSC), polarizing optical microscopy (POM), X-ray diffraction, dielectric spectroscopy, visible absorbance spectroscopy.

5.1.4 Results and Discussion

5.1.4.1 Thermotropic Behaviour

The thermal behavior of all the compounds was investigated by polarizing optical microscopy (POM) and differential scanning calorimetry (DSC). In the all the cases classical textures of discotic columnar mesophases appeared upon cooling from the isotropic liquid as shown in Figure 5.2 (a-d).

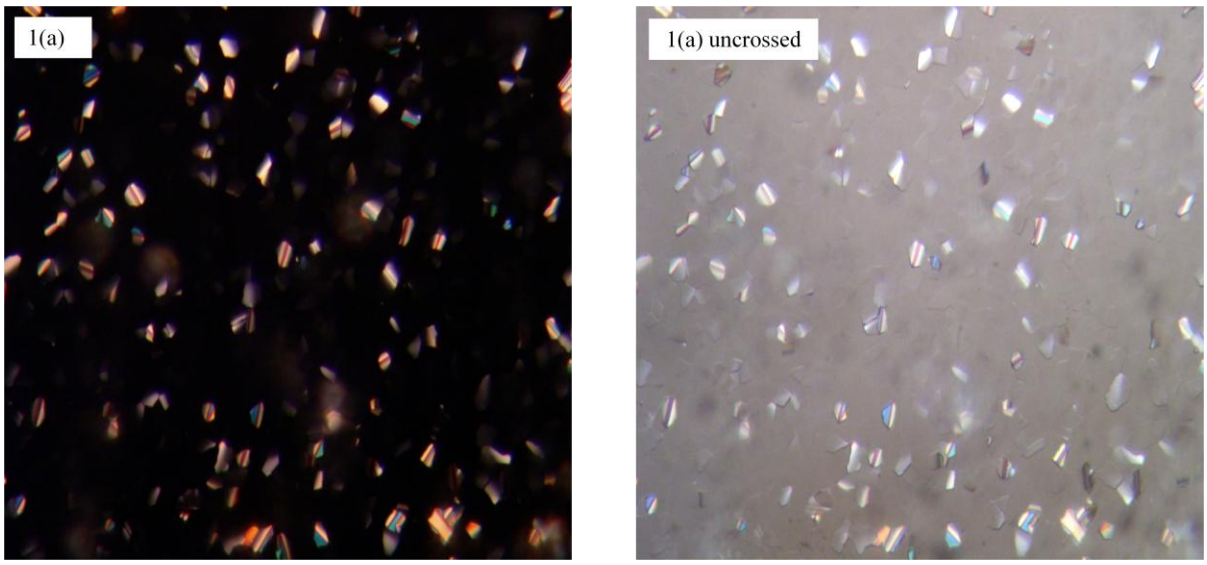

Figure 5.2 (a) POM images of complex 1(a) at room temperature upon cooling from isotropic phase under crossed and uncrossed polarizer.

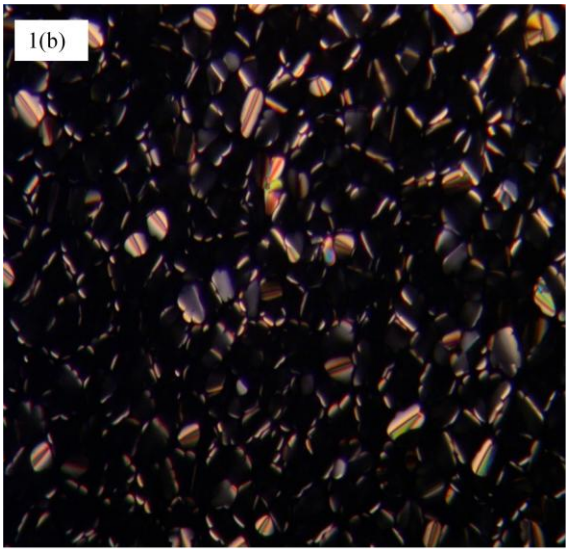

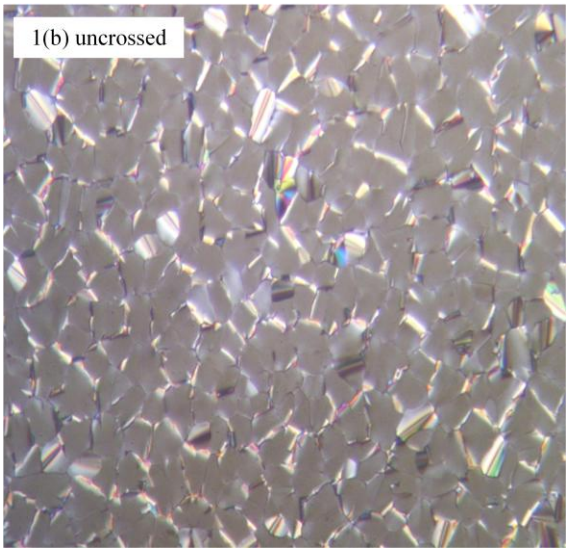

Figure 5.2 (b) POM images of complex 1(b) at room temperature upon cooling from isotropic phase under crossed and uncrossed polarizer.

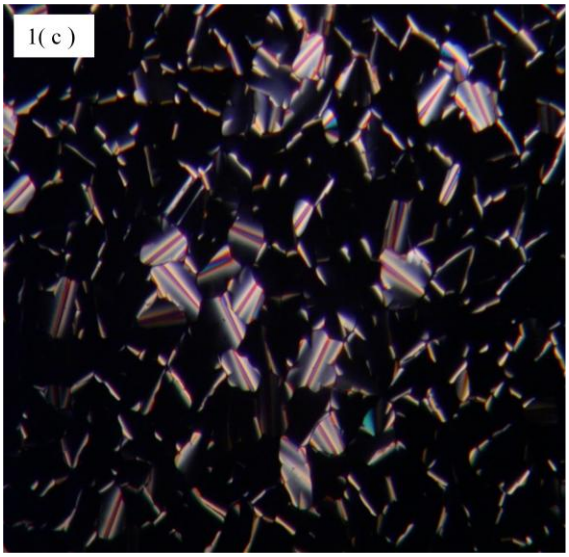

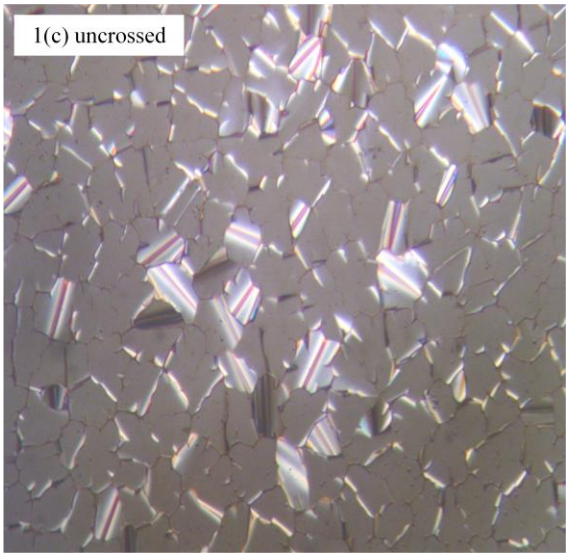

Figure 5.2 (c) POM images of complex 1(c) at room temperature upon cooling from isotropic phase under crossed and uncrossed polarizer.

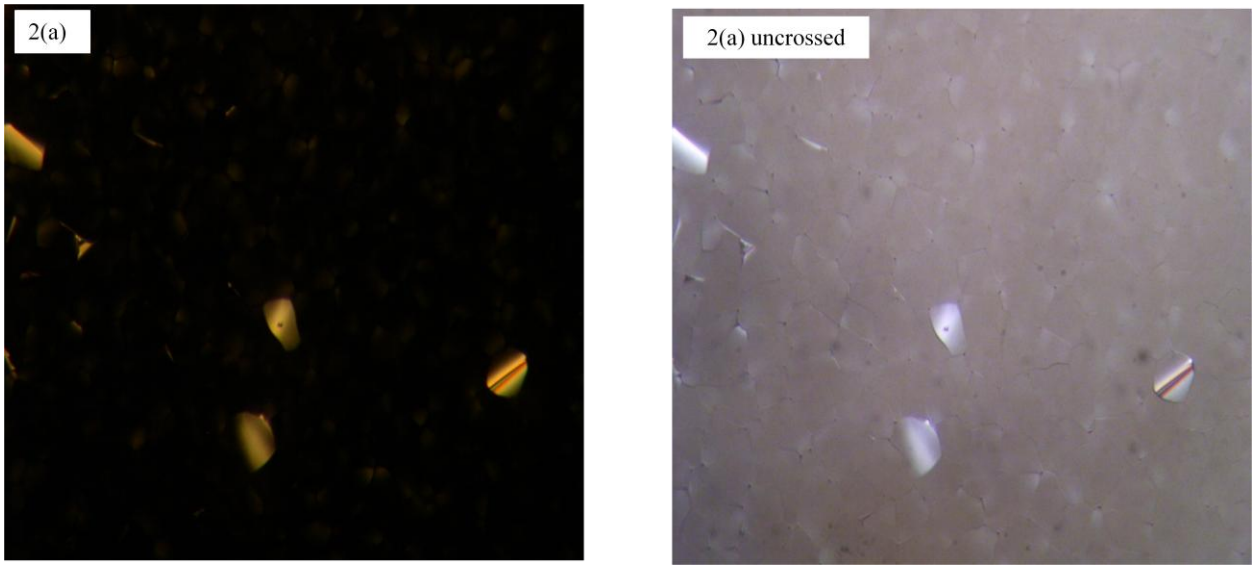

Figure 5.2 (d) POM images of complex 2(a) at room temperature upon cooling from isotropic phase under crossed and uncrossed polarizer.

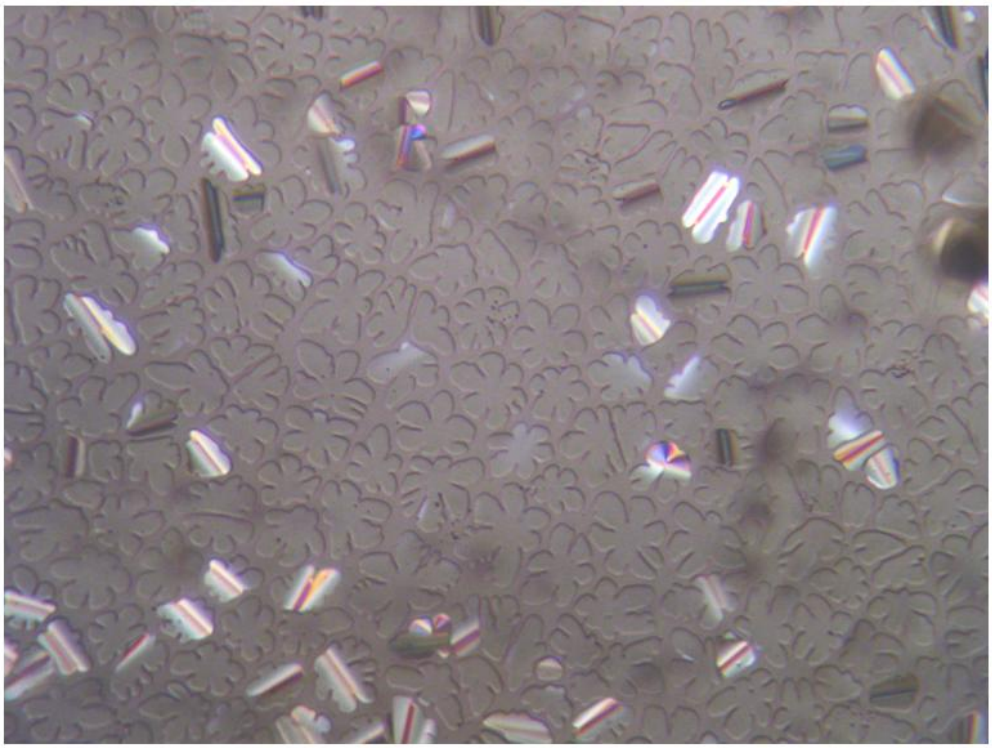

Figure 5.3 POM image of CT complex 1(c) upon cooling from isotropic phase at 180^{o}C under uncrossed polarizer.

All CT complexes developed similar POM textures (uncrossed polarizer) as shown in Figure 5.3 upon cooling from isotropic phase. When the isotropic phase is cooled, one sees growing germs resembling flowers. They coalesce and form a mosaic of domains. Most of these domains do not show any polarization colors, and this means that the flat molecules are horizontal, the negative optical axis being vertical (parallel to the microscope axis). Certain germs and domains however, show brilliant colors and are not homeotropic. The ability to control their stable molecular assembly and orientation plays very important role in determining the utility of discotic materials in devices. Alignment of thin films of complex was investigated and observed using polarized optical microscopy. It was found that slow cooling from its melt yielded near perfect homeotropically aligned samples. This is clearly seen from the growing hexagonal domains that are optically extinct when viewed between crossed polarizer. This approach to achieve molecular orientation without crystallization via a charge-transfer complex process involving triphenylene based DLCs could prove particularly useful and versatile in organic optoelectronic device applications. These alignments appear to be stable at room temperature.

The transition temperature data obtained from the heating and cooling cycles of DSC are collected in Table 5. 1. In their DSC thermograms, they display a soft solid to mesophase transition followed by mesophase to isotropic transition on heating. Upon cooling they show only isotropic to mesophase transition and the mesophase remains stable down to room temperature. Compound **1** shows columnar helical phase upon heating and upon cooling it crystallize from columnar hexagonal phase and pure compound **2** shows columnar plastic

phase along with columnar hexagonal phase. In case of CT complexes only single phase is present. Other phases of pure compounds are suppressed respectively. As typical example the DSC thermogram of CT **1 (b)** complex is shown in Figure 5. 4. For all CT complexes a broad transition peak (isotropic to mesophase) is observed. Precise measurements of transition temperatures are hard to determine due to weak phase transition temperatures and slowly developing optical textures. POM studies of CT complexes combined with DSC were used to study the phase transition temperature.

Table 5.1 DSC data for CT complexes upon cooling from isotropic phase.

CT complexes	Phase transition temperature upon cooling cycle
1(a)	Col_h 98.8^oC I
1(b)	Col_h 158^oC I
1(c)	Col_h 235.7^oC I
2(a)	Col_h 208.5^oC I

5.1.4.2 X-ray Diffraction

In order to reveal the mesophase structure and hence the supramolecular organization of these complexes, X-ray diffraction experiments were carried out using unoriented samples. X-ray diffraction patterns for all the complexes were recorded while cooling from the isotropic phase. The X-ray diffraction patterns of the mesophase exhibited by all the samples are almost similar and are supportive of a discotic hexagonal columnar arrangement. As typical example, one dimensional intensity *vs* theta (θ) graph derived from the pattern are shown in the Figure 5.5. Qualitatively all the compounds show similar X-ray diffraction

patterns. As can be seen from the Figure 5.5, in the small angle region, two sharp peaks, one very strong and one weak reflection are seen whose *d*-spacings are in the ratio of $1:1/\sqrt{3}$, consistent with a two-dimensional hexagonal lattice. In the wide angle region two diffuse reflections are seen. The broad one centered at 4.62 Å corresponds to the liquid like order of the aliphatic chains. The reflection at higher *theta* (θ) value and well separated from the previous one is due to the stacking of the molecular cores one on the top of the other. The diffuse nature of this peak implies that the stacking of the discs within each column is correlated over short distances only. The average stacking distance (core-core separation) was found to be 3.66 Å and falls in the range observed for a number of materials exhibiting discotic columnar phase. So the discotic molecules stack one on top of the other to form the columns and these columns in turn arrange themselves on a two dimensional hexagonal lattice for both the series of compounds. In these unoriented samples, we do not observe any additional small angle peak for the formation of any superlattice with the two dimensional hexagonal lattice. Therefore, it was concluded that the triphenylene and TNF units arrange themselves statistically to form a columnar hexagonal phase.

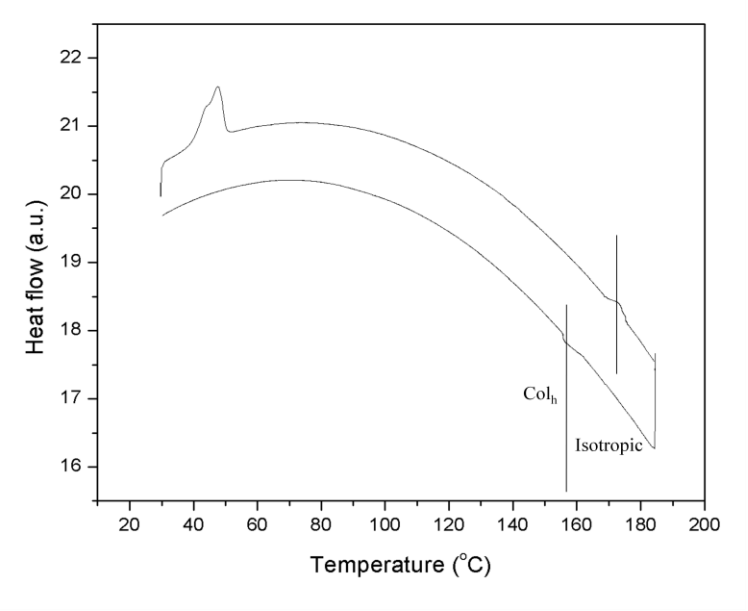

Figure 5.4 DSC thermogram of CT complex **1(b**).

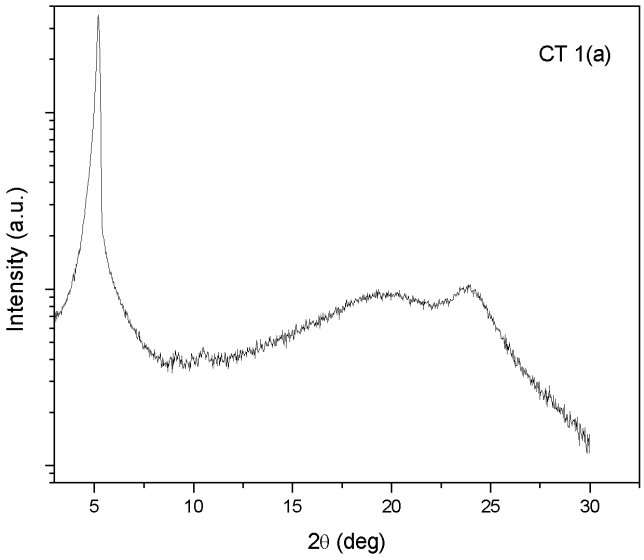

Figure 5.5 I-2θ profile obtained in the Col_h mesophase of CT complex **1(b).**

5.1.4.3 Visible Absorbance Spectroscopy

The optical properties of charge-transfer complexes of the above TP based DLCs and related discotic electron donor compounds with TNF acceptor have been studied in solution. Initial evidence to support the formation of a charge-transfer complex was their changes in colors and hence in absorption spectra. UV–Vis absorption was measured in chloroform as solvent. Pure compounds **1, 2** and TNF have almost no absorption in the visible spectral range, while a broad absorption at longer wavelength was developed in all complexes (Figure 5.6). This low energy absorption indicates the formation of the charge-transfer complex in the mixture.

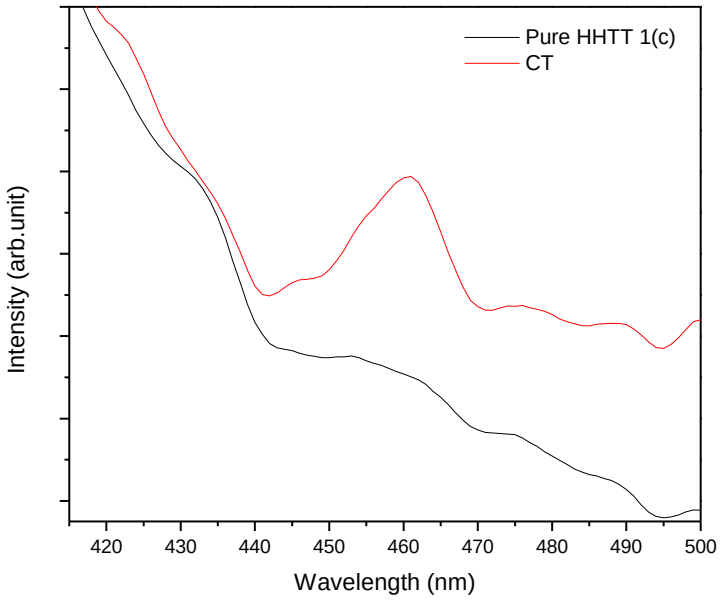

Figure 5.6 Visible absorbance spectroscopy of the Compound **1** and CT **1(c).**

5.1.4.4 Dielectric Spectroscopy

All CT complexes were study for dielectric relaxation spectroscopy in temperature range 30^{o}C to 170^{o}C and frequency range 0.1 Hz to 20 MHz. Pure compound HHTT **(1)** doesn't show any relaxation process due to symmetry and lack of net dipole moment. No relaxation

process for its CT complex **1(a)** was observed in this temperature and frequency range. CT complexes **1(b)** and **1(c)** show single relaxation process in low frequency region with very high value of dielectric loss. Therefore this relaxation process is attributed to ionic conduction. Temperature dependent relaxation curves for CT complex **1(c)** are shown in Figure 5.7 and Figure 5.8.

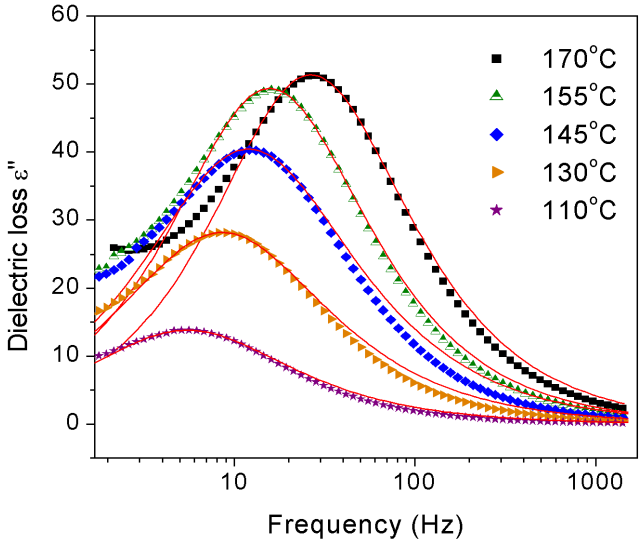

Figure 5.7 Dielectric loss ε″ as function of frequency at different temperatures CT **1(c)**.

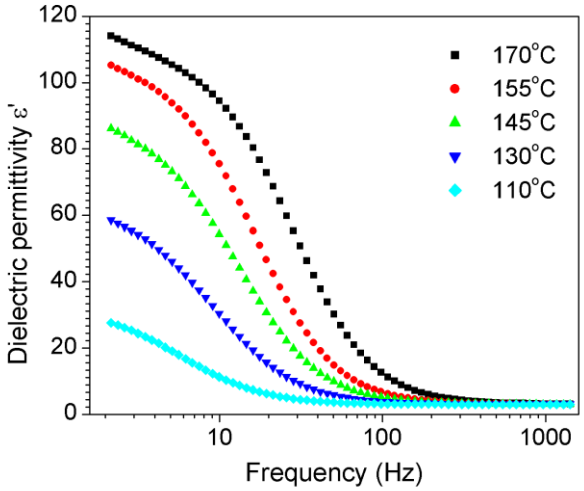

Figure 5.8 Dielectric permittivity ε′ as function of frequency for CT **1(c)**.

Pure compound C_4MNTP (**2)** shows single relaxation α process (temperature dependent). For CT complex **2(a)**, the relaxation curves are damped and relaxation frequency shifts to lower frequency side. Arrhenius temperature dependent relaxation time plot for pure and CT complex is shown in Figure 5.10. Since CT complexes involve strong interactions, the disc motion becomes slower. However in this temperature and frequency range, we didn't observe any extra relaxation process.

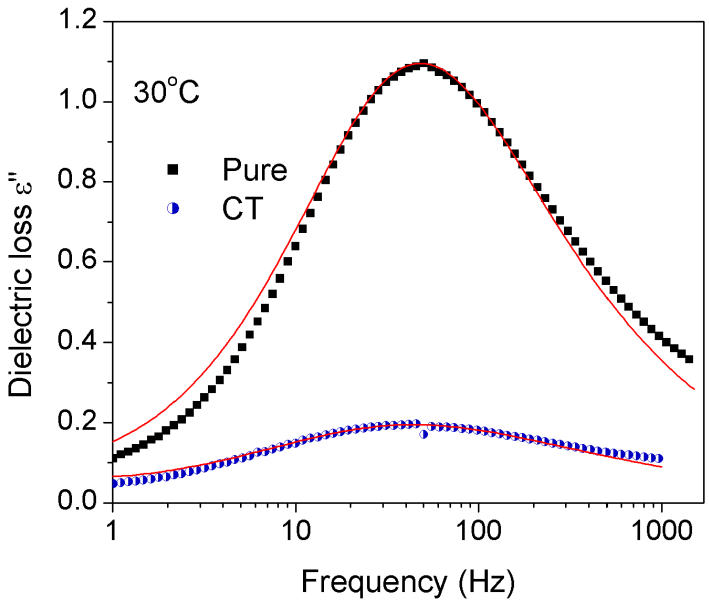

Figure 5.9 Dielectric loss ε″ as function of frequency at 30°C for pure **2** and CT **2(a)**.

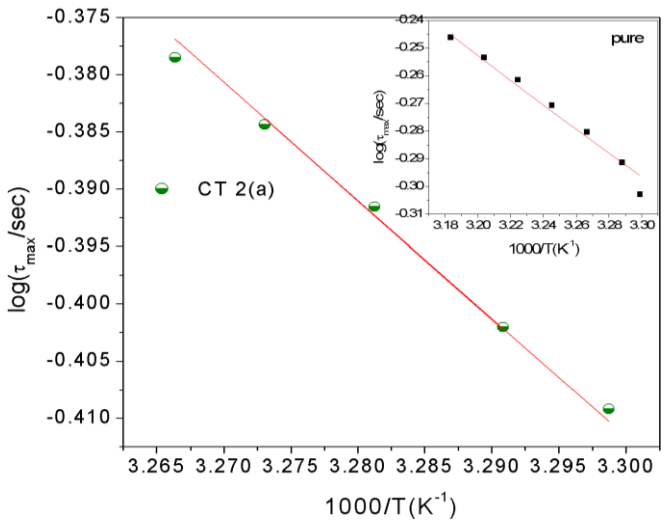

Figure 5.10 Arrhenius temperature dependent relaxation time plot for pure compound **2** and CT **2(a)**.

5.1.4.5 Conclusions

We successfully prepared donor–acceptor charge-transfer complex of DLCs derived from triphenylene core with 2, 4, 7-trinitrofluorenone (TNF). The resulting CT complex has been investigated using visible absorbance spectroscopy, polarized optical microscopy, thermal analysis, and X-ray diffraction and dielectric spectroscopy. The charge-transfer complexes exhibits single columnar mesophase formation over a wide temperature range suppressing other mesophase present in pure DLCs. The mesophase was identified as a hexagonal columnar mesophase by its characteristic texture, and X-ray diffraction indicates that the columnar order remains at room temperature. More importantly, it was discovered that with this complex, a homeotropic molecular orientation can be easily achieved on glass substrates. These alignments appear to be stable at room temperature. This approach to achieve molecular orientation without crystallization via a charge-transfer complex process involving

a symmetrically and unsymmetrically substituted triphenylene could prove particularly useful and versatile in organic optoelectronic device applications.

Part 2

5.2 Induction of Mesophase in Non Mesomorphic Materials.

5.2.1 Induction of Hexagonal Columnar Mesophase in Non Mesomorphic Derivative of Triphenylene Core

5.2.1.1 Abstract

We now report on mesophase induction via CT interactions between a non-mesomorphic compound composed of TP derivative and flat 2, 4, 7-trinitrofluorenone molecules (TNF). The phenomenon of induction of mesophase in two non-liquid crystalline compounds, appearance of another mesophase, stabilization of mesophase (broadening of temperature range of the mesophase) by CT interactions is well known from decades [4]. Mesophase induction via CT interaction between electron rich disc-like molecules and the flat electron acceptor TNF is very fascinating finding. Based on detailed experimental studies using polarizing optical microscopy, differential scanning calorimetry, and X-ray diffraction, we have reported the induction of columnar mesophase in mixture of two non mesomorphic materials.

5.2.1.2 Materials and Experimental

Compound under present study is pyridinium bromides containing hexaalkoxytriphenylene units (Py-TP) **3**. Synthesis of this compound is reported by S. Kumar *et al.* [25]. They observed that by increasing the number of carbon atoms on the peripheral chains of the triphenylene core stabilized the columnar phase while increasing the spacer length

connecting the triphenylene unit with the pyridine moiety destabilized the mesophase. Compound with largest spacer length (n=5) is non liquid crystalline in nature. Chemical structure of this compound is shown in Figure 5.11. We have used this compound to form charge transfer complex with TNF. CT complex was prepared (**3(a)**) by dissolving compound **3** and with 10% weight ratio of TNF in chloroform, sonicating for two hours, evaporating the solvent, and drying the residues in a vacuum. Compound **3** and TNF were pale yellow powders. When they were dissolved in chloroform, the color of the solutions changed to deep red. Initial evidence to support the formation of a charge-transfer complex was therefore their changes in color. The complex thus prepared was analyzed by differential scanning calorimetry (DSC), polarizing optical microscopy (POM), X-ray diffraction.

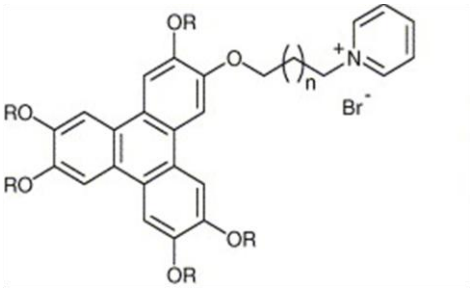

n = 5, R = n-C_4H_9,

Figure 5.11 Chemical structure of pyridinium bromide containing hexaalkoxytriphenylene units (Py-TP) with n = 5, R = n-C_4H_9.

5.2.1.3 Result and Discussion

5.2.1.3.1 Mesomorphic Behaviour

Liquid crystalline properties of CT complex **3(a)** were studied initially with POM and then with DSC. CT complex **3(a)** was very viscous and sticky in nature. Upon slow cooling from isotropic phase optical textures started appearing very slowly. Textures thus appeared resemble broken fan textures (Figure 5.12), characteristic of hexagonal columnar phase. DSC

thermogram of **3(a)** is shown in Figure 5.13. It exhibits a very broad melting peak centered around 205^{o}C. CT complex shows very broad range of mesophase down to room temperature.

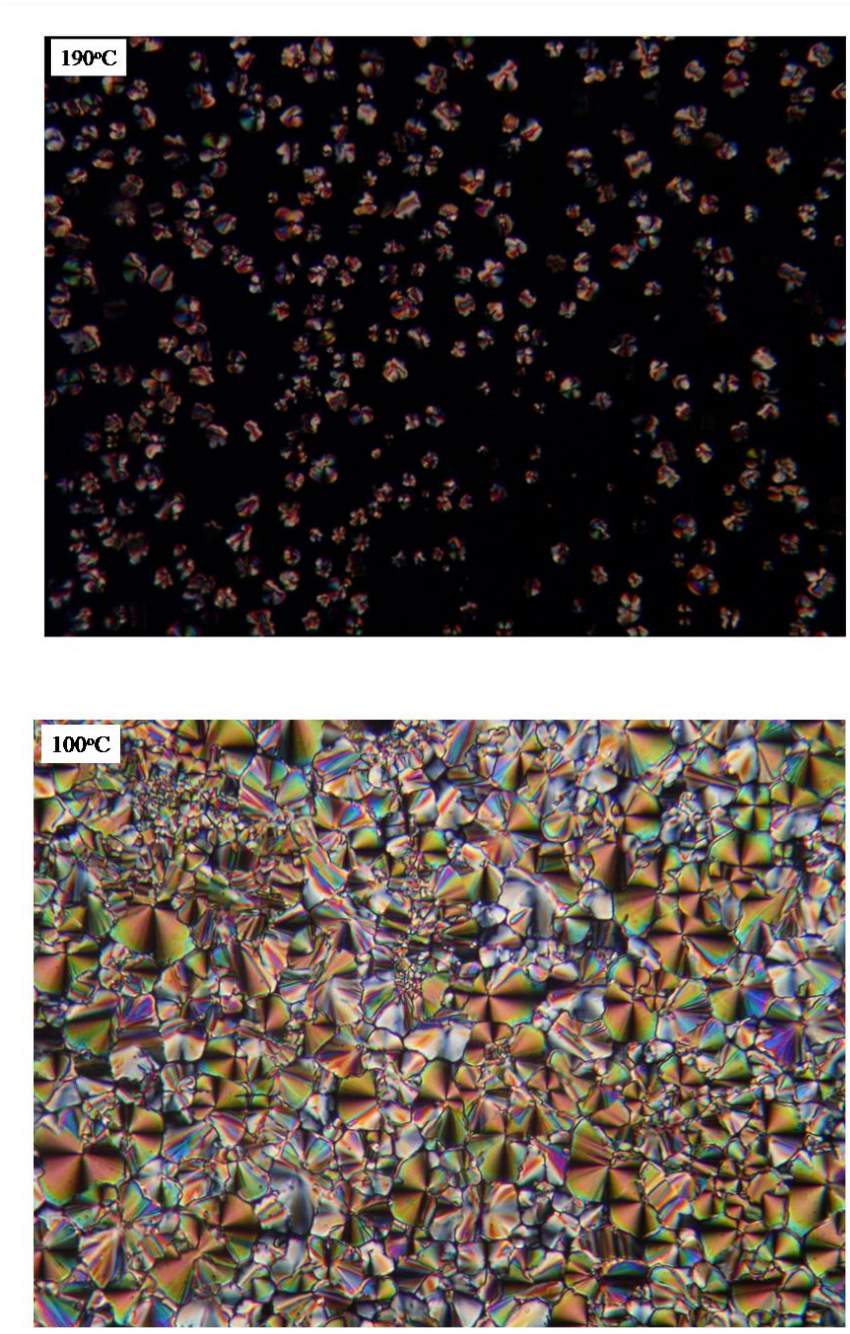

Figure 5.12 POM image of CT complex **3(a)** on cooling from isotropic phase at 190^{o}C and 100^{o}C.

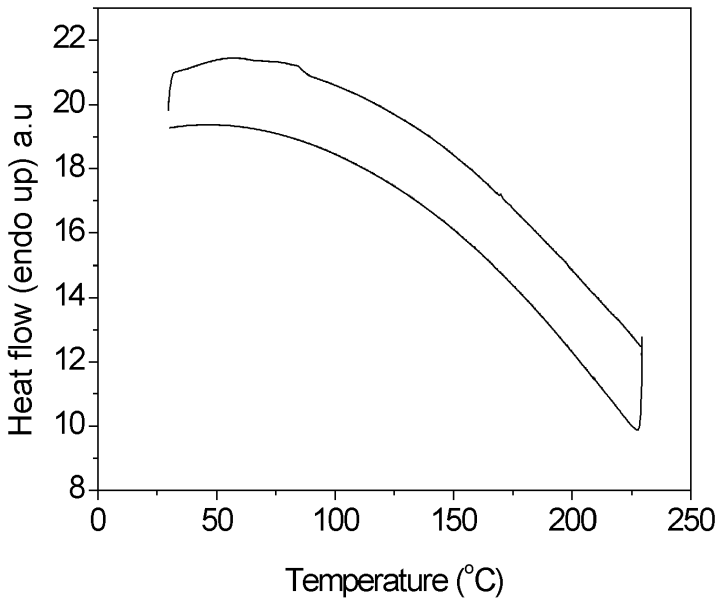

Figure 5.13 DSC thermogram of complex **3(a)**.

5.2.1.3.2 X-ray Diffraction

As can be seen from the pattern (Figure 5.14) there is one peak at 18.47 Å in small angle region corresponding to (10) reflection from (10) plane of 2D hexagonal columnar lattice. Unfortunately, we did not get any other peak corresponding to higher reflections (11, 20 and so on) in small angle region. The pattern in wide angle region has one broad peak at $\theta \sim 10^{o}$. This broad peak with a *d*-spacing of ~ 4.5 Å was due to the liquid like packing of the aliphatic chains. A relatively sharper peak with a *d*-spacing of ~ 3.4 Å was observed due to stronger core-core interaction.

Combining the results of POM, DSC and XRD we can assign the induced mesophase as columnar hexagonal mesophase.

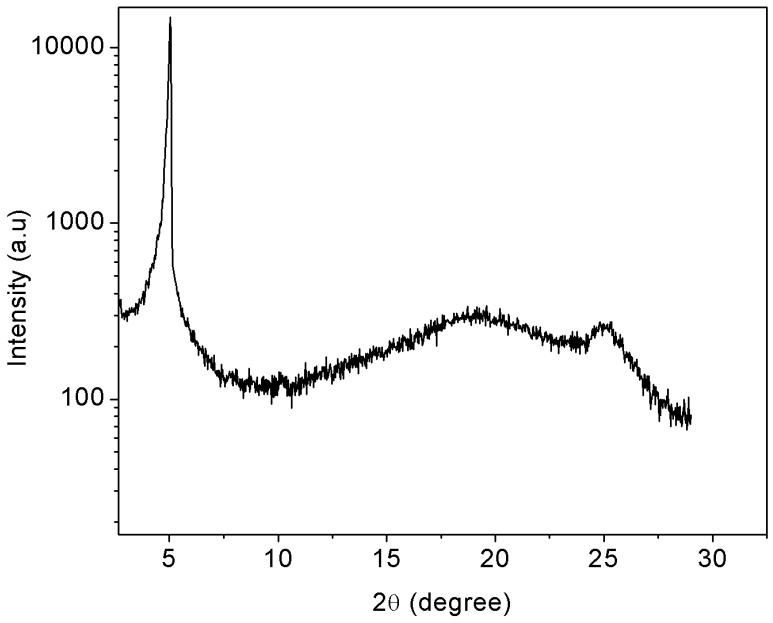

Figure 5.14 I-2θ profile obtained in the Col_h mesophase of CT complex **3(a).**

5.2.1.4 Conclusions

Combine study of POM, DSC, and XRD measurements show that columnar mesophase was induced into the binary mixture of compound **3** and TNF. Both compounds are non liquid crystalline in nature in pure form. Formation of charge transfer complex between electron acceptor and electron donor molecules resulted into induction of columnar mesophase.

5.2.2 Induced Smectic A Phase in Binary Mixtures of a Non Mesomorphic Compound Composed of Disc-like Molecules and 2, 4, 7-trinitrofluorenone

5.2.2.1 Abstract

Charge Transfer (CT) interactions have been known to (a) induce mesophases in mixtures of two non-liquid crystalline compounds (b) form new mesophases not present in either of the liquid crystalline compounds forming the mixtures and (c) broaden the mesophase range. In

the case of disc-like molecules, these interactions usually result in the induction of columnar hexagonal or columnar nematic phases. We now report on mesophase induction via CT interactions between a non-mesomorphic compound composed of disc-like molecules and flat 2, 4, 7-trinitrofluorenone molecules (TNF). Interestingly the induced mesophase is lamellar in nature and corresponds to a smectic A like phase as show by prelimnary experimental studies using polarizing optical microscopy, differential scanning calorimetry.

5.2.2.2 Introduction

After the discovery of discotic liquid crystal (DLC) in 1977[26], there is revolution in the field of synthesis of DLC. Rufigallol has found to function as core fragment for a remarkable family of DLC. Rufigallol has attracted immense interest owing to their ease synthesis and various applications in different fields. More than 100 different DLC derivatives of rufigallol have been synthesized. Most of them exhibit well ordered two dimensional columnar hexagonal arrangement. Mixed tail rufigallol hexaethers having normal alkyl chain are found to be non liquid crystal in nature [27-34]. However it is observed that a branched chain substituted tetraalkoxy derivatives shows broad room temperature mesophase [35-36]. Nature of aliphatic chains attached to the aromatic core plays an important role in deciding the mesomorphic behavior of DLC. Also**,** Structure and mesomorphic properties of disc like molecules comprising of rigid aromatic core with peripheral alky chains depend upon the stacking of the molecular discs which forms columns. Moreover, specific inter and intra molecular interactions like charge-transfer (CT), electrostatic interactions (ion-dipole, dipole-dipole), hydrogen bonding, π-π stacking, Van der waals forces etc and the molecular shape of the constituent unit plays very crucial role in formation of different types of mesophases and other thermotropic liquid crystalline properties of organic materials. The phenomenon of

induction of mesophase in two non-liquid crystalline compounds, appearance of another mesophase, stabilization of mesophase (broadening of temperature range of the mesophase) by CT interactions is well known from decades [37-39]. Mesophase induction via CT interaction between electron rich disc-like molecules and the flat electron acceptor 2, 4, 7-trinitrofluorenone (TNF) is very fascinating finding. In case of disc-like molecules, these interactions usually results into induction of columnar hexagonal or columnar nematic phases. Usually the induction or stabilization of smectic A phase by addition of electron acceptor molecule (TNF) has been reported for calamatic liquid crystals [40-42] and there are less report of columnar phase forming electron donors which display an induction of smectic liquid crystalline structures by mixing with nitrofluorenone based acceptors [43].

In this work, we have reported preliminary but interesting finding on the induction of smectic A phase in non liquid crystalline mixed tail rufigallol hexaethers derivative via complexation with TNF. Usually rufigallol cores are electron deficient. But in comparison to very strong electron acceptor TNF molecule, disc like molecule behaves as electron donor. This mesophase induction is a rather amazing finding because no typical electron donor is present. Identification of the complex and induction of liquid crystalline phase was investigated by polarizing optical microscopy (POM), differential scanning calorimetry (DSC).

5.2.2.3 Materials and Methods

Disc like molecule used in the present study is be 1, 5-dihydroxy-2, 3, 6, 7-terakishexyloxy-anthraquinone (**4**) and was synthesized as reported [31].

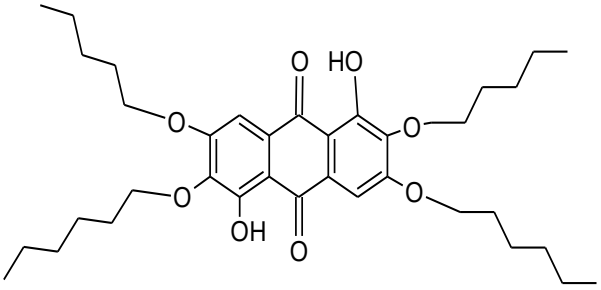

Figure 5.15 Molecular structure 1, 5-dihydroxy-2, 3, 6, 7-terakishexlyoxy-anthraquinone (**4**).

It is a non liquid crystalline in nature. The structure of the molecule is shown in Figure 20(a). Second component 2, 4, 7, trinitrofluorenone was selected as acceptor to prepare complexes by mixing with component **4**. TNF has been widely cited as an electron acceptor molecule and form charge transfer complexes with wide variety of polynuclear hydrocarbons. Binary mixtures of non mesomorphic rufigallol derivative with different mole ratios of TNF were prepared by sonicating both components in dichloromethane. Removal of solvent subsequently gave the complexes. We observed the mesophase starts appearing with 10% TNF and with 40% of TNF the induced phase was stabilized. Higher concentration of TNF leads to separation of two components. Results are shown for 40% of TNF in compound **4**.

Textural and thermal properties of the induced mesophase were studied by POM (Olympus BX51) combined heating stage (Mettler FP82HT) and central processor (Mettler FP90) along with DSC (Perkin, Elmer, model Pyres 1D) respectively. DSC was performed at scanning rate of $5^{o}C/min^{-1}$ both on cooling and heating.

5.2.2.4 Results and Discussions

5.3.2.4.1 Thermotropic Behaviour

The observed drastic change in properties of CT complexes formation was on thermal behavior. Compound **4** is a crystalline compound. TNF is also a crystalline material with a melting temperature 176-177^{o}C. The complex showed completely different phase transition. Induced liquid crystalline phase with their corresponding temperatures were first observed by POM. Accurate measurement of phase transition temperature and their associated enthalpies were measured by DSC. At room temperature the sample was crystalline in nature and on heating some textures started appearing and it cleared at around 140^{o}C. To identify the phase sample was cooled slowly from isotropic phase and textures were observed under POM. We observed that on cooling from isotropic phase batonnets textures from isotropic liquid started appearing and on further cooling typical fan shaped textures appeared and finally it got crystallized. Textures that appeared in mesophase are characteristic of smectic A phase. Optical photomicrographs for mixture on cooling are shown in Figure 5.15. Similar textures have been observed for smectic A phase of nanophase segregated rod –disc oligomers [44]. No phase separation was observed and the mixture was found to be thermodynamically stable.

The DSC thermogram (Figure 5.16) of the binary mixture shows two first order transition corresponding to isotropic phase to mesophase transition and mesophase to crystallization on cooling cycle. The mesophase exhibited between the temperature range 115.45^{o}C and 137.28^{o}C. The associate enthalpy observed for the isotropic to mesophase transitions is 0.62 kJ/mol and for mesophase to crystalline is 11.5kJ/mol which is higher than later [44]. In present case TNF molecule induces lamellar phase instead of columnar or discotic nematic

phase probably because of the uneven distribution of the TNF molecules in disc like molecule which results in the distorted geometry. Induction of mesophase and supramolecular organization of mesophase is also determined by various other specific intra-inter molecular interactions along with the geometry of constituent molecules.

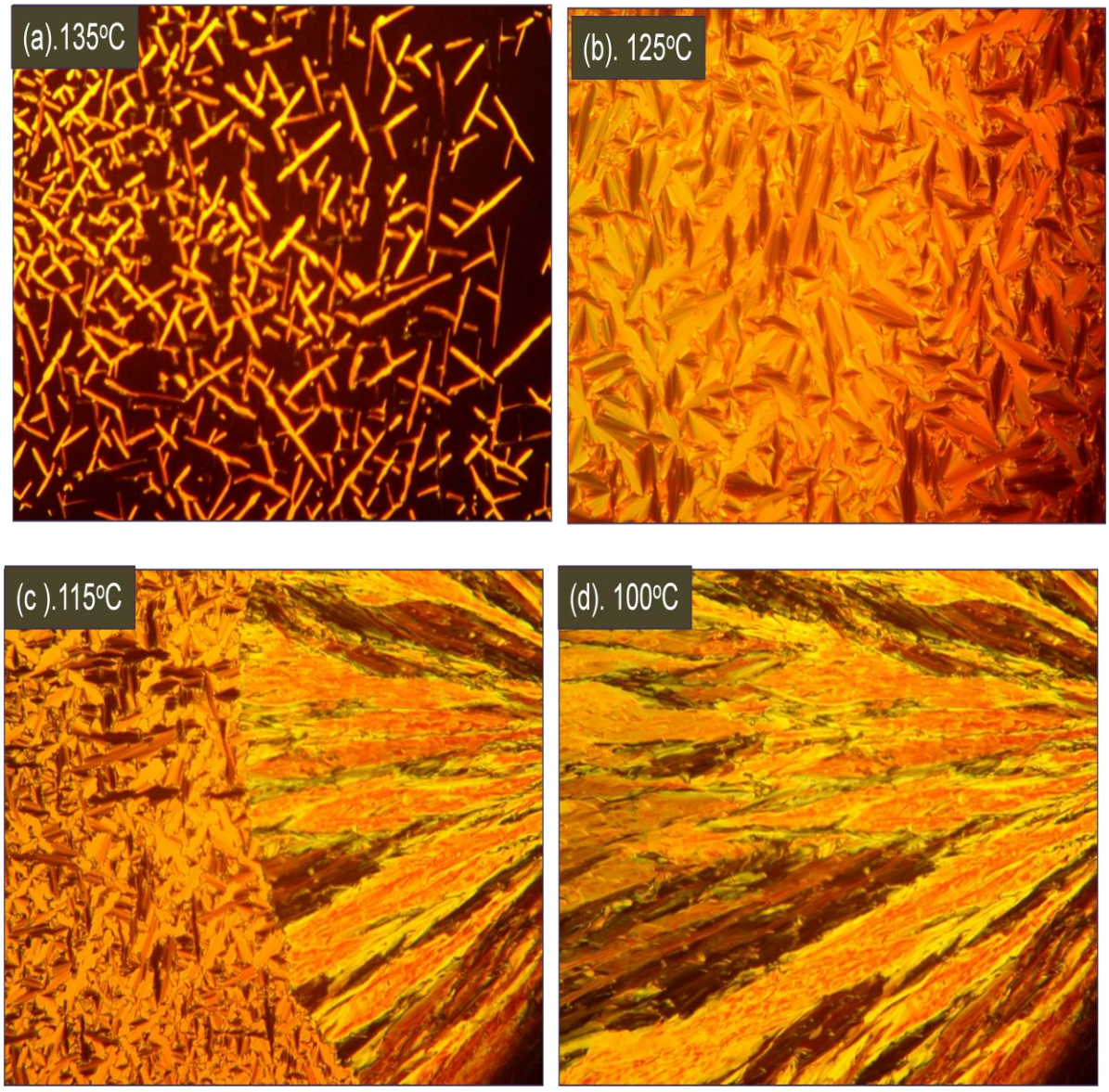

Figure 5.16 Polarizing optical microscopy (POM) observations of the show phase transitions and on cooling from isotropic phase this exhibit batonnets (a) and on further cooling focal

conic texture (b) characteristic of a smectic A (SmA) appear. On further cooling transition from mesophase to crystallization occurs (c) and finally crystallizes (d).

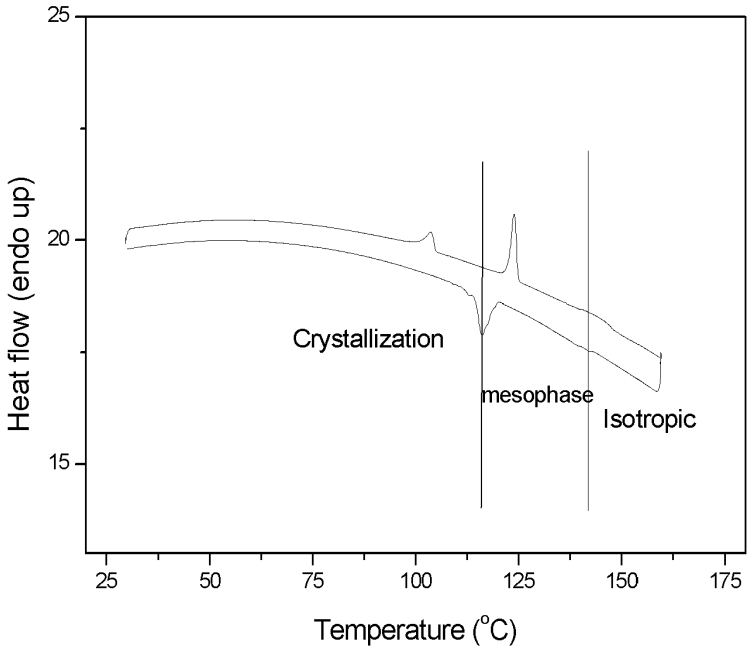

Figure 5.17 DSC scan of binary mixture.

5.2.2.4.2 Visible Absorbance Spectroscopy

Initial evidence to support the formation of charge transfer complex was slight change in the color of the complex. UV/visible spectroscopy of the complex (Figure 5.17) shows broadening of peak and appearance of shoulder in region 310 nm to 390 nm support the modeling of π-π interactions of charge transfer type. Moreover blue shift in the peak of the complex can be attributed to the occurrence of the CT from disc like molecule to TNF in the complex [45].

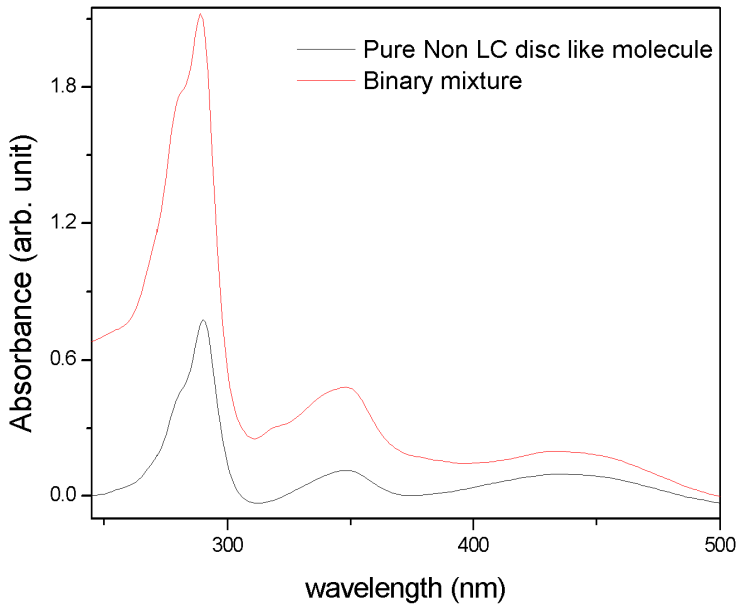

Figure 5.18 UV/Visible spectroscopy of the binary mixture.

5.2.2.5 Conclusions

We have successfully induced a stabilized mesophase between two non mesomorphic compounds composed of disc like molecules and flat TNF molecules respectively. The simultaneous studies of POM, DSC us to assign the phase. Induced phase was found to correspond to smectic A like phase. More detail studies are required to study the induced phase and mutual orientation of disc like molecules and TNF molecules.

References

[1] O. Kruglova, E. Mencles, Z. Yildirim, M. Wubbenhorst, F. M. Mulder, J. A. Stride, S. J. Picken, G. J. Kearley, J. *Chemphyschem.*,, *8*, 1338, (2007).

[2] Usol'tseva, A. Smirnova , *Mol. Cryst. Liq. Cryst.*, 397, 161, (2003).

[3] N. Boden, R. J. Bushby, O. R. Lozman, *Mol. Cryst. Liq. Cryst.*, 411, 1387, (2004).

[4] H. Ringsdorf, R. Wustefeld, E. Zerta, M. Ebert, J. H. Wendorff, *Angew. Chem*., 101, 934 (1989), *Angew. Chem., Int. Ed. Engl.* , 28, 9, (1989).

[5] C. Destrade, P. Foucher, H. Gasparoux, H. T. Nguyen, A.-M. Levelut, J. Malthete, *Mol. Cryst. Liq. Ctyst*.,106, 12, (1994) and references cited therein.

[6] (a) H. Bengs, M. Ebert, O. Karthaus, B. Kohne, K. Praefcke, H. Ringsdorf, J. H. Wendorff. R. Wiistefeld, *Adv. Mater*., 2, 141 (1990). (b) M. Ebert, G. Frick, C. Baehr, J. H. Wendorff, R. Wiistefeld, H. Ringsdorf, *Liq. Cryst*., 11, 293, (1992).

[7] A. Bubnov, V. Hamplová, M. Kašpar, A. Vajda, M. Stojanović, D. Z. Obadović, N. Éber, Katalin Fodor-Csorba, *J. Thermal Analysis and Calorimetry* , 90, 431, (2007).

[8] D. Z. Obadović, A. Vajda, M. Garić, A. Bubnov, V. Hamplová, M. Kašpar, Fodor Csorba K, *J.Thermal Analysis and Calorimetry,* 82, 519, (2005).

[9] D. Markovitsi, H. Bengs, H. Ringsdorf, *J. Chem. Soc., Faraday Trans.,* 88, 127, (1992).

[10] W. G. Blann, C. A. Fyfe, J. R. Lyerla, C. S. Yannoni, *J. Am. Chem. Soc.*, 103, 4030, (1981).

[11] R. S. Mulliken, *J. Phys. Chem., 56*, 801, (1952).

[12] T. Hirose, T. Yumoto, K. Matsumoto, S. Mitsushio, O. Kawakami, M. Yasutake, M. *Mol. Cryst. Liq. Cryst., 524*, 68, (2010).

[13] K. Praefcke, J. D. Holbrey, *J. Inclusion Phenom. Mol. Recognit. Chem., 24*, 19, (1996).

[14] Y. Kamikawa, T. Kato, T. *Org. Lett., 8*, 2463, (2006).

[15] V. Percec, M. R. Imam, M. Peterca, D. A. Wilson, R. Graf, H. W.Spiess, V. S. K. Balagurusamy, P. A. Heiney, *J. Am. Chem. Soc.*, 131, 7662, (2009).

[16] G. B. M. Vaughan, P. A. Heiney, J. P. Mccauley, A. B. Smith, A. B. *Phys. Rev. B, 46*, 2787, (1992).

[17] P. Davidson, A. M. Levelut, H. Strzelecka, V. Gionis, *J. Phys., Lett.*, 44, L823, (1983).

[18] P. H. J. Kouwer, W. F. Jager, W. J. Mijs, S. J. Picken, *Macromol.*, 35, 4322, (2002).

[19] V. Percec, M. Glodde, T. K. Bera, Y. Miura, I. Shiyanovskaya, K. D. Singer, V. S. K. Balagurusamy, P. A. Heiney, I. Schnell, A. Rapp, H. W.Spiess, S. D. Hudson, H. Duan, *Nature*, *419*, 384, (2002).

[20] N. Boden, R. J. Bushby, J. Clements, R. Luo, R. *J. Mater. Chem.*, *5*, 1741, (1995).

[21] P. S. Kumar, S. Kumar, V. Lakshminarayanan, *J. Phys. Chem. B*, 112, 4865, (2008).

[22] K. J. Donovan, K. Scott, M. Somerton, J. Preece, M. Manickam, M. *Chem. Phys.*, 322, 471, (2006).

[23] D. Markovitsi, S. Marguet, J. Bondkowski, S. Kumar, *J. Phys. Chem. B*, 105, 1299, (2001)

[24] Y. Yamamoto, T. Fukushima, Y. Suna, N. Ishii, A. Saeki, S. Seki, S. Tagawa, M. Taniguchi, T. Kawai, T. Aida, *Science*, *314*, 1761, (2006).

[26] S. Chandrasekhar, B. K. Sadashiva, K A Suresh, *Pramana*, 9, 471, (1977).

[27] A. Queguiner, A. Zann, J. C. Dubois and J. Billard, *Proceedings of International Conference on Liquid Crystals*, Bangalore, ed. S. Chandrasekhar, Heyden and Son, London, 34, (1980).

[28] C. Carfugna, A. Roviello and A. Sirigu, *Mol. Cryst. Liq. Cryst*., 122, 151, (1985).

[29] M. Werth, J. Leisen, C. Boeffel, R. Y. Dong and H-W Spiess, *J. Phys. II Fr.*, 3, 53, (1993).

[30] J. Billard, Z. Luz, R. Poupko and H. Zimmermann, *Liq. Cryst*., 16, 333, (1994).

[31] K. S. Raja, S. Ramakrishnan and V. A. Raghunathan, *Chem. Mater*., 9, 1630, (1997).

[32] V. Prasad, K. Krishnan and V. S. K. Balagurusamy, *Liq. Cryst.*, 27, 1075, (2000).

[33] S. Kumar, J. Naidu and S. K. Varshney, *Mol. Cryst. Liq. Cryst*. , 411, 355, (2004).

[34] S, Kumar, *Phase Transitions*, 81, 113, (2008).

[35] H. K. Bisoyi and S. Kumar, *Tetrahedron Lett.*, 48, 4399, (2007).

[36] H. K. Bisoyi and S. Kumar, *New J. Chem.*,32, 1974, (2008).

[37] H. Bengs, M. Ebert, O. Karthaus, B. Kohne, K. Praefcke, H. Ringsdorf, J. H. Wendorff, and R. Wustefeld, *Adv. Mater*., 2 , 141 (1990).

[38] M. Ebert, G. Frick, C. Baehr, J. H. Wendorff, R. Wustefeld, and H. Ringsdorf, *Liq. Cryst*., 11 , 293, (1992).

[39] K. Praefcke and J. D. Holbrey, *J. Incl. Phenom. Mol. Recog. Chem.*, 24 , 19, (1996).

[40] K. Praefcke, D. Singer, In Handbook of Liquid Crystals; D Demus, J W Goodby, G W Gray, H W Spiess, Vill, V., Eds.; Wiley VCH: New York, 2B, 945, (1998).

[41] K. A. Suresh, *Mol. Cryts. Liq. Cryst*,, 97,417, (1983)

[42] K. A.Suresh, *Mol. Cryts. Liq. Cryst.*, 32, 99, (1986) .

[43] D. Goldmann, A. Nordsieck, T. Janietz, C. Schmidt, J. H. Wendroff, *Mol. Cryst. Liq. Cryst*., 411, 337, (2004).

[44] H. K. Bisoyi, V. A. Raghunathan, S. Kumar, *Chem. Commun.*, 7003, 7003, (2009).

[45] P. S. Kumar, S. Kumar, and V. Lakshminarayanan, *J. Phys. Chem. B*, 112, 486, (2008).

Chapter 6

Summary

In this chapter, I have summarized some of the important results and conclusions derived from this thesis work, which deals with **"Electrical and Optical Investigations on Dispersed Discotic Liquid Crystal Composite Systems".** I have briefly discussed the possibilities and scope for future work based on the results obtained from our experimental work. Chapter wise description of the thesis has been given below:

Chapter 1 gives an over view of thermotropic liquid crystals and their brief history and focuses in greater detail on the physical properties of discotic liquid crystals, making them ideal candidates for various optical and electronic devices. We have revised the recent developments in this subject and proposed aim of our work.

Chapter 2 provides information regarding the DLC materials. It includes various characterization techniques (like structural, spectroscopic, thermal and electro-optic) employed to characterize them. Design of experiment is also mentioned.

Chapter 3 presents results and discussing chararterisation of pure and ZnO nanoparticles dispersed rufigallol based discotic liquid crystal. Chapter 3 is divided into two parts. Part (1) deals with temperature-dependent dielectric spectroscopy of pure discotic liquid crystal with rufigallol core having wide temperature range hexagonal columnar (Col_h) mesophase in frequency range 1 Hz to 10 MHz. The mesophase and its transition temperature have been determined by using polarizing optical microscopy and differential scanning calorimeter. SAXS showed the existence of hexagonal columnar phase. The molecular dynamics of rufigallol core in liquid crystalline and isotropic phase were also

studied. Part (2) is an experimental characterization of dispersions of ZnO nanoparticles (NPs) in the columnar matrix of a discotic liquid crystal. Thermophysical properties were investigated by absorbance spectroscopy, differential scanning calorimetry (DSC), polarizing optical microscopy, dielectric measurements, dc conductivity, X-ray diffraction and infrared (IR) dichroism technique. The experimental results show that inclusion of ZnO NPs into the columnar matrix enhances the orientational order in the columnar phase and does not affect the two dimensional hexagonal lattice. The alignment in homeotropic samples is also found to be better with the addition of the NPs. The real (ε′) and imaginary parts (ε″) of the permittivity increase by a small amount in the dispersions and a new loss process appears in the isotropic phase. The order parameter measured using the IR dichroism technique in the face on geometry (homeotropic alignment) shows an enhancement for the composite system. The dc conductivity is also found to increase by an order of magnitude by addition of the NPs. These results suggest an improved stacking of the disc-like molecules within the columns by the insertion of the ZnO NPs possessing high electron mobility. Such composite systems would be highly beneficial for potential applications like organic conductors.

Chapter 4 discusses the synthesis of hexanethiolate-stabilized gold nanoparticles (GNP) and their dispersion in hexaalkyloxytriphenylene H10T (**1**) and mono nitro substituted triphenylene based discotic liquid (MNTP4). Compound **1** is a room temperature crystalline material and shows wide range of columnar hexagonal mesophase (Col_h). Whereas, compound **2** shows columnar plastic phase along with columnar hexagonal phase at higher temperature before going to isotropic phase. The composite systems were characterized by DSC, POM, XRD, dielectric spectroscopy, visible absorbance spectroscopy and IR dichroic technique. This chapter is also divided into two part. Part (1) deals with the dispersion of

GNP in symmetrically substituted hexaalkyloxytriphenylene (HATn), n=10. POM, DSC and dielectric results show that GNPs are well dispersed into the columnar matrix without affecting the hexagonal arrangements of columns of DLC. Part (2) deals with the dispersion of gold nanoparticles in plastic columnar phase. DSC, POM, XRD, IR-dichroic technique, dielectric spectroscopy results show the inclusion of GNPs in DLC matrix. The nature of mesophases is not altered by GNPs but a shift in transition temperature was observed. Though there is decrease in order parameter and the disc motion about the column axis is hindered, dc conductivity increases with GNPs. These GNP-DLC composite systems may be important for many device applications such as photovoltaic solar cell, photoconduction, light emitting diodes, thin film transistors etc.

Chapter 5 deals with the CT complexes of triphenylene based DLC with 2,4,7-trinitrofluoren-9-one (TNF). It also deals with induction of mesomorphism in non mesogenic disc like molecules via CT complexes with TNF. The thermotropic mesomorphic behavior of the CT complexes was studied by differential scanning calorimetry (DSC), polarizing optical microscopy (POM), and X-ray diffraction (XRD) measurement. This approach to achieve molecular orientation without crystallization via a charge-transfer complex process involving derivatives of triphenylene could prove particularly useful and versatile in organic optoelectronic device applications.

As final conclusions, it may be affirmed that the thesis deals with the **Electrical and Optical Investigations on Dispersed Discotic Liquid Crystal Composite Systems** prepared by incorporation of nanomaterials in the supramolecular order of the columnar phase forming discotic liquid crystals. We have shown that properties of pure DLCs can be

tuned, enhanced, varied according to their application in opto-electronic devices by preparing different dispersed DLC composite systems.

- Alignment and order parameter of DLC can be enhanced by dispersing ZnO nanoparticles in columnar matrix and by preparing charge transfer complexes of DLC.
- Conductivity enhancement by order of two can be achieved by dispersing gold nanoparticles in the columnar matrix.
- Transition temperatures variation, stablization and induction of mesophases can be achieved by forming charge transfer complexes of DLC with TNF.

These inorganic-organic liquid crystal hybrid systems may be extremely important for many device applications such as photovoltaic solar cell, photoconduction, light emitting diodes, thin film transistors etc. Also, composite systems between columnar liquid crystals and polymers, inorganic solids, and biomolecules have only been rarely explored. It is our opinion that the field of liquid-crystal research and in particular the columnar systems will lead to exciting new discoveries

Some of the findings of this thesis have been published/communicated in the following international journals.

List of Publications

In journals:

1. Supreet, S. Kumar, K.K. Raina and R. Pratibha. Enhanced stability of the columnar matrix in a discotic liquid crystal by insertion of ZnO nanoparticles, Liquid Crystals, 2013; 40:228–236.

2. Supreet, S. Kumar, R. Pratibha and K.K. Raina. Effect of dispersion of gold nanoparticles on the optical and electrical properties of discotic liquid crystal Liquid Crystals, 2014, 41:933-39.

3. Supreet, S. Kumar, Rishi Kumar, R. Pratibha and K.K. Raina. Gold Nanoparticles in Columnar Matrix of Discotic Liquid Crystal, AIP Conference Proceeding, 2013;1536:67-68.

4. Rishi Kumar, Supreet, and K. K. Raina. Morphological responses of polymer dispersed liquid crystal composites for photonic display applications, AIP Conference Proceeding,2013;1536:743-744.

5. Supreet, S. Kumar, R. Pratibha K.K. Raina. Orientational Order Parameter Measurements of Discotic Liquid Crystal, AIP Conference Proceeding, 2013;1591:180-182.

In Conference Proceedings:

1. Supreet, S. Kumar, R. Pratibha R, and K. K. Raina. Dielectric and Thermo-physical Studies of Discotic Liquid Crystal Dispersed with Gold Nanoparticles, International Workshop on Soft Matter Chemistry, Nov. 9-11, 2011, organized by Raman Research Institute, pp 42.

2. Supreet, K. K. Raina, Sandeep Kumar. Dielectric spectroscopy of nematic liquid crystals disperesed with discotic liquid crystals, 18^{th} National conference on liquid crystal, Nov. 15-17 2011, organized by NERIST Itanagar, Arunachal Pradesh, Nov. 15-17 2011, pp 66.

3. Supreet, R. Pratibha, S. Kumar, and K. K. Raina. ZnO-Columnar Hexagonal Discotic Nanocomposites: Dielectric and Thermophysical Properties, 23rd Annual General Meeting-Materials Research Society of India (MRSI), February 13-15, 2012, organized by Thapar University, Patiala, pp 148.

4. Supreet, R. Pratibha, S. Kumar, and K. K. Raina. Induced smectic A phase in binary mixtures of a non mesomorphic compound composed of disc-like molecules and 2, 4, 7-trinitrofluorenone, 19th National conference on liquid crystals, Nov 21-22, 2012, organized by Thapar University, Patiala, pp 52.

5. Supreet, R. Pratibha, S. Kumar, and K. K. Raina. Thermophysical studies on rufigallol based discotic liquid crystal, NCFM, Sept 24-25, 2012, organized by GVMGC Sonipat, Haryana, pp 23.

6. Supreet, Pratibha R., Sandeep Kumar, and K.K. Raina. Charge transfer complex of discotic liquid crystal, DAVIET-2013, May 30-31, 2013, organized by DAVIET Jalandhar Punjab, pp 34.

7. Supreet, Pratibha R., Sandeep Kumar, and K.K. Raina. Thermal analysis and X-ray study of disc like molecules forming columnar mesophase, National Conference on Recent Developments in Physics (NCRDP-2014), March 29-30, 2014, organized by S. D. (PG) College, Sonipat, Haryana.

8.Supreet, Pratibha R., Sandeep Kumar, and K.K. Raina. Gold Nanoparticles-Discotic Liquid Crystal Composite Systems for Opto-Electronic Devices, International conference on electron microscopy (EMSI-2014), July 9-11, 2014, organized by Delhi University, Delhi IC034.